DISPERSION IN SLOWLY MOVING FLUIDS

by

WOLTER A. M. TE RIELE M.Sc.(Eng.)

A thesis submitted in partial fulfilment of the requirements for the degree of Doctor of Philosophy in the Department of Chemical Engineering, University of Natal, Durban. March, 1970.

ABSTRACT

This work is concerned with the characterization of slowly moving fluids and was carried out on the flow of water through a narrow sedimentation tank. Dispersion in the type of flow structure involved is caused mainly by the presence of large eddies and, due to the fact that shear stresses are saml1, these eddies persist for a considerable period of time.

Two flow models are presented :

The first model assumes the X- Y- velocity component pair to form a discrete state Markov process in time and dispersion equations for the mean concentration at a point, the variance as well as concentration cross-correlations are generated.

In the second model the velocity fluctuation components are assumed to be independent, time-stationary Markov processes with normal probability density functions. The stochastic differential equation describing dispersion of tracer is formulated with and without the effect of molecular diffusion and solutions to both cases are presented.

Comparison of the model with experimental data obtained from tracer and anemometer measurements show that the model is capable of describing mean dispersion in a relatively small region of the tank and that the tracer experiments were insensitive to molecular diffusion.

ACKNOWLEDGEMENTS

The author wishes to express his appreciation to Professor E.T. Woodburn and Dr. R.P. King for their able supervision and guidance throughout the course of this work.

Assistance received from the following people is gratefully acknowledged :

- Staff and students of this department for many helpful suggestions and discussions;
- Workshop staff for the construction of apparatus;
- Staff of the Electronics Workshop of the department of Electrical Engineering for the construction and use of electronic equipment;
- Computer Centre staff for help with running of programmes;
- Miss Françoise Maingard for the skilful typing of these pages.

The author thanks the National Institute for Metallurgy for financing the project.

LIST OF CONTENTS

LIST OF CONTENTS (Continued)

LIST OF CONTENTS (Continued)

LIST OF CONTENTS (Continued)

Page

APPENDIX (Continued)

LIST OF FIGURES

LIST OF PHOTOGRAPHS

LIST OF SYMBOLS

A	Area under Lagrangian-time Correlation Curve, Equation 1.B
c, $c(x,y,t)$	Realisation of C.
$C, C(x,y,t)$	Tracer Concentration at the point (x,y) and time t; Random Process.
$\overline{C}(s,p,t)$	Two-sided Laplace Transform of C(x,y,t); Random Process.
d	Switching Time (Decision Interval) of Pseudo-Random Binary Sequence.
d_p	Width of rectangular input pulse.
D	Molecular Diffusion Coefficient
E	Eddy Diffusion Coefficient
$E\{\ \}$	Expected Value of $\{\ \}$.
$f(v)$	Distribution Density Function of V(t)
$f\{u_{x1}, u_{x2}(\tau, \sigma_0^2, \beta)\}$	Joint Probability Density Function for $U_x'(t)$ and $U_x'(t+\tau)$.
$f(w_x, w_y, t, \tau)$	Joint Probability Density Function for W_x and W_y.
$f(w_x, t, \tau)$, $f(w_y, t, \tau)$	Probability Density Functions for W_x, W_y.
$G_i(w) G_o(w)$	Frequency Content of Mean Response pulses.
F_i	Frequency of occurrence of velocity v_i.
$H(w)$	Amplitude Ratio in Bode Plot.
i,j,k	States of Discrete Space Flow Model.
$I_o(z)$	Modified Bessel Function of Zero Order.
J	Auxiliary Variable for R_{Qf}; Equation 5.10

LIST OF SYMBOLS (Continued)

K	Characteristic Function of $f\{u_{x1}, u_{x2}(\tau, \sigma_0^2, \beta)\}$
$L\{\ \}$	Laplace Transform of $\{\ \}$
$m_{1x}, m_{1x,1}, m_{1x,2}$	Mean of W_x; Equations 3.15, 3.29
$m_{1y}, m_{1y,1}, m_{1y,2}$	Mean of W_y; Equations 3.15, 3.29
n	Number of Concentration Readings per Station in experimental Crosscorrelation.
N	Total Number of Pulses in Mean Response Expt.
N_c	Number of V(t) readings correlated.
N_p	Number of decisions in P.R.B.S.
N_v	Total number of Hot Film Anemometer readings.
$N_\alpha, N_\alpha(t)$	Random Impact Force with White Noise properties and Gaussian Distribution Density.
p	Laplace transformed coordinate y.
$p(i)$	Stationary Probability of system being in flow state i; discrete space model.
$p(j;t)$	Probability of system being in flow state j at time t; discrete space model.
$p(c,q)$	Stationary Probability for observing a source strength q and concentration c at the point (x,y); discrete space model.
$p(j,c;t)$	Probability density for observing the concentration c at the point (x,y) while the flow is in state j at time t; discrete space model.

LIST OF SYMBOLS (Continued)

$p(i,j:\tau)$ — Probability of system being in flow state i and a time τ later in flow state j, discrete space model.

$p(j,q,c;t)$ — Probability density for observing a source strength q and a concentration c at the point (x,y), while the flow is in state j at time t; discrete space model.

$p(i;t,j;t+\tau)$ — Probability of system being in flow state i at time t and in flow state j at time $t+\tau$; discrete space model.

$p(i,q;t,j,c;t+\tau)$ — Prob. density for observing a source strength q and flow state i at time t and a concentration c at the point (x,y) and flowstate j at time $t+\tau$; discrete space model.

P — Period of pulse train for Mean Response experiment.

$PSD_{u'}(w)$ — Power Spectral Density of velocity fluctuations.

$PSD_Q(w)$ — Power Spectral Density of Pseudo-Random Binary Sequence.

PSD_{N_α} — Power Spectral Density of $N_\alpha(t)$

q — Amplitude of rectangular tracer input pulse (flowrate).

q(t) — Tracer flow rate injected at origin.

Q(t) — Random, time-stationary tracer source function.

LIST OF SYMBOLS (Continued)

$r_{1,2,..n}$	Eigen values of switching rates matrix; discrete space model.
r	Normalised covariance; equation 3.43.
R_N	Normalised Lagrangian autocorrelation of velocity fluctuations.
R_Q	Autocorrelation of Pseudo-Random Binary Sequence.
R_{Qf}	Autocorrelation of filtered Pseudo-Random Binary Sequence, Equation 5.10.
$R_{j,q,q}$	Partial autocorrelation of stationary source strength; discrete space model.
R_{qq}	Autocorrelation of Q(t); discrete space model.
R_{ox}, R_{oy}, R_o	Autocorrelation of velocity fluctuation components.
R_{v^2}	Autocorrelation of $V^2(t)$
R_{N_α}	Autocorrelation of $N_\alpha(t)$.
$s(j,x,y;t)$	Partial Mean square concentration; discrete space model.
s	Laplace transformed coordinate x.
T_p	Period of Pseudo-Random Binary Sequence.
T_c	Time constant of tracer injection system.
$\bar{u}_x, \bar{u}_y$	Components of mean fluid velocity.
u_x, u_y	Realisations of U_x, U_y.
u_{xi}, u_{yi}	Realisations of U_x, U_y in flowstate i; discrete space model.
U_x, U_y	X-,Y-component of fluid velocity; random process.

LIST OF SYMBOLS (Continued)

U'_x, U'_y	Fluid velocity fluctuation component; random process.
v	Realisation of $V(t)$.
$V(t)$	Vector sum of U_x and U_y; random process.
V_c	Volume of liquid used in calibration of light probes; Appendix 7.
w_x, w_y	Realisations of W_x, W_y.
W_x, W_y	Random process defined by equation 3.11.
w	Frequency in radians per second.
x, y	Coordinates with respect to point of tracer injection.
X, Y	Coordinates of fluid particle; random process.
X_R, Y_L	Right hand and Left hand Eigen vectors of switching rates matrix; discrete space model.
$\overline{x^2}(t)$	Variance of position of fluid particle in random flow field.
z	Dummy variable; Equation 5.12.
$\alpha, \alpha'_1, \alpha'_2$	Power Spectral Density of $N_\alpha(t), N_{\alpha'_1}(t)$ and $N_{\alpha'_2}(t)$
α_1, α_2	Auxiliary variables for crosscorrelation with molecular diffusion; Equations 3.45.
$\alpha_c, \alpha(\ )$	Derivate moment in Kolmogorov equations for term involving $\frac{\partial}{\partial c}$
α_q	Derivate moment in Kolmogorov equations for term involving $\frac{\partial}{\partial q}$

LIST OF SYMBOLS (Continued)

β_1, β_2	Auxiliary variables for crosscorrelation with molecular diffusion; Equation 3.45.
$\beta, \beta_1', \beta_2' (\beta_x, \beta_y)$	Flow scale parameters in Lagrangian time-correlation of (X-and Y-) velocity fluctuations.
γ_1, γ_2	Auxiliary variable in crosscorrelation with molecular diffusion; Equations 3.45
δ_{ij}	Kronecker Delta.
$\delta(\ )$	Dirac Function.
$\Phi_{ex.}$	Experimental concentration crosscorrelation between points (x_1, y_1) and (x_2, y_2).
Φ	Model crosscorrelation between points (x_1, y_1) and (x_2, y_2).
$\Phi_{q,c}$	Crosscorrelation between source strength and concentration at the point (x,y); discrete space model.
$\Phi_{j,q,c}$	Partial crosscorrelation between source strength and concentration at the point (x,y); discrete space model.
χ_x, χ_y	Variance parameters for velocity processes in Kolmogorov Equation 1.4.
λ_{ij}	Mean switching rate from state i to state j; discrete space model.
$\mu_{ex}(t_i)$	Experimental Mean Response curve.
$\mu(x,y,t)$	Mean concentration; continuous space model.
$\mu(j,x,y;t)$	Partial mean concentration; discrete space model.

LIST OF SYMBOLS (continued)

ν_x, ν_y	Drift parameters for velocity processes in Equation 1.4.
$\pi(j\|i:\tau)$	Transitional probability for transfer from flow state i to j in time interval τ ; discrete space model.
$\pi(j,q_1,c\|i,q:\tau)$	Stationary transitional probability for transfer from flow state i and source strength q to flow state j, source strength q_1 and concentration c at the point (x,y) in time interval τ; discrete space model.
$\pi(j,q_1,c;t+\tau\|i,q;t)$	Transitional probability for the transfer from flow state i and source strength q at time t to flow state j and source strength q_1 and concentration c at the point (x,y) at time t + τ ; discrete space model.
$\pi(u_x,u_y,c;t\|u_{x0},u_{y0},c_o;t_o)$	Transitional probability for the transfer from velocities u_{xo},u_{yo} and concentration c_o at time t_o to velocities u_x,u_y and concentration c at time t.
$\rho(t,\tau_1;t,\tau_2)$	Covariance of $W_x(t,\tau_1)$ and $W_x(t,\tau_2)$; $W_y(t,\tau_1)$ and $W_y(t,\tau_2)$
σ_o^2, $(\sigma_{ox}^2,\sigma_{oy}^2)$	Variance of continuous space velocity (components) processes.
$\sigma_{1x}^2,\sigma_{1y}^2,\sigma_1^2$	Variance of W_x,W_y,W
	Lag in auto- and crosscorrelations; time interval.

LIST OF SYMBOLS (continued)

τ_1, τ_2	Variable space for crosscorrelation; Equation 3.31.
$\sigma^2_{1,1}, \sigma^2_{1,2}$	Variance of W defined by Equations 3.42.
θ', θ''	Dummy variables of integration.
θ_1, θ_2	Variable space for crosscorrelation; Equation 3.31.
ξ_1, ξ_2	Variable space of characteristic function K.

CHAPTER I

INTRODUCTION

Our interest lies in the flow structure developed when large masses of fluids move comparatively slowly. To illustrate the type of dispersion obtained in such a flow structure one may observe the smoke from the tip of a stationary cigarette in a well ventilated room. The character of the dispersion action may be roughly split into two parts:

Firstly, a randomly varying velocity responsible for large scale dispersion and secondly the effect of a diffusion type mechanism. Under these circumstances the shear stresses within the fluid are low giving rise to large scale turbulence of low intensity.

Tracer experiments were carried out on the flow of water through a narrow sedimentation tank. The photographs on page 2 show the path taken by a dye solution injected continuously at a point in the tank. They were taken at intervals of about thirty seconds and show clearly that the general direction of flow varies substantially, even though the flows into and out of the tank had been constant for a considerable period of time. Furthermore, the jagged paths indicate that the general direction of flow is the same throughout the region shown and changes fairly slowly with time. (See photograph on page 3). Under these conditions the velocity history of a fluid particle is identical to that recorded by a stationary observer noting the fluid velocity at a point. The gradual

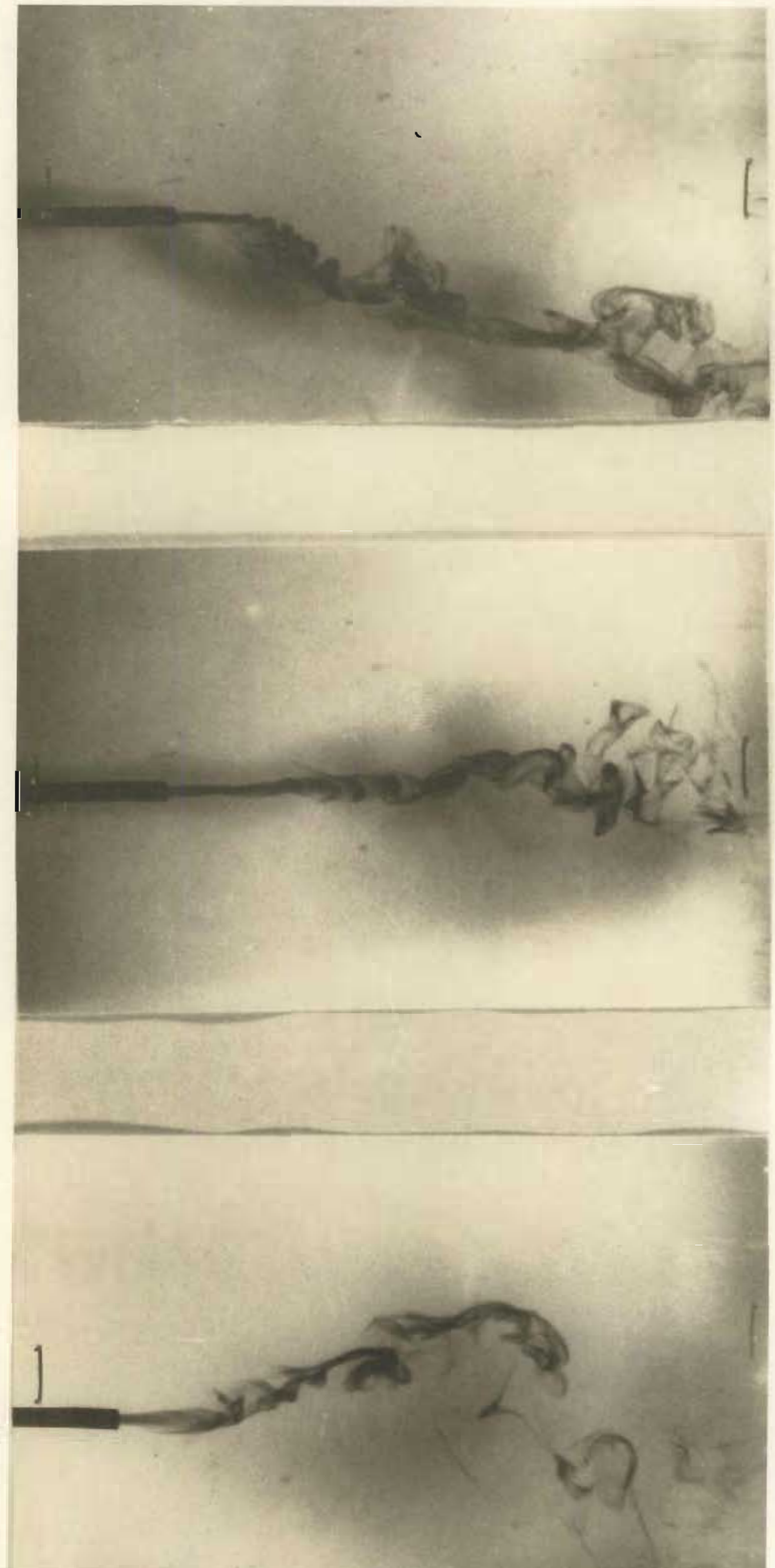

widening of the dye path indicates the presence of a small scale, diffusion-type dispersion mechanism. The flow situation is therefore interesting from a theoretical point of view, because, to a close approximation, the Eulerian and Lagrangian statistics are identical.

The stochastic nature of the flow was further illustrated by the widely differing paths taken by pulses of tracer material injected intermittently at a point in the tank. Clearly the above flow structure cannot be realistically described by the well-used Eddy Diffusion model applicable to dispersion in highly turbulent fluids. The latter is associated with large shear stresses and small, high frequency eddies superimposed on a constant mean velocity. The inadequacy of this model for the flow structure considered here is shown in more detail below.

The dispersion of tracer material may be described by the following stochastic partial differential equation:

$$\frac{\partial C}{\partial t} = - U_x(x,y,t)\frac{\partial C}{\partial x} - U_y(x,y,t)\frac{\partial C}{\partial y} + q(t)\delta(x)\delta(y) \qquad 1.1$$

where,

C = tracer concentration at the point x,y and time t.

$q(t)$ = tracer flow rate injected at the origin.

$U_x(x,y,t)$ = X-component of velocity.

$U_y(x,y,t)$ = Y-component of velocity.

Both $U_x(x,y,t)$ and $U_y(x,y,t)$ are stochastic processes. The solution to the above equation is unknown at present, because the stochastic processes $U_x(x,y,t)$ and $U_y(x,y,t)$ are functions of both position and time; (1) i.e. the equation is an Eulerian description of dispersion. If, however, the velocities are interpreted in a Lagrangian sense, they become effectively functions of time only and equation 1.1 may be written:

$$\frac{\partial C}{\partial t} = - U_x(t)\frac{\partial C}{\partial x} - U_y(t)\frac{\partial C}{\partial y} + q(t)\delta(x)\delta(y) \qquad 1.2$$

Hence, Lagrangian statistics of the velocity processes must be used to obtain statistical properties of the solution functions C(x,y,t). This method of interpreting and solving equation 1.2 yields results identical to the solution of the familiar Lagrangian equations :

$$\frac{dX}{dt} = U_x(t) \quad ; \quad \frac{dY}{dt} = U_y(t) \qquad 1.3$$

first investigated by Taylor (2) as a model for turbulent flow. This correspondence might appear surprising at first sight and is developed in detail below.

In order to solve equation 1.2 we assume the velocities U_x and U_y to be Markov processes; in addition, the solution C(x,y,t) together with U_x and U_y form a composite Markov process and hence the associated Kolmogorov equation must exist :(3)

$$\frac{\partial \pi}{\partial t} = - \frac{\partial}{\partial c}(\alpha_c \pi) - \frac{\partial}{\partial u_x}(\nu_x \pi) - \frac{\partial}{\partial u_y}(\nu_y \pi) + \tfrac{1}{2}\frac{\partial^2}{\partial u_x^2}(\chi_x \pi) + \tfrac{1}{2}\frac{\partial^2}{\partial u_y^2}(\chi_y \pi) \qquad 1.4$$

where,

$\pi(u_x,u_y,c;t|u_{xo},u_{yo},c_o;t_o)$ = transition prob. density.

$$\alpha_c = - u_x\frac{\partial c}{\partial x} - u_y\frac{\partial c}{\partial y} \qquad 1.5$$

$\nu_x,\nu_y,\chi_x,\chi_y$ = drift and variance parameters respectively for the velocity processes.

This equation, however, cannot be used to generate a closed system of moment equations due to the non-linear coupling between the velocities and concentrations in α_c. We therefore investigated two possible assumptions to overcome this difficulty.

In the first case, the velocity can only assume a finite number of fixed values; i.e. $U_{x,y}(t)$ has discrete state space. This model was inspired by the work of Krambeck, Shinnar and Katz (4). These workers modelled a flow reactor by a network of perfectly stirred tanks. The volumes of the tanks remain constant, whilst the interstage flow rates between them are allowed to switch randomly in time between discrete levels according to a stationary Markov process. Clearly, the physical significance of this model is limited and cannot be applied directly to the present problem. Their treatment is adapted by assuming the X-and-Y-velocity component pair to be a discrete state, time-stationary Markov process. Equations describing the development of a number of concentration moments are derived from a consideration of the appropriate Kolmogorov equations. The major drawback of this model, however, lies in the difficulty of obtaining solutions to these equations as well as in its large number of parameters. Consequently, no attempt was made to compare the predictions of this model with experimental data. The model is presented in Chapter II and the reader may omit this chapter on first reading without loss of continuity.

In the second case we make an a priori assumption regarding the probability density function for the velocity process. $U_{x,y}(t)$ has continuous state space and thus provides a more realistic description of the flow structure under consideration. The above Kolmogorov equation (Equation 1.4) was not used in the solution, as a direct method of solution was available, and is presented in Chapter III.

To illustrate the correspondence of the results developed in Chapter III with those obtained by Taylor (5), Doob (6), a.o. we may examine the expression for the mean concentration : (see Equation 3.25)

$$\mu(x,t) = \int_0^\infty q(\tau) \frac{1}{\{2\pi\sigma_1^2(t,\tau)\}^{\frac{1}{2}}} \exp - \frac{\{x - m_{1x}(t,\tau)\}^2}{2\sigma_1^2(t,\tau)} \, d\tau \qquad 1.6$$

If tracer enters the system as an instantaneous point source then: $q(\tau)=\delta(\tau)$ and the resultant response for the mean concentration is seen to be Gaussian. Furthermore, development of the model results in the following expressions for the mean and variance of this distribution:

$$m_{1x} = \bar{u}_x t \qquad 1.7$$

$$\sigma_1^2(t) = \frac{\alpha}{\beta} \{\exp(-\beta t) - 1 + \beta t\} \qquad 1.8$$

(compare Equations 3.15, 3.17)

Taylor (2) developed the following expression for the variance of particle position in a turbulent velocity field :

$$\overline{X^2(t)} = 2\sigma_0^2 \int_0^t \int_0^{\tau_1} R_N(\tau) \, d\tau \, d\tau_1 \qquad 1.9$$

where,

$R_N(\tau)$ = Normalised Lagrangian autocorrelation of

σ_o^2 = Variance of velocity fluctuations.

Substitution of the assumed form of $R(\tau)$ (see Equation 3.3) in Equation 1.9 and integrating yields a result identical to Equation 1.8. Clearly, when the flow field suffers a mean displacement velocity $\bar{u}_x$, then $\overline{X^2(t)}$ relates to the variance about the point $\bar{u}_x t$.

In order to show the correspondence in more detail we require the form of the probability density function for X(t). Doob (6) a.o. make use of the following two equations to obtain this function:

$$\frac{dU(t)}{dt} + \beta U(t) = N_\alpha(t) \qquad 1.10$$

$$U(t) = \frac{dX(t)}{dt} \qquad 1.11$$

where,

β = damping parameter.

$N_\alpha(t)$ = random impact force with White Noise properties and Gaussian distribution density.

These workers showed that both the probability density for position p(x,t) and velocity p(u,t) have a Gaussian form.

Hence, the results derived by Taylor, Doob a.o. for the motion of a single particle are similar to those developed in Chapter III and the equivalence is complete if the probability density for the position of a single particle is interpreted as the concentration resulting from the release of a large number of tracer particle at the origin. The correspondence between the mean concentration $\mu(x,t)$ and the probability density p(x,t) is, of course, easy to justify for fully developed turbulence, tainly not be true due to the slow variation of the instantaneous velocity.

The use of a pseudo Eulerian formulation of Equation 1.2 may be justified for three reasons :

Firstly, it allows one to work directly with tracer concentration.

Secondly, molecular diffusion terms may be written in directly :

$$\frac{\partial C}{\partial t} = -U_x(t)\frac{\partial C}{\partial x} + D\frac{\partial^2 C}{\partial x^2} - U_y(t)\frac{\partial C}{\partial y} + D\frac{\partial^2 C}{\partial y^2} + q(t)\delta(x)\delta(y) \qquad 1.12$$

where,

D = molecular diffusion coefficient.

Thirdly, the model is not restricted to periods of dispersion which are considerably longer than the lag at which the Lagrangian autocorrelation of velocity has reached zero. This restriction does apply to the Eddy Diffusion model :

$$\frac{\partial c}{\partial t} = -\overline{u}_x\frac{\partial c}{\partial x} + E\frac{\partial^2 c}{\partial x^2} \qquad 1.13$$

where,

$\overline{u}_x$ = constant mean velocity

E = Eddy Diffusion Coeficient

Taylor (7) has shown that E may be expressed as :

$$E = \tfrac{1}{2}\sigma_0^2 \int_0^\infty R_N(\tau)\, d\tau \qquad 1.14$$

The above expression for E, however, is based on the following approximation:

$$\overline{X}^2(t) = 2\sigma_0^2 At \quad \text{where, } A = \int_0^\infty R_N(\tau)\, d\tau \qquad 1.14;\ 1.15$$

If $R\ (\tau)$ reaches zero at lag $\tau = t_1$ and $t > t$ ...

becomes :

$$\overline{X}^2(t) = 2\sigma_0^2 At - 2\sigma_0^2 \int_0^{t_1}\int_{\tau_1}^{t_1} R_N(\tau)\, d\tau\, d\tau_1 \qquad 1.17$$

It can be shown that for the tracer experiments carried out in this work errors of the order of thirty per cent result when the second term is neglected. (Appendix I)

Equations 1.2 and 1.12 are solved by assuming the velocity components to be independent, time stationary Markov processes with Gaussian probability density functions. Solutions for both the mean concentration at a point as well as the concentration cross correlation between two points are obtained in terms of model parameters and tracer input function. The validity of this model was tested experimentally in two ways :

Firstly, tracer experiments were carried out to obtain experimental estimates of concentration moments for a number of positions. Comparisons with model predictions provided a means for evaluation of the parameters as well as a measure for the ability of the model to describe dispersion.

Secondly, the fluid velocity at a point was measured directly with the aid of a Hot Film Anemometer. This experiment provided a test of the physical significance of the model parameters together with an independent estimate of their values.

CHAPTER II

DISCRETE STATE SPACE FLOW MODEL

2.1. INTRODUCTION

The model is based on the assumption that the velocity of the fluid may be represented by a stationary, discrete state Markov process. The instantaneous velocity components in the X-and-Y coordinate directions $U_x(t)$, $U_y(t)$ can therefore assume any of a finite number of pair values (u_{xj}, u_{yj}); the flow process is said to be in flow state j. The randomness of the model is introduced by allowing instantaneous switching to occur from one flow state to another as a random function of time. Furthermore, it is assumed that the statistical properties of the flow process do not vary with time. This assumption will hold when the process has been in progress long enough, so that start-up conditions have no influence on the state of the system. The flow process is assumed to be Markov and therefore may be described by a matrix of transition probability densities:

$$||\pi(j|i:\tau)||$$

where $\pi(j\,|i:\tau)$ represents the probability of the flow process switching from state i to state j in a time interval τ .

2.2 FLOW STATE EQUATIONS

The following properties of such a Markov process are known and will be used below:

$$\sum_j \pi(i|j:\tau) = 1 \qquad 2.1$$

$$\pi(i|j:\tau) = \delta_{ij} + \lambda_{ij}\tau + O(\tau) \qquad 2.2$$

where,

$$\delta_{ij} = 0 \quad ; \quad i \neq j$$
$$= 1 \quad ; \quad i = j$$

λ_{ij} = constant and may be interpreted as a measure of the mean switching rate from state i to state j.

$$\lim_{\tau \to 0} \frac{O(\tau)}{\tau} = 0$$

From Equations 2.1 and 2.2 it follows that :

$$\sum_j \lambda_{ij} = 0$$

If p(i;t) represents the probability that the flow process is in state i at a time t, then :

$$p(j;t+\tau) = \sum_i p(i;t)\ \pi(j|i:\tau) \qquad 2.4$$

From Equations 2.2 and 2.4 it follows that

$$\frac{dp(j;t)}{dt} = \sum_i \lambda_{ij} p(i;t) \qquad 2.5$$

When the process has become stationary Equation 2.5 becomes :

$$\sum_i \lambda_{ij} p(i) = 0 \qquad 2.6$$

Equation 2.6 together with

$$\sum_i p(i) = 1 \qquad 2.7$$

may be solved uniquely for the stationary flow state probabilities p(i), provided zero is a single (i.e. not multiple) Eigen - value of the matrix $||\lambda_{ij}||$.

2.2.1

AUTOCORRELATION OF VELOCITY PROCESS

If $p(i;t,j;t+\tau)$ is defined as the joint probability that the X-component of velocity (U_x) has the value u_{xi} at time t and u_{xj} at time $t+\tau$, then the autocorrelation may be written as :

$$R_{ox}(\tau) = \int_{-\infty}^{\infty}\int_{-\infty}^{\infty} u_{xi}u_{xj}p(i;t,j;t+\tau)\ du_{xi}\ du_{xj}$$

For a time stationary, discrete process this may be simplified as follows:

$$\begin{aligned} R_{ox}(\tau) &= \sum_j \sum_i u_{xi}u_{xj}p(i,j:\tau) \\ &= \sum_j \sum_i u_{xi}u_{xj}p(i)\ \pi(j|i:\tau) \end{aligned} \qquad 2.8$$

It can be shown (8) that the transition probability density matrix as a function of time may be written as :

$$||\pi(j|i:\tau)|| = |X_R|\ \text{diag}||\exp(r_1\tau),..\exp(r_n\tau)|||Y_L| \qquad 2.9$$

where $|X_R|$ and $|Y_L|$ are the Righthand and Lefthand Eigen-vectors of the matrix λ_{ij} and $r_{1..n}$ the Eigen-values. $\text{diag}||\exp(r_1\tau), \ldots \exp(r_n\tau)||$ is a square matrix with elements $\exp(r_1\tau), \ldots \exp(r_n\tau)$ on the diagonal and all other elements equal to zero.

Hence, from a knowledge of the switching rate matrix λ_{ij} and the allowable values of U_x and U_y both the stationary flow state probabilities p(i) and the component autocorrelations $R_{ox}(\tau)$, $R_{oy}(\tau)$ may be calculated. Figure 1.1 shows a typical autocorrelation $R_{ox}(\tau)$ as a function of τ for a three-state flow structure. The autocorrelation fuunction has an exponential type decay typical of Markov processes. This model could only be expected to be useful for modelling flow systems having such a velocity autocorrelation.

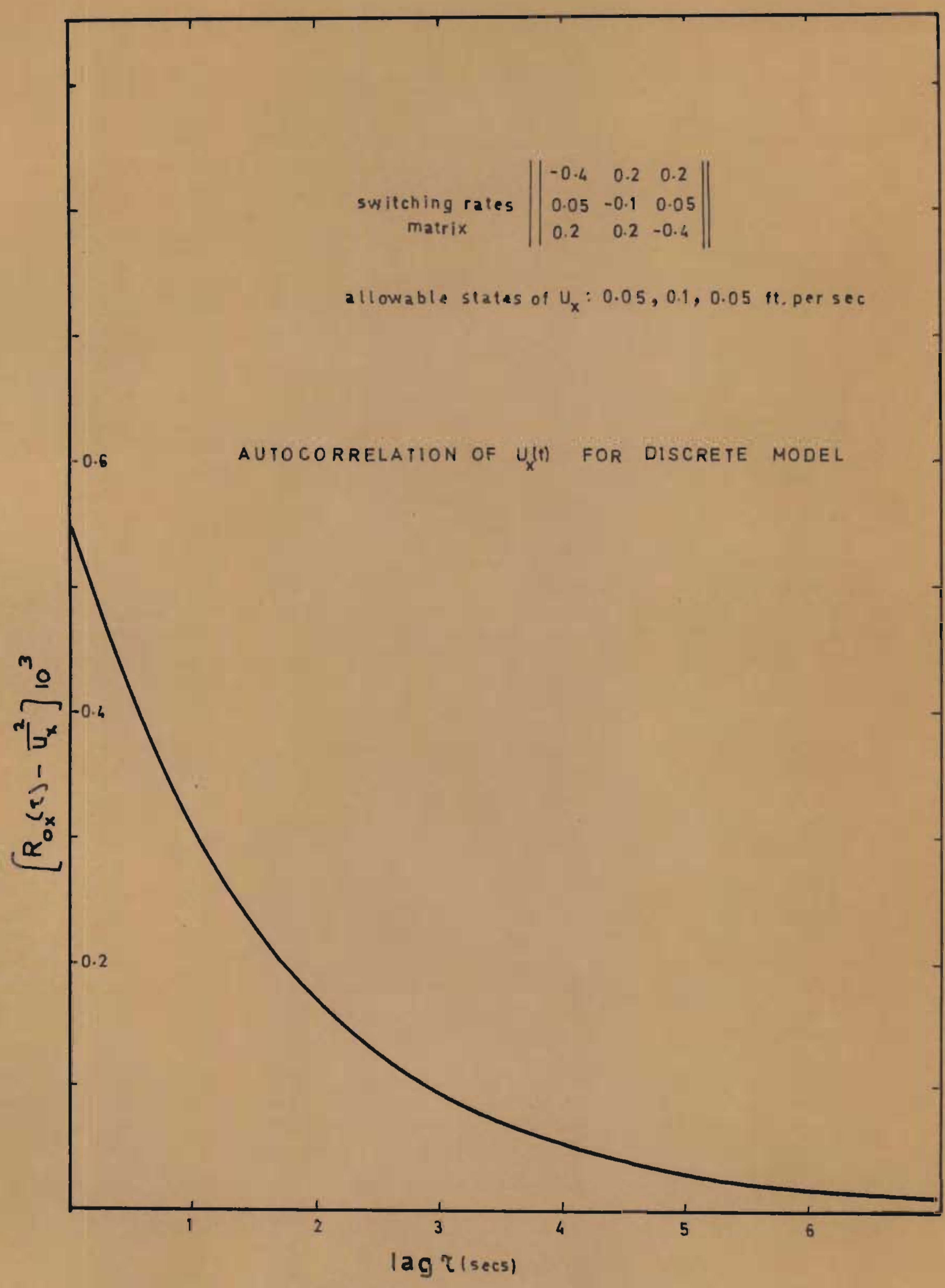
switching rates matrix
-0·4 0·2 0·2
0·05 -0·1 0·05
0·2 0·2 -0·4
allowable states of U_x : 0·05, 0·1, 0·05 ft. per sec
AUTOCORRELATION OF U_x(t) FOR DISCRETE MODEL
0·6
0·4
0·2
[R_ox(τ) - U_x^2] 10^3
1
2
3
4
5
6
lag τ (secs)

FIG. 1.1

2.3 MIXING EQUATIONS

In order to describe the dispersion of tracer material in the above flow process we now introduce a composite Markov process, whose state comprises the discrete flow states p(i) and the continuous states of tracer concentration c and spatial coordinates x,y. Hence $p(j,c;t)$ dc represents the joint probability of the flow being in state j and of the concentration at the point x,y having a value between c and c+dc at a time t. The forward Kolmogorov equation associated with $p(j,c;t)$ may be show to have the following form: (Appendix 2)

$$\frac{\partial p(j,c;t)}{\partial t} = \sum_i \lambda_{ij} p(i,c;t) - \frac{\partial}{\partial c}\{\alpha_c(j,c;t)p(j,c;t)\} \qquad 2.10$$

where,

$$\alpha_c(j,c;t) = \lim_{\Delta t \to o} \frac{1}{\Delta t} E\{C(t+\Delta t)-C(t)\,|\,C(t)=c,\text{flow state}=j\} \qquad 2.11$$

If the system is excited by means of a point source of tracer then the dispersive action of the flow process is described by the following stochastic partial differential equation :

$$\frac{\partial C(t)}{\partial t} = - U_x \frac{\partial C(t)}{\partial x} - U_y \frac{\partial C(t)}{\partial y} + q(t)\delta(x)\delta(y) \qquad 2.12$$

where,

q(t) = tracer flow rate.

Hence from Equation 2.11 :

$$\alpha_c(j,c;t) = - u_{xj}\frac{\partial c}{\partial x} - u_{yj}\frac{\partial c}{\partial y} + q(t)\delta(x)\delta(y) \qquad 2.13$$

2.3.1 MOMENTS EQUATIONS

The most convenient way of testing prediction of the model and of estimating the model parameters is to compare the moments of the distribution of concentration with those measured experimentally. We define the Partial Mean Concentration at the point (x,y) as :

$$\mu(j,x,y,t) = \int_0^\infty c\, p(j,c;t)\, dc \tag{2.14}$$

and the Partial Mean Square Concentration as :

$$s(j,x,y,t) = \int_0^\infty c^2\, p(j,c;t) \tag{2.15}$$

The development of these moments in time is obtained by differentiation:

$$\frac{\partial\mu}{\partial t}(j,x,y,t) = \int_0^\infty c\, \frac{\partial p}{\partial t}(j,c;t)\, dc \tag{2.16}$$

$$\frac{\partial s}{\partial t}(j,x,y,t) = \int_0^\infty c^2\, \frac{\partial p}{\partial t}(j,c;t)\, dc \tag{2.17}$$

Substituting Equations 2,10 and 2.13 and integrating by parts yields :

$$\frac{\partial\mu}{\partial t}(j,x,y,t) = \sum_i \lambda_{ij}\mu(i,x,y,t) - u_{xj}\frac{\partial\mu}{\partial x}(j,x,y,t) - u_{yj}\frac{\partial\mu}{\partial y}(j,x,y,t) + q(t)p(j)\delta(x)\delta(y) \tag{2.18}$$

$$\frac{\partial s}{\partial t}(j,x,y,t) = \sum_i \lambda_{ij}s(i,x,y,t) - u_{xj}\frac{\partial s}{\partial x}(j,x,y,t) - u_{yj}\frac{\partial s}{\partial y}(j,x,y,t) + 2q(t)p(j)\mu(j,x,y,t)\delta(x)\delta(y) \tag{2.19}$$

Crosscorrelation between the source strength Q(t) and tracer concentration C(t) at point (x,y).

Tracer material is injected at the origin at a rate Q(t). If Q(t) is a time-stationary, random function then Q(t), C(t) and flow state form a composite Markov process. Hence we may define a probability density function p(j,q,c;t), such that p(j,q,c;t) dq dc represents the joint probability of the system being in flow state j, the tracer flow rate having a value between q and q + dq and the tracer concentration at the point (x,y) having a value between c and c + dc at time t. The associated Kolmogorov equation has the following form : (Appendix 2)

$$\frac{\partial p(j,q,c;t)}{\partial t} = \sum_k \lambda_{kj} p(k,q,c;t) - \frac{\partial}{\partial q}\{\alpha_q(j,q,c;t)p(j,q,c;t)\}$$
$$- \frac{\partial}{\partial c}\{\alpha_c(j,q,c;t)p(j,q,c;t)\} \qquad 2.20$$

where,

$$\alpha_q(j,q,c;t) = \lim_{\Delta t \to o} \frac{1}{\Delta t} E\{Q(t+\Delta t)-Q(t)\,|\,Q(t)=q,$$
$$C(t)=c, \text{flow state}=j\} \qquad 2.21$$

$$\alpha_c(j,q,c;t) = \lim_{\Delta t \to o} \frac{1}{\Delta t} E\{C(t+\Delta t)-C(t)\,|\,Q(t)=q,$$
$$C(t)=c, \text{flow state}=j\} \qquad 2.22$$

Similarly, a transitional probability density function $\pi(j,q_1,c;t+\tau\,|\,i,q;t)$ may be defined such that $\pi(j,q_1,c;t+\tau\,|\,i,q;t)\, dq_1\, dc$ represents the joint probability of the system being in flow state j and the concentration at the point (x,y) having a value between c and c + dc and the source strength between q_1 and $q_1 + dq_1$ at t+τ, knowing that at time t the system the source strength had a value q. If the process is time-stationary this function will be independent of t and the appropriate Kolmogorov equation becomes : (Appendix 2)

$$\frac{\partial \pi(j,q_1,c|i,q:\tau)}{\partial \tau} = \sum_k \lambda_{kj} \pi(k,q_1,c|i,q,:\tau) - \frac{\partial}{\partial c}\{\alpha_c(j,q_1,c)\pi\} - \frac{\partial}{\partial q_1}\{\alpha_q(j,q_1,c)\pi\} \quad 2.23$$

where,

$$\alpha_q(j,q_1 c) = \lim_{\Delta t \to o} \frac{1}{\Delta t} E\{Q(t+\Delta t) - Q(t)|Q(t)=q_1, C(t)=c,\text{flow state}=j\}$$

$$\alpha_c(j,q_1,c) = \lim_{\Delta t \to o} \frac{1}{\Delta t} E\{C(t+\Delta t) - C(t)|C(t)=c, Q(t)=q_1,\text{flow state}=j\} \quad 2.24$$

The Crosscorrelation between the source strength Q(t) and tracer concentration at the point (x,y) is defined as :

$$\Phi_{qc}(t,\tau) = \sum_j \sum_i \int_o^\infty \int_o^\infty qc\ p(i,q;t,j,c;t+\tau)\ dq\ dc \quad 2.25$$

If the system is time-stationary we define a Partial Crosscorrelation as :

$$\Phi_{jqc}(\tau) = \sum_i \int_o^\infty \int_o^\infty \int_o^\infty qc\ p(i,q)\ \pi(j,q_1,c|i,q:\tau)\ dq\ dc\ dq_1 \quad 2.26$$

Differentiating Equation 2.26, substituting from Equations 2.23 and 2.13 and integrating by parts yields :

$$\frac{\partial \Phi_{jqc}(\tau)}{\partial \tau} = \sum_k \lambda_{kj} \Phi_{kqc}(\tau) - u_{xj}\frac{\partial \Phi_{jqc}(\tau)}{\partial x} - u_{yj}\frac{\partial \Phi_{jqc}(\tau)}{\partial y} + R_{jqq}(\tau)\delta(x)\delta(y) \quad 2.27$$

where,

$$R_{jqq}(\tau) = \text{Partial Autocorrelation of } Q(t)$$

$$= \sum_i \int_0^\infty \int_0^\infty qq_1 \; p(i,q) \; \pi(j,q_1|i,q:\tau) \; dq \; dq_1 \qquad 2.28$$

In order to solve Equation 2.27 we require initial conditions $\Phi_{jqc}(o)$:

$$\Phi_{jqc}(o) = \int_0^\infty \int_0^\infty qc \; p(j,q,c;t) \; dq \; dc \qquad 2.29$$

Differentiating Equation 2.29 with respect to t and substituting from Equation 2.20, assuming the process to be time-stationary yields: (Appendix 3)

$$o = \sum_k \lambda_{kj} \Phi_{kqc}(o) - \frac{1}{T_c} \Phi_{jqc}(o) - u_{xj} \frac{\partial \Phi_{jqc}}{\partial x}(o) - u_{yj} \frac{\partial \Phi_{jqc}}{\partial y}(o) \qquad 2.30$$

$$+ \frac{1}{T_c} \; E\{N_w(t) | Q(t)=q\} \mu(j,x,y) + R_{qq}(o) p(j) \delta(x) \delta(y)$$

where,

$$R_{qq}(\tau) = \text{Autocorrelation of } Q(t).$$

The source strength Q(t) is the output of a first order filter (time constant T_c) with input $N_w(t)$.

Hence the solution of Equations 2.30 serves as initial conditions for Equations 2.27. A similar set of equations may be developed for concentration autocorrelations and crosscorrelations between two points (x_1,y_1) and (x_2,y_2).

In order to solve the non-time-stationary forms of Equations 2.18 and 2.19 in an infinite plane a numerical approach must be adopted. It will be realised that each case involves the simultaneous solution of a number of partial differential equations equal to the number of allowable flow states. Hence the time consuming effort and high cost of computation required f complete solution of the above equations for a realistic number of flow states are not considered warranted.

CHAPTER III

CONTINUOUS STATE SPACE FLOW MODEL.

3.1 VELOCITY PROCESS.

The model is based on the following assumptions:

Firstly, the instantaneous fluid velocity U(t) is regarded to consist of a mean component $\bar{u}$ and a fluctuating component U'(t). Hence

$$\begin{aligned} U_x(t) &= \bar{u}_x + U_x'(t) \\ U_y(t) &= \bar{u}_y + U_y'(t) \end{aligned} \qquad 3.1$$

Secondly, the stochastic processes $U_x'(t)$ and $U_y'(t)$ are time-stationary and have continuous state Markov properties as well as Gaussian probability density functions. (Ornstein-Uehlenbeck processes)

Thirdly, it is assumed that the random motion is isotropic as far as rotations about the X-axis are concerned; the X- and Y-motions may then be shown to be uncorrelated.(9) Since their distributions are Gaussian they are also independent.(10)

Mean of U'(t) :

$$E\{U_x'(t)\} = E\{U_y'(t)\} = o \qquad 3.2$$

Autocorrelation of U'(t) :

$$\begin{aligned} R_{ox}(\tau) &= E\{U_x'(t)U_x'(t+\tau)\} = \sigma_{ox}^2 \exp(-\beta_x|\tau|) \\ R_{oy}(\tau) &= E\{U_y'(t)U_y'(t+\tau)\} = \sigma_{oy}^2 \exp(-\beta_y|\tau|) \end{aligned} \qquad 3.3$$

Crosscorrelation between $U_x'(t)$ and $U_y'(t)$:

$$E\{U_x'(t)U_y'(t+\tau)\} = o \qquad 3.4$$

for all τ.

3.2 MIXING EQUATIONS.

Neglecting the effect of molecular diffusion dispersion of tracer material originating from a point source at a rate q(t) is described by the following partial stochastic differential equation :

$$\frac{\partial C}{\partial t} = - U_x(t)\frac{\partial C}{\partial x} - U_y(t)\frac{\partial C}{\partial y} + q(t)\delta(x)\delta(y) \qquad 3.5$$

We define a two-sided Laplace Transform by :

$$L\{C(x,y,t)\} = \int_{-\infty}^{\infty}\int_{-\infty}^{\infty} C(x,y,t)\exp(-sx)\exp(-py)\ dx\ dy \qquad 3.6$$

Hence

$$L\{\frac{\partial C}{\partial x}\} = \int_{-\infty}^{\infty}\int_{-\infty}^{\infty} \frac{\partial C}{\partial x} \exp(-sx)\exp(-py)\ dx\ dy$$

Integrating by parts and noting that $C(x,y,t) = o$ @ $x,y = -\infty$, we obtain :

$$L\{\frac{\partial C}{\partial x}\} = s\overline{C}(s,p,t) \qquad 3.7$$

Taking the Laplace Transform of Equation 3.5 we obtain :

$$\frac{d\overline{C}}{dt} = - U_x(t)\overline{C}s - U_y(t)\overline{C}p + q(t) \qquad 3.8$$

Using the initial condition :

$$c(x,y,o) = o \quad ; \quad \overline{c}(s,p,o) = o \qquad 3.9$$

this ordinary stochastic differential equation may be solved to give :

$$\overline{C}(s,p,t) = \int_0^t q(\tau)\ \exp-\{sW_x(t,\tau) + pW_y(t,\tau)\}\ d\tau \qquad 3.10$$

where,

$$W_x(t,\tau) = \int_\tau^t U_x(\theta')\ d\theta'$$

$$W_y(t,\tau) = \int_\tau^t U_y(\theta')\ d\theta' \qquad 3.11$$

Inverting the transform of Equation 3.10 gives :

$$C(x,y,t) = \int_0^t q(\tau)\ \delta\{W_x(t,\tau)-x\}\delta\{W_y(t,\tau)-y\}\ d\tau \qquad 3.12$$

The corresponding solution for a time-stationary, random source is :

$$C(x,y,t) = \int_{-\infty}^t Q(\tau)\ \delta\{W_x(t,\tau)-x\}\delta\{W_y(t,\tau)-y\}\ d\tau \qquad 3.13$$

3.3 W(t,τ) - PROCESS

In order to obtain expressions for the moments of C(x,y,t) and compare these with values determined experimentally we must first derive corresponding expressions for the random processes $W_x(t,\tau)$ and $W_y(t,\tau)$. (subscripts x,y are omitted where not explicitly required.)

Using Equations 3.1 and 3.11 we may write :

$$W(t,\tau) = \int_\tau^t U(\theta')\ d\theta' = \int_\tau^t U'(\theta')\ d\theta' + \bar{u}(t-\tau)$$

Mean $m_1(t,\tau)$:

$$m_1(t,\tau) = E\{\int_\tau^t U'(\theta')\ d\theta'\} + \bar{u}(t-\tau)$$

$$= \int_\tau^t E\{U'(\theta')\}\ d\theta' + \bar{u}(t-\tau)$$

Hence from Equation 3.2 it follows that

$$m_1(t,\tau) = \bar{u}(t-\tau) \qquad 3.15$$

Variance $\sigma_1^2(t,\tau)$:

Using Equations 3.14 and 3.15 we may write :

$$\sigma_1^2(t,\tau) = E\{\left[W(t,\tau)-m_1(t,\tau)\right]^2\} = E\{\left[\int_\tau^t U'(\theta')\ d\theta'\right]^2\}$$

Substituting Equation 3.3 and integrating yields :

$$\sigma_1^2(t,\tau) = \frac{2\sigma_o^2}{\beta^2}\left[\exp\{-\beta(t-\tau)\} + \beta(t-\tau) - 1\right] \quad 3.17$$

Autocorrelation $\rho(t,\tau_1 t,\tau_2)$

Similarly, substituting Equation 3.3 and integrating we obtain :

$$\rho(t,\tau_1;t,\tau_2) = E\{\left[W(t,\tau_1)-m_1(t,\tau_1)\right]\left[W(t,\tau_2)-m_1(t,\tau_2)\right]\}$$

$$= \frac{\sigma_o^2}{\beta^2}\left[2\beta(t-\tau_2) + \exp\{-\beta(t-\tau_2)\} + \exp\{-\beta(t-\tau_1)\} - \exp\{-\beta(\tau_2-\tau_1)\} - 1\right] \qquad \tau_2 > \tau_1 \quad 3.18$$

It can be shown that if U(t) has a Gaussian distribution density function, $W(t,\tau)$ will likewise have one. This relationship does not hold generally for distributions other than Gaussian (12) and the analysis relies heavily on the choice of this distribution. Furthermore, since $U_x(t)$ and $U_y(t)$ are independent the same will be true for $W_x(t,\tau)$ and $W_y(t,\tau)$.

3.4 MOMENTS EQUATIONS

3.4.1 MEAN CONCENTRATION $\mu(x,y,t)$

$$\mu(x,y,t) = E\{C(x,y,t)\} \quad 3.19$$

Substituting from Equation 3.12 yields :

$$\mu(x,y,t) = \int_0^t q(\tau)\; E\{\delta\left[W_x(t,\tau)-x\right]\delta\left[W_y(t,\tau)-y\right]\}\, d\tau \quad 3.20$$

$$= \int_0^t q(\tau)\int_{-\infty}^{\infty}\int_{-\infty}^{\infty}\delta\left[w_x(t,\tau)-x\right]\delta\left[w_y(t,\tau)-y\right] f(w_x,w_y,t,\tau)$$

where,

$f(w_x,w_y,t,\tau)$ = Joint probability density of $W_x(t,\tau)$ and $W_y(t,\tau)$.

Noting that

$$f(w_x,w_y,t,\tau) = f(w_x,t,\tau)\ f(w_y,t,\tau) \qquad 3.21$$

and integrating Equation 3.20 yields :

$$\mu(x,y,t) = \int_0^t q(\tau)\ f(x,t,\tau)\ f(y,t,\tau)\ d\tau \qquad 3.22$$

where,

$$f(x,t,\tau) = \frac{1}{(2\pi\sigma_{1x}^2)^{\frac{1}{2}}} \exp\left(-\frac{(x-m_{1x})^2}{2\sigma_{1x}^2}\right)$$

$$3.23$$

$$f(y,t,\tau) = \frac{1}{(2\pi\sigma_{1y}^2)^{\frac{1}{2}}} \exp\left(-\frac{(y-m_{1y})^2}{2\sigma_{1y}^2}\right)$$

If it is assumed that :

$$\beta_x = \beta_y = \beta \quad ; \quad \sigma_{ox}^2 = \sigma_{oy}^2 = \sigma_o^2 \qquad \text{and hence}$$

$$3.24$$

$$R_{ox}(\tau) = R_{oy}(\tau) = R_o(\tau) \quad ; \quad \sigma_{1x}^2 = \sigma_{1y}^2 = \sigma_1^2$$

Equation 3.22. becomes :

$$\mu(x,y,t) = \int_0^t \frac{q(\tau)}{2\pi\sigma_1^2} \exp\left(-\frac{(x-m_{1x})^2 + (y-m_{1y})^2}{2\sigma_1^2}\right) d\tau \qquad 3.25$$

3.4.2 CROSSCORRELATION $\Phi(x_1,y_1,x_2,y_2,t,\tau)$

The concentration crosscorrelation between two points (x_1,y_1) and (x_2,y_2) is defined as :

$$\Phi(x_1,y_1,x_2,y_2,t,\tau) = E\{C(x_1,y_1,t)\ C(x_2,y_2,t+\tau)\} \qquad 3.26$$

If the tracer source function Q(t) is time-stationary we may substitute Equation 3.13 :

$$E\left\{\int_{-\infty}^{t+\tau}\int_{-\infty}^{t} Q(\tau_1)Q(\tau_2)\ \delta\left[W_x(t,\tau_1)-x_1\right]\ \delta\left[W_x(t+\tau,\tau_2)-x_2\right]\ \delta\left[W_y(t,\tau_1)-y_1\right]\ \delta\left[W_y(t+\tau,\tau_2)-y_2\right]\ d\tau_1 d\tau_2\right\} \tag{3.27}$$

$$= \int_{-\infty}^{t+\tau}\int_{-\infty}^{t} E\{Q(\tau_1)Q(\tau_2)\}\ E\left\{\delta\left[W_x(t,\tau_1)-x_1\right]\ \delta\left[W_x(t+\tau,\tau_2)-x_2\right]\ \delta\left[W_y(t,\tau_1)-y_1\right]\ \delta\left[W_y(t+\tau,\tau_2)-y_2\right]\right\}\ d\tau_1 d\tau_2$$

The above equation makes use of the fact that the source and the flow process are independent.

Taking the Expected Values yields :

$$\Phi(x_1,y_1,x_2,y_2,t,\tau) = \int_{-\infty}^{t+\tau}\int_{-\infty}^{t} R_Q(|\tau_2-\tau_1|) \tag{3.28}$$

$$\int_{-\infty}^{\infty}\int_{-\infty}^{\infty} \delta\{w_x(t,\tau_1)-x_1\}\ \delta\{w_x(t+\tau,\tau_2)-x_2\}\ f(w_{x1},w_{x2})\ dw_{x1}\ dw_{x2}$$

$$\int_{-\infty}^{\infty}\int_{-\infty}^{\infty} \delta\{w_y(t,\tau_1)-y_1\}\ \delta\{w_y(t+\tau,\tau_2)-y_2\}\ f(w_{y1},w_{y2})dw_{y1}dw_{y2}d\tau_1 d\tau_2$$

where,

$R(|\tau_2-\tau_1|)$ = Autocorrelation of tracer source Q(t).

$f(w_{x1},w_{x2})$ = Joint probability density function for the pair of Normal random variables $W_x(t,\tau_1)$ and $W_x(t+\tau,\tau_2)$

$f(w_{y1},w_{y2})$ = Joint probability density function for the pair of Normal random variables $W_y(t,\tau_1)$ and $W_y(t+\tau,\tau_2)$.

The above density functions are Normal themselves. (13)

Writing

$$m_{1x,1} = m_{1x}(t,\tau_1) \qquad ; \quad m_{1y,1} = m_{1y}(t,\tau_1)$$

3.29

$$\sigma_{1x,1} = \sigma_{1x}(t,\tau_1) \quad ; \quad \sigma_{1y,1} = \sigma_{1y}(t,\tau_1)$$

$$\sigma_{1x,2} = \sigma_{1x}(t+\tau,\tau_2) \quad ; \quad \sigma_{1y,2} = \sigma_{1y}(t+\tau,\tau_2)$$

$$r_x(t,\tau_1;t+\tau,\tau_2) = \frac{\rho(t,\tau_1;t+\tau,\tau_2)}{\sigma_{1x,1}\sigma_{1x,2}} \quad ; \qquad 3.29$$

$$r_y(t,\tau_1;t+\tau,\tau_2) = \frac{\rho(t,\tau_1;t+\tau,\tau_2)}{\sigma_{1y,1}\sigma_{1y,2}}$$

and carrying out the integrations with respect to w_{x1}, w_{x2}, w_{y1}, and w_{y2} we obtain :

$$\Phi(x_1,y_1,x_2,y_2:\tau) =$$

$$\int_{-\infty}^{t+\tau}\int_{-\infty}^{t} \frac{R_Q(|\tau_2-\tau_1|)}{(2\pi)^2\sigma_{1x,1}\,\sigma_{1x,2}\,\sigma_{1y,1}\,\sigma_{1y,2}}$$

$$\frac{1}{(1-r_x^2(t,\tau_1;t+\tau,\tau_2))^{\frac{1}{2}}\,(1-r_y^2(t,\tau_1;t+\tau,\tau_2))^{\frac{1}{2}}}$$

$$\exp\{-\frac{1}{1-r_x^2(t,\tau_1;t+\tau,\tau_2)}\left(\frac{(x_1-m_{1x,1})^2}{\sigma_{1x,1}^2}\right.$$

$$\left.-\frac{2r_x(t,\tau_1;t+\tau,\tau_2)(x_1-m_{1x,1})(x_2-m_{1x,2})}{\sigma_{1x,1}\,\sigma_{1x,2}}+\frac{(x_2-m_{1x,2})^2}{\sigma_{1x,2}^2}\right)\}$$

$$\exp\{-\frac{1}{1-r_y^2(t,\tau_1;t+\tau,\tau_2)}\left(\frac{(y_1-m_{1y,1})^2}{\sigma_{1y,1}^2}\right.$$

$$\left.-\frac{2r_y(t,\tau_1;t+\tau,\tau_2)(y_1-m_{1y,1})(y_2-m_{1y,2})}{\sigma_{1y,1}\,\sigma_{1y,2}}+\frac{(y_2-m_{1y,2})^2}{\sigma_{1y,2}^2}\right)\}d\tau_1 d\tau_2$$

3.30

If both the tracer source function Q(t) and the velocity process are time-stationary the concentration crosscorrelation must likewise be time-stationary. In order to eliminate t from the above expression we make the following transformation of variables :

$$\begin{aligned} t - \tau_1 &= \tau - \theta_1 \\ t + \tau - \tau_2 &= \tau - \theta_2 \end{aligned} \tag{3.31}$$

It is interesting to note that the mean and variance of the random processes $W(t,\tau_1)$ and $W(t+\tau,\tau_2)$ depend only on the size of the time interval on which they are defined. Hence we may write :

$$\begin{aligned} m_{1x}(\tau,\theta_1) &= m_{1x}(t,\tau_1) \quad ; \quad m_{1y}(\tau,\theta_1) = m_{1y}(t,\tau_1) \\ m_{1x}(\tau,\theta_2) &= m_{1x}(t+\tau,\tau_2) \quad ; \quad m_{1y}(\tau,\theta_2) = m_{1y}(t+\tau,\tau_2) \\ \sigma^2_{1x}(\tau,\theta_1) &= \sigma^2_{1x}(t,\tau_1) \quad ; \quad \sigma^2_{1y}(\tau,\theta_1) = \sigma^2_{1y}(t,\tau_1) \\ \sigma^2_{1x}(\tau,\theta_2) &= \sigma^2_{1x}(t+\tau,\tau_2) \quad ; \quad \sigma^2_{1y}(\tau,\theta_2) = \sigma^2_{1y}(t+\tau,\tau_2) \end{aligned} \tag{3.32}$$

The covariance $r(t,\tau_1;t+\tau,\tau_2)$ however, depends not only on the size of the time intervals $(t-\tau_1)$ and $(t+\tau-\tau_2)$, but more importantly on the amount of overlap of these intervals. Hence, since the amount of overlap is not preserved by the transformation of variables (Equation 3.31),

$$r(\tau,\theta_1;\tau,\theta_2) \neq r(t,\tau_1;t+\tau,\tau_2)$$

This may best be illustrated by considering the case when $\theta_1 = \theta_2$. The time intervals for $W(\tau,\theta_1)$ and $W(\tau,\theta_2)$ are then identical resulting in a covariance of one. This situation is clearly impossible for $W(t,\tau_1)$ and $W(t+\tau,\tau_2)$ for any positive value of τ. Expressions for the covariance between $W(t,\tau_1)$ and $W(t+\tau,\tau_2)$ must therefore be derived before the new variables θ_1, θ_2, may be substituted.

Consider $\rho(t,\tau_1;t+\tau,\tau_2) = E\{W(t,\tau_1)W(t+\tau,\tau_2)\} - m_1(t,\tau_1)m_1(t+\tau,\tau_2)$

Noting that at all times

$\tau > 0 \quad ; \quad t \geq \tau_1 \quad ; \quad t+\tau \geq \tau_2$

we distinguish three cases :

<u>case A</u> $\quad t + \tau > t > \tau_2 \geq \tau_1$

<u>case B</u> $\quad t + \tau > t > \tau_1 \geq \tau_2$

<u>case C</u> $\quad t + \tau > \tau_2 \geq t > \tau_1$

From Equations 3.11 and 3.3 it follows that :

$$\rho(t,\tau_1;t+\tau,\tau_2) = \int_{\tau_2}^{t+\tau}\int_{\tau_1}^{t} E\{U(\theta')U(\theta'')\}\, d\theta'\, d\theta''$$

$$= \int_{\tau_2}^{t+\tau}\int_{\tau_1}^{t} \sigma_o^2 \exp\{-\beta(|\theta'-\theta''|)\, d\theta'\, d\theta'' \qquad 3.33$$

Performing the integration for each case separately (Appendix 4) yields :

<u>case A</u>

$$\frac{\sigma_o^2}{\beta^2}\Big(-\exp\{-\beta\tau\} + \exp\{-\beta(t+\tau-\tau_1)\} + 2\beta(t-\tau_2) - \exp\{-\beta(\tau_2-\tau_1)\} + \exp\{-\beta(t-\tau_2)\}\Big)$$

<u>case B</u>

$$\frac{\sigma_o^2}{\beta^2}\Big(-\exp\{-\beta\tau\} + \exp\{-\beta(t+\tau-\tau_1)\} + 2\beta(t-\tau_1) + \exp\{-\beta(t-\tau_2)\} - \exp\{-\beta(\tau_1-\tau_2)\}\Big)$$

<u>case C</u>

$$\frac{\sigma_o^2}{\beta^2}\Big(-\exp\{-\beta\tau\} + \exp\{-\beta(t+\tau-\tau_1)\} + \exp\{-\beta(\tau_2-t)\} - \exp\{-\beta(\tau_2-\tau_1)\}\Big) \qquad 3.34$$

Substituting the new variables (Equations 3.31) in the above expressions yields :

case A $\quad 0 > \theta_2 \geqslant \theta_1 - \tau$

$$\frac{\sigma_o^2}{\beta^2}\Big[-\exp\{-\beta\tau\} + \exp\{-\beta(2\tau-\theta_1)\} - 2\beta\theta_2$$
$$- \exp\{-\beta(\tau-\theta_1+\theta_2) \quad + \exp\{\beta\theta_2\}\Big]$$

case B $\quad 0 > \theta_1 - \tau \geqslant \theta_2$

$$\frac{\sigma_o^2}{\beta^2}\Big[-\exp\{-\beta\tau\} + \exp\{-\beta(2\tau-\theta_1)\}- 2\beta(\tau-\theta_1)$$
$$- \exp\{-\beta(\theta_1-\theta_2-\tau)\}+ \exp\{\beta\theta_2\}\Big]$$

case C $\quad \theta_2 \geqslant 0$

$$\frac{\sigma_o^2}{\beta^2}\Big[-\exp\{-\beta\tau\} + \exp\{-\beta(2\tau-\theta_1)\} - \exp\{-\beta(\tau-\theta_1+\theta_2)\}$$
$$+ \exp\{-\beta\theta_2)\}\Big] \tag{3.35}$$

Transforming the limits of integration we note that

$$\begin{aligned} \text{when} \quad \tau_1 &= -\infty \;, & \theta_1 &= -\infty \\ \tau_2 &= -\infty \;, & \theta_2 &= -\infty \\ \tau_1 &= t \;, & \theta_1 &= \tau \\ \tau_2 &= t+\tau, & \theta_2 &= \tau \end{aligned} \tag{3.36}$$

and Equation 3.30 becomes :

$$\Phi(x_1,y_1,x_2,y_2:\tau) = \int_{-\infty}^{\tau}\int_{-\infty}^{\tau} R_Q(|\tau-\theta_1+\theta_2|)$$
$$f(x_1,x_2,\tau,\theta_1;\tau,\theta_2)\; f(y_1,y_2,\tau,\theta_1;\tau,\theta_2)\; d\theta_1\; d\theta_2 \tag{3.37}$$

where,

$f(x_1,x_2,\tau,\theta_1;\tau,\theta_2)$ and $f(y_1,y_2,\tau,\theta_1;\tau,\theta_2)$ are joint Normal density functions of $\{W_x(\tau,\theta_1),W_x(\tau,\theta_2)\}$ and $\{W_y(\tau,\theta_1),W_y(\tau,\theta_2)\}$ respectively, with

$w_x(\tau,\theta_1) = x_1$, $w_x(\tau,\theta_2) = x_2$, $w_y(\tau,\theta_1) = y_1$ and $w_y(\tau,\theta_2) = y_2$. The appropriate correlation coefficients are given by Equations 3.35

Thus the transformation (Equations 3.31) has eliminated the time, t, from the expression for the crosscorrelation function.

3.5 THE EFFECT OF MOLECULAR DIFFUSION

When the effect of molecular diffusion is included the following stochastic partial differential equation describes the dispersion of tracer material :

$$\frac{\partial C}{\partial t} = - U_x\frac{\partial C}{\partial x} + D\frac{\partial^2 C}{\partial x^2} - U_y\frac{\partial C}{\partial y} + D\frac{\partial^2 C}{\partial y^2} + q(t)\delta(x)\delta(y) \qquad 3.38$$

where,

D = Coefficient of Molecular Diffusion.

The method of obtaining expressions for the mean concentration and crosscorrelation is exactly analogous to that used for the continuous model without molecular diffusion; the details have been included in Appendix 5. The main results are :

Concentration at the point (x,y) and time t :

$$C(x,y,t) = \int_0^t \frac{q(\tau)}{4\pi D(t-\tau)} \exp\left[\frac{-\{x-W_x(t,\tau)\}^2 - \{y-W_y(t,\tau)\}^2}{4D(t-\tau)}\right] d\tau \qquad 3.39$$

Mean concentration at the point (x,y) and time t :

$$\mu(x,y,t) = \int_0^t \frac{q(\tau)}{8\pi D(t-\tau)\ \sigma_{1x}\ \sigma_{1y}}$$

$$\left(\frac{\frac{1}{2}\sigma_{1x}^2 + D(t-\tau)}{2D(t-\tau)\sigma_{1x}^2}\right)^{-\frac{1}{2}} \left(\frac{\frac{1}{2}\sigma_{1y}^2 + D(t-\tau)}{2D(t-\tau)\sigma_{1y}^2}\right)^{-\frac{1}{2}}$$

$$\exp\left(\frac{-1}{2D(t-\tau)\sigma_{1x}^2}\left(\frac{-\frac{1}{4}\{\sigma_{1x}^2 x + D(t-\tau)2m_{1x}\}^2}{\frac{1}{2}\sigma_{1x}^2 + D(t-\tau)} + \frac{1}{2}\sigma_{1x}^2 x^2 + D(t-\tau)m_{1x}^2\right)\right)$$

$$\exp\left(\frac{-1}{2D(t-\tau)\sigma_{1y}^2}\left(\frac{-\frac{1}{4}\{\sigma_{1y}^2 y + D(t-\tau)2m_{1y}\}^2}{\frac{1}{2}\sigma_{1y}^2 + D(t-\tau)} + \frac{1}{2}\sigma_{1y}^2 y^2 + D(t-\tau)m_{1y}^2\right)\right)d\tau \qquad 3.40$$

If it is assumed that

$\beta_x = \beta_y = \beta \ ; \quad \sigma_{ox}^2 = \sigma_{oy}^2 = \sigma_o^2$ and hence

$\sigma_{1x}^2 = \sigma_{1y}^2 = \sigma_1^2 \ ;$

the above equation reduces to :

$$\mu(x,y,t) = \int_0^t \frac{q(\tau)}{4\pi\{\frac{1}{2}\sigma_1^2 + D(t-\tau)\}} \exp\left(\frac{-1}{2D(t-\tau)\sigma_1^2}\left(\frac{-\frac{1}{4}}{\frac{1}{2}\sigma_1^2 + D(t-\tau)}\right.\right.$$

$$\left[\{\sigma_1^2 x + D(t-\tau)2m_{1x}\}^2 + \{\sigma_1^2 y + D(t-\tau)2m_{1y}\}^2\right]$$

$$\left.\left. + \frac{1}{2}\sigma_1^2(x^2 + y^2) + D(t-\tau)(m_{1x}^2 + m_{1y}^2)\right)\right) d\tau \qquad 3.41$$

Crosscorrelation :

Making the same assumptions as in Equation 3.41 and writing :

$$\sigma_{1x,1}^2 = \sigma_{1y,1}^2 = \sigma_{1,1}^2 \ ; \quad \sigma_{1x,2}^2 = \sigma_{1y,2}^2 = \sigma_{1,2}^2 \qquad 3.42$$

and $$r = \frac{\rho(\tau,\theta_1;\tau,\theta_2)}{\sigma_{1,1}\sigma_{1,2}} \quad \text{(see Equations 3.29, 3.32)} \qquad 3.43$$

the expression for the crosscorrelation may be shown to have the following form :

$$\Phi(x_1,y_1,x_2,y_2:\tau) = \int_{-\infty}^{\tau}\int_{-\infty}^{\tau} \frac{R_Q(|\tau-\theta_1+\theta_2|)}{(4\pi D)^2(\tau-\theta_1)(\tau-\theta_2)\{2\pi\sigma_{1,1}\sigma_{1,2}(1-r^2)^{\frac{1}{2}}\}^2}$$

$$\pi^2\{\frac{1}{\alpha_1}+\frac{1}{\beta_1}\}^{-1}\left(\frac{1}{\alpha_2}+\frac{1}{\beta_2}-\{\frac{1}{\alpha_1}+\frac{1}{\beta_1}\}^{-1}\frac{r^2}{(1-r^2)^2\gamma^2}\right)^{-1}$$

$$\exp-\left(\frac{x_1^2}{\alpha_1}+\frac{x_2^2}{\alpha_2}+\frac{m_{1x,1}^2}{\beta_1}+\frac{m_{1x,2}^2}{\beta_2}-\frac{2rm_{1x,1}m_{1x,2}}{(1-r^2)\gamma}-\right.$$

$$\left.\{\frac{1}{\alpha_1}+\frac{1}{\beta_1}\}^{-1}\left(\{\frac{x_1}{\alpha_1}+\frac{m_{1x,1}}{\beta_1}\}^2+\frac{r^2m_{1x,2}^2}{(1-r^2)^2\gamma^2}-\frac{2rm_{1x,2}}{(1-r^2)\gamma}\{\frac{x_1}{\alpha_1}+\frac{m_{1x,1}}{\beta_1}\}\right)\right)$$

$$\exp\left(\left(\frac{1}{\alpha_2}+\frac{1}{\beta_2}-\{\frac{1}{\alpha_1}+\frac{1}{\beta_1}\}^{-1}\frac{r^2}{(1-r^2)^2\gamma^2}\right)^{-1}\left(\frac{x_2}{\alpha_2}-\frac{rm_{1x,1}}{(1-r^2)\gamma}+\frac{m_{1x,2}}{\beta_2}\right.\right.$$

$$\left.\left.+\{\frac{1}{\alpha_1}+\frac{1}{\beta_1}\}^{-1}[\frac{r}{(1-r^2)\gamma}\{\frac{x_1}{\alpha_1}+\frac{m_{1x,1}}{\beta_1}\}-\frac{r^2m_{1x,2}}{(1-r^2)^2\gamma^2}]\right)^2\right)$$

$$\exp-\left(\frac{y_1^2}{\alpha_1}+\frac{y_2^2}{\alpha_2}+\frac{m_{1y,1}^2}{\beta_1}-\frac{m_{1y,2}^2}{\beta_2}-\frac{2rm_{1y,1}m_{1y,2}}{(1-r^2)\gamma}-\{\frac{1}{\alpha_1}+\frac{1}{\beta_1}\}^{-1}\right.$$

$$\left.\left(\{\frac{y_1}{\alpha_1}+\frac{m_{1y,1}}{\beta_1}\}^2+\frac{r^2m_{1y,2}^2}{(1-r^2)^2\gamma^2}-\frac{2rm_{1y,2}}{(1-r^2)\gamma}\{\frac{y_1}{\alpha_1}+\frac{m_{1y,1}}{\beta_1}\}\right)\right)$$

$$\exp\left(\left(\frac{1}{\alpha_2}+\frac{1}{\beta_2}-\{\frac{1}{\alpha_1}+\frac{1}{\beta_1}\}^{-1}\frac{r^2}{(1-r^2)^2\gamma^2}\right)^{-1}\left(\frac{y_2}{\alpha_2}-\frac{rm_{1y,1}}{(1-r^2)\gamma}+\frac{m_{1y,2}}{\beta_2}\right.\right.$$

$$\left.\left.+\{\frac{1}{\alpha_1}+\frac{1}{\beta_1}\}^{-1}[\frac{r}{(1-r^2)\gamma}\{\frac{y_1}{\alpha_1}+\frac{m_{1y,1}}{\beta_1}\}-\frac{r^2m_{1y,2}}{(1-r^2)^2\gamma^2}]\right)^2\right)d\theta_1\,d\theta_2 \qquad 3.44$$

where,

$$\alpha_1 = 4D(\tau-\theta_1) \quad ; \quad \alpha_2 = 4D(\tau-\theta_2)$$

$$\beta_1 = (1-r^2)\sigma_{1,1}^2 \quad ; \quad \beta_2 = (1-r^2)\sigma_{1,2}^2$$

$$\gamma = \sigma_{1,1}\,\sigma_{1,2} \qquad 3.45$$

CHAPTER IV

EXPERIMENTAL

4.1 GENERAL

The experiments were carried out in a narrow, Perspex tank, six inches wide and four feet long, which was provided with an inlet duct (4 inches x 6 inches) at one end. A double weir arrangement at the other end permitted continuous withdrawal from the surface and bottom of the tank. (see photograph on page 34)

A constant-head tank ensured a steady inlet flow rate which was measured with a rotameter and controlled with a one - inch globe valve. The water level in the tank and the outlet flows were controlled by the heights of the two weirs.

4.2 TRACER INJECTION

Tracer material consisting of a water soluble dye solution was injected at a point through a ¼-inch diameter copper tube and its concentration at two points further downstream was continuously monitored. In order to ensure isokinetic injection, the tracer flow rate was measured and the pressure drop across the injection line was kept constant by means of a small constant head tank with overflow circulation. (See Figure 4.1 on page 36). The on-off type of the tracer flow was controlled by means of a shift register circuit (photograph on page 63) operating an 80V DC solenoid valve in the injection line. This circuit was capable of generating precisely and automatically the required pattern of tracer injection.

.3 TRACER DETECTION AND RECORDING

0.2% solution of a watersoluble, green dye was used as :acer material; it was an iron complex of 1-notroso-2-

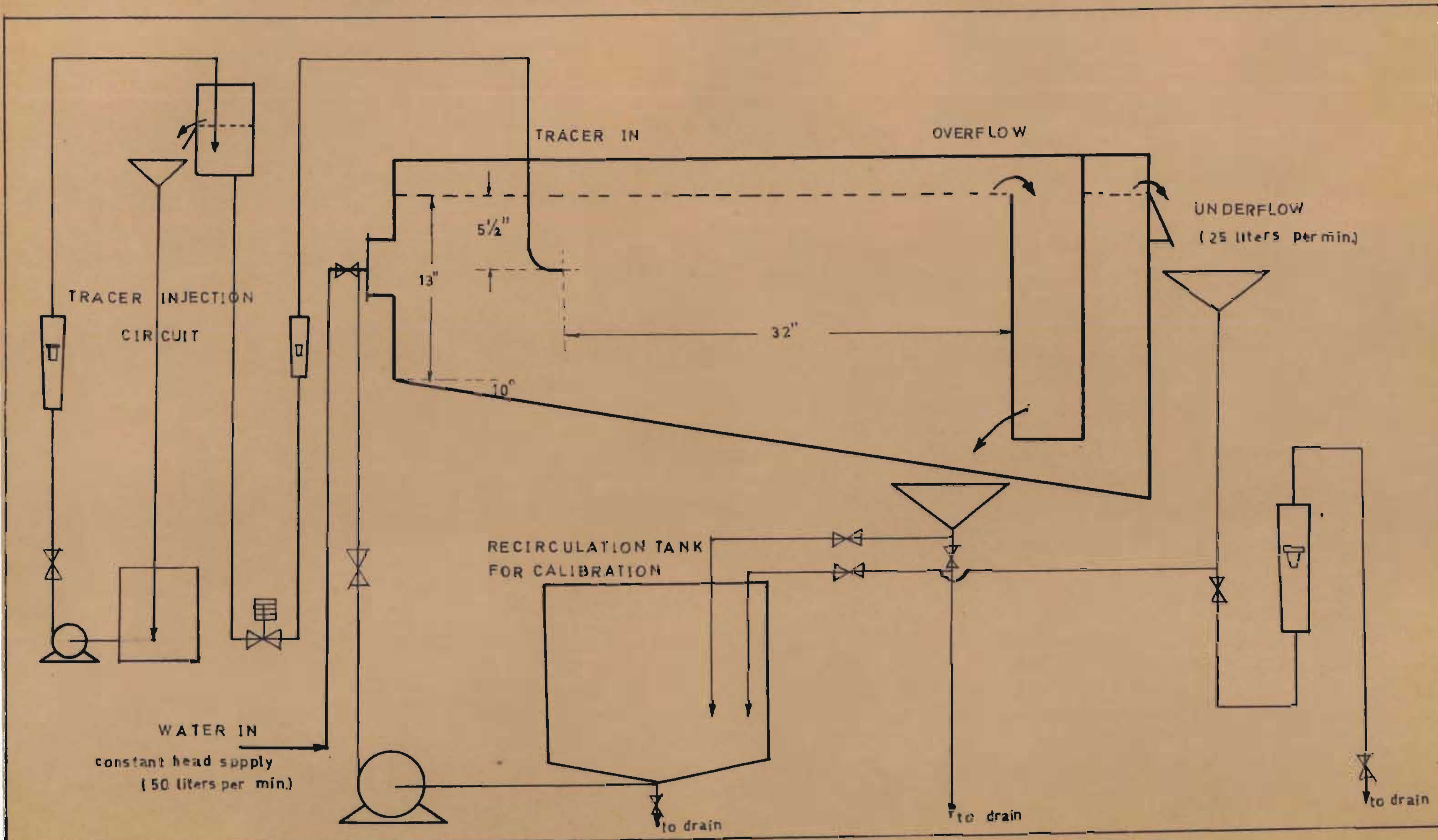
TRACER IN
OVERFLOW
UNDERFLOW
(25 liters per min.)
5½"
13"
32"
10°
TRACER INJECTION
CIRCUIT
RECIRCULATION TANK
FOR CALIBRATION
WATER IN
constant head supply
(50 liters per min.)
to drain
to drain
to drain

FIG. 4·1

naphthol-6-sodium-sulphonate and strongly absorbed light emitted from an incandescent globe. By means of a system of lenses and attenuators a narrow beam (¼ inch) of parallel light was focussed across the width of the tank. On the opposite side a photoelectric cell mounted at the far end of a tube, was positioned such that only the light of the parallel beam reached its photosensitive surface. Two probes were constructed in this way; probe and light source supports were constructed in such a way that the concentration at any point in the tank could be monitored. The photograph on page 38 shows the two probes mounted in position. The output of the photo-cells was suitably off-set, amplified, and frequency modulated before being recorded on magnetic tape. (See Figure 4.2 on page 40) The taperecorders were capable of operating at four different tape speeds and of recording two signals simultaneously.

Speed variations of the tape recorders during recording and playback would destroy the required synchronism as well as the accuracy of the time base of the two signals. For this reason a special timing pulse generator was used to record markers on the second track of each tape for the duration of the run. Each marker consisted of a short burst of a 10 Kc/second signal and for all runs a frequency of 5 markers per second was used. In this way the frequency modulated concentration signal at each monitoring station was recorded and simultaneously subdivided into 0.2 second intervals. Thus, even though speed variations between the two tape recorders may occur,

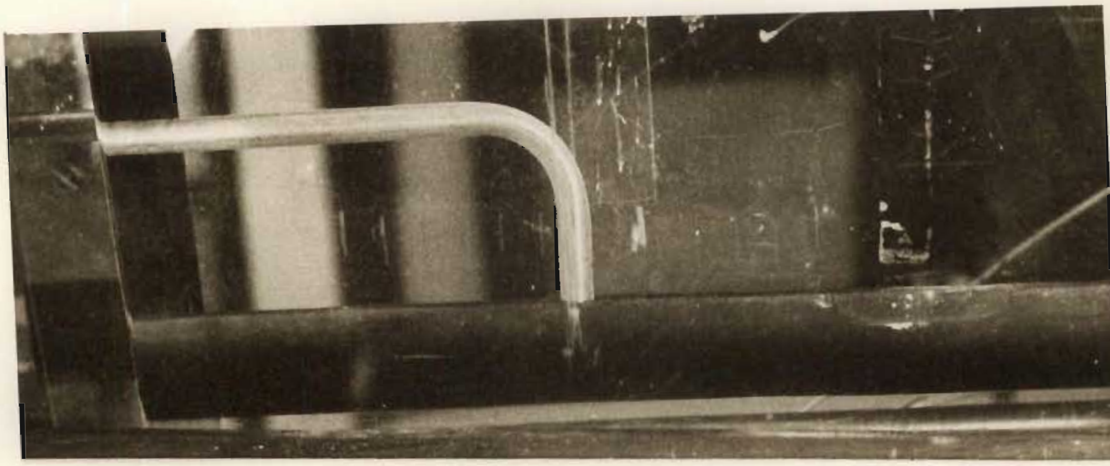

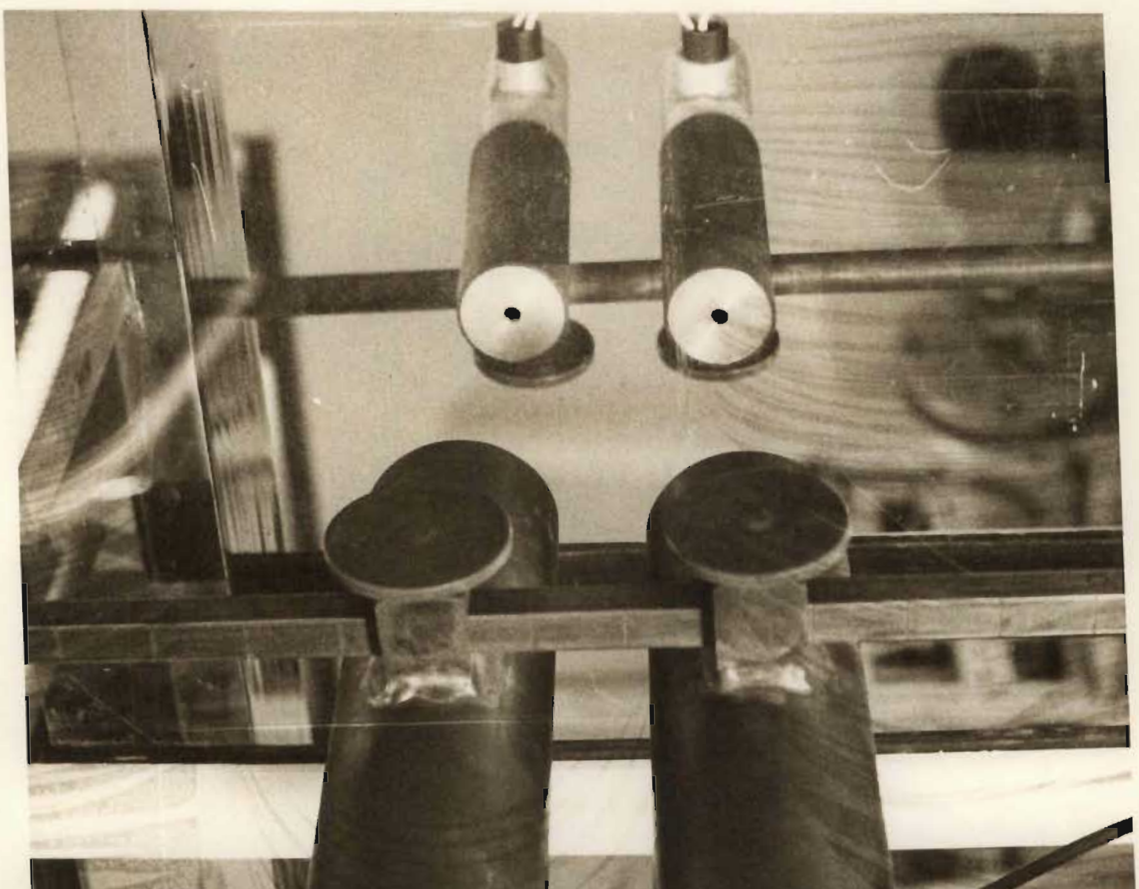

time during the run. Hence the total signal count between e.g. the 50th and 51st marker for each tape is a measure of the average concentration which occured at the corresponding monitoring station in the interval between 9.8 seconds and 10.0 seconds measured from the start of the run.

On playback both the time marker track and signal track were monitored. The counting equipment consisted of two scalers and an output controller. (See Figure 4.2 on page 40). The arrival of the first timing marker causes scaler 1 to start counting the signal track. With the arrival of the second timing marker the input to scaler 1 is blocked and scaler 2, previously re-set to zero, takes over the counting of the signal track. During this second interval the count of scaler 1 is read by the printer controller,which in turn feeds it to an I.B.M. punching machine; scaler 1 is then re-set to zero. During the next time interval the roles of the two scalers are reversed and the count of scaler 2 is read, punched and re-set to zero, whilst scaler 1 is counting the signal track. In this way it was possible to obtain an accurate, digitalised concentration versus time record, punched on computer cards. Details of the equipment used for both recording and playback are given in Appendix 8.

The operation of the counting equipment was slow and in order to obtain maximum time resolution, the signals were recorded at the fastest tape speed ($8\frac{1}{2}$ inches per second) and played back at the slowest speed ($\frac{15}{16}$ inches per second).

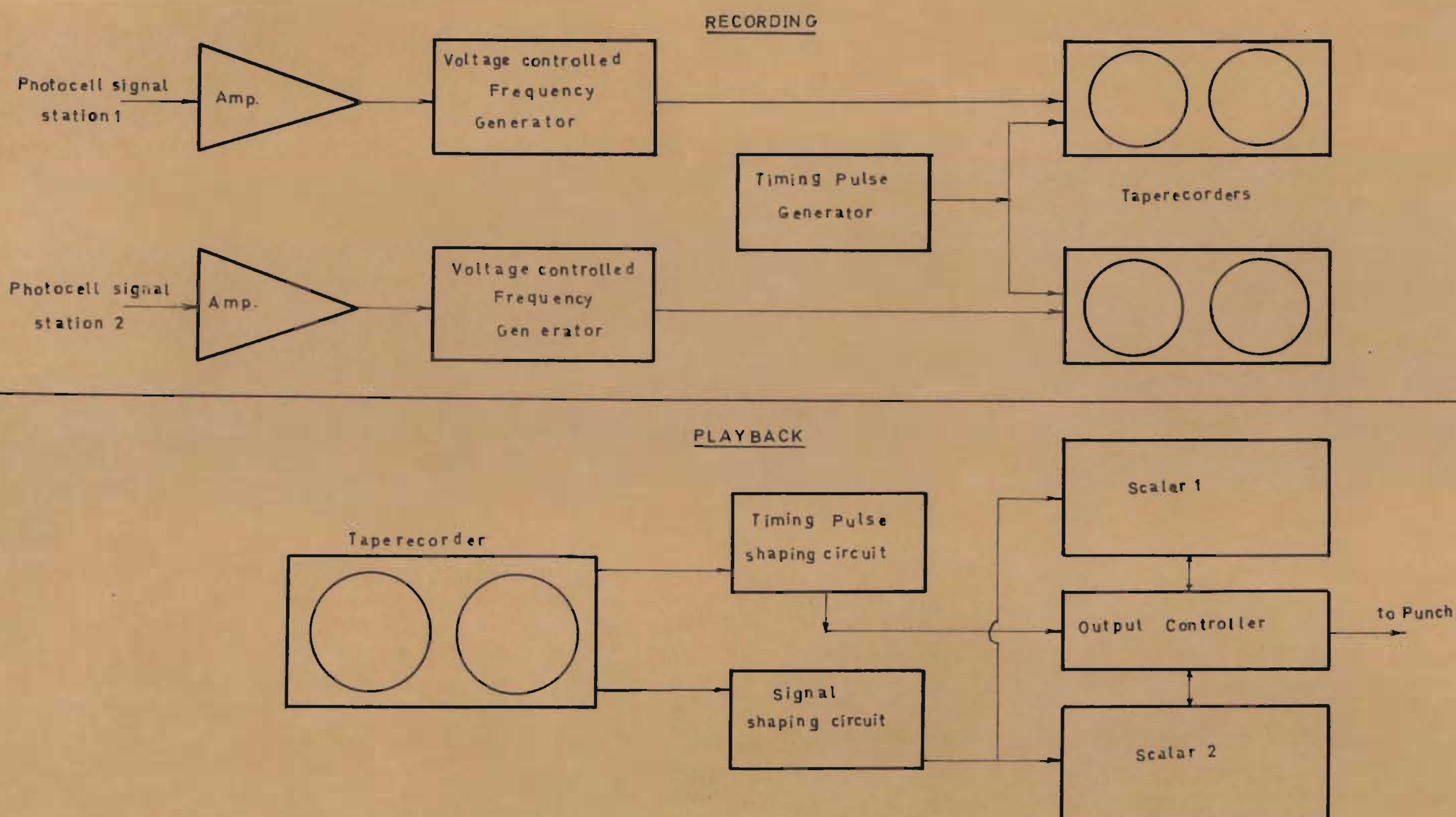
RECORDING
Photocell signal station 1
Amp.
Voltage controlled Frequency Generator
Timing Pulse Generator
Taperecorders
Photocell signal station 2
Amp.
Voltage controlled Frequency Gen erator
PLAYBACK
Taperecorder
Timing Pulse shaping circuit
Signal shaping circuit
Scaler 1
Output Controller
to Punch
Scalar 2

FIG. 4-2

4.4 CALIBRATION OF TRACER DETECTORS

From BEER - LAMBERTS law of light absorption it follows that the output signal due to the presence of tracer depends only on the total amount of tracer in the light beam and not on the tracer concentration profile along the beam. Probes could, therefore, be calibrated in situ by adding known amounts of concentrated tracer to a fixed volume of water and making sure that the tracer was evenly distributed before recording the probe outputs. By isolating the system from the fresh water supply and recirculating through a mixing vessel and pump the tracer was quickly and effectively dispersed. (See Figure 4.1 on page 36). Figure 4.3 shows a calibration curve obtained in this way.

4.5 HOT FILM ANEMOMETER

In order to obtain an independent estimate of the model parameters derived from tracer experiments, the water velocity at a point was measured directly with a Hot-Film probe. It was a standard cylindrical film anemometer probe (Flow Corporation type B-1N) and consisted of a small Pyrex glass rod coated with a thin strip of platinum making electrical contact with needle-supports at each end of the rod. The photograph on page 42 shows details of the sensor together with a millimetre scale. It was operated in the Constant Temperature Mode so that the output was a measure of the current required to keep the resistance and hence the temperature of the probe constant. The essential features of the circuit are shown in Figure A.1 in Appendix 8.

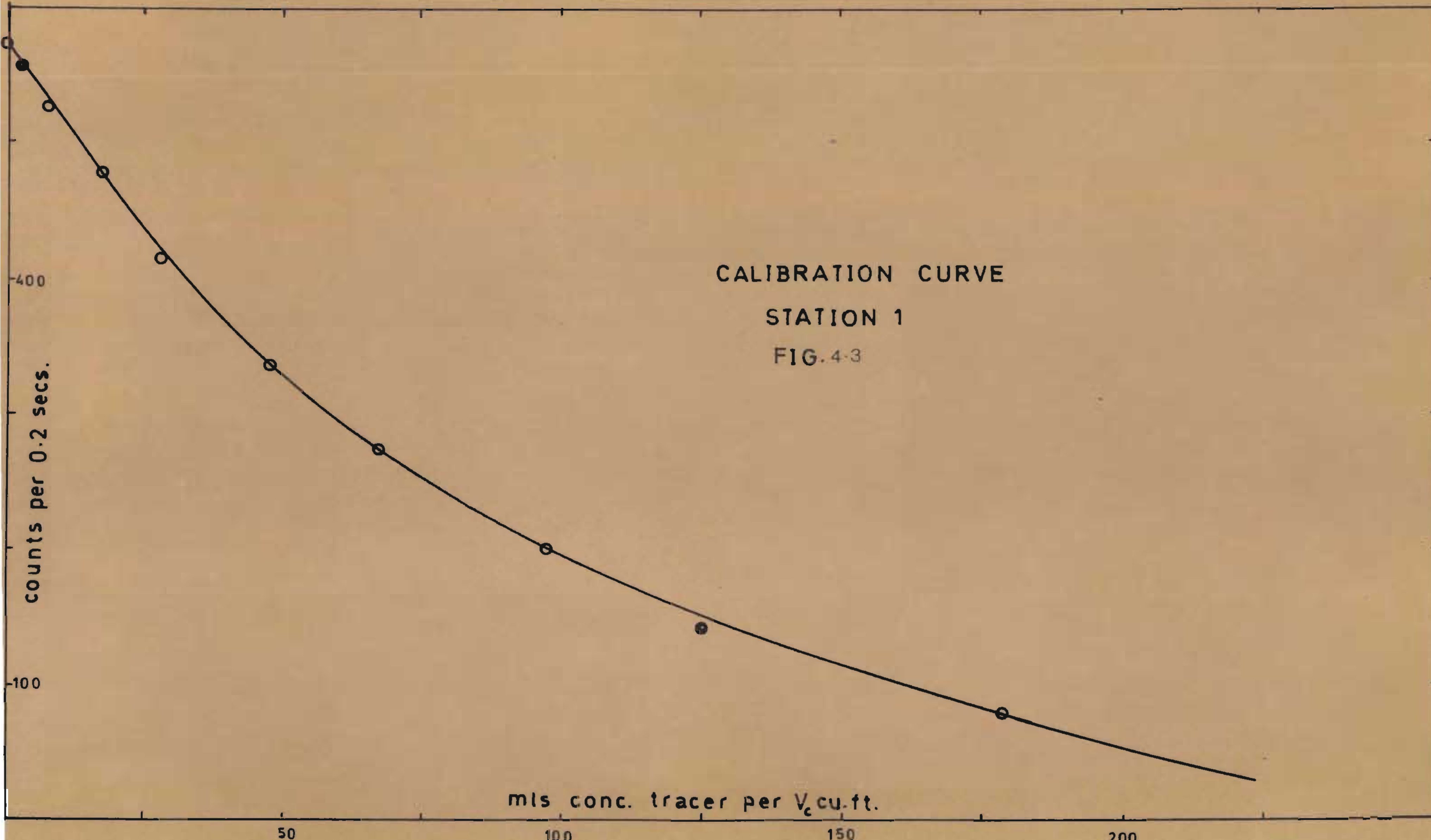

CALIBRATION CURVE
STATION 1
FIG. 4·3

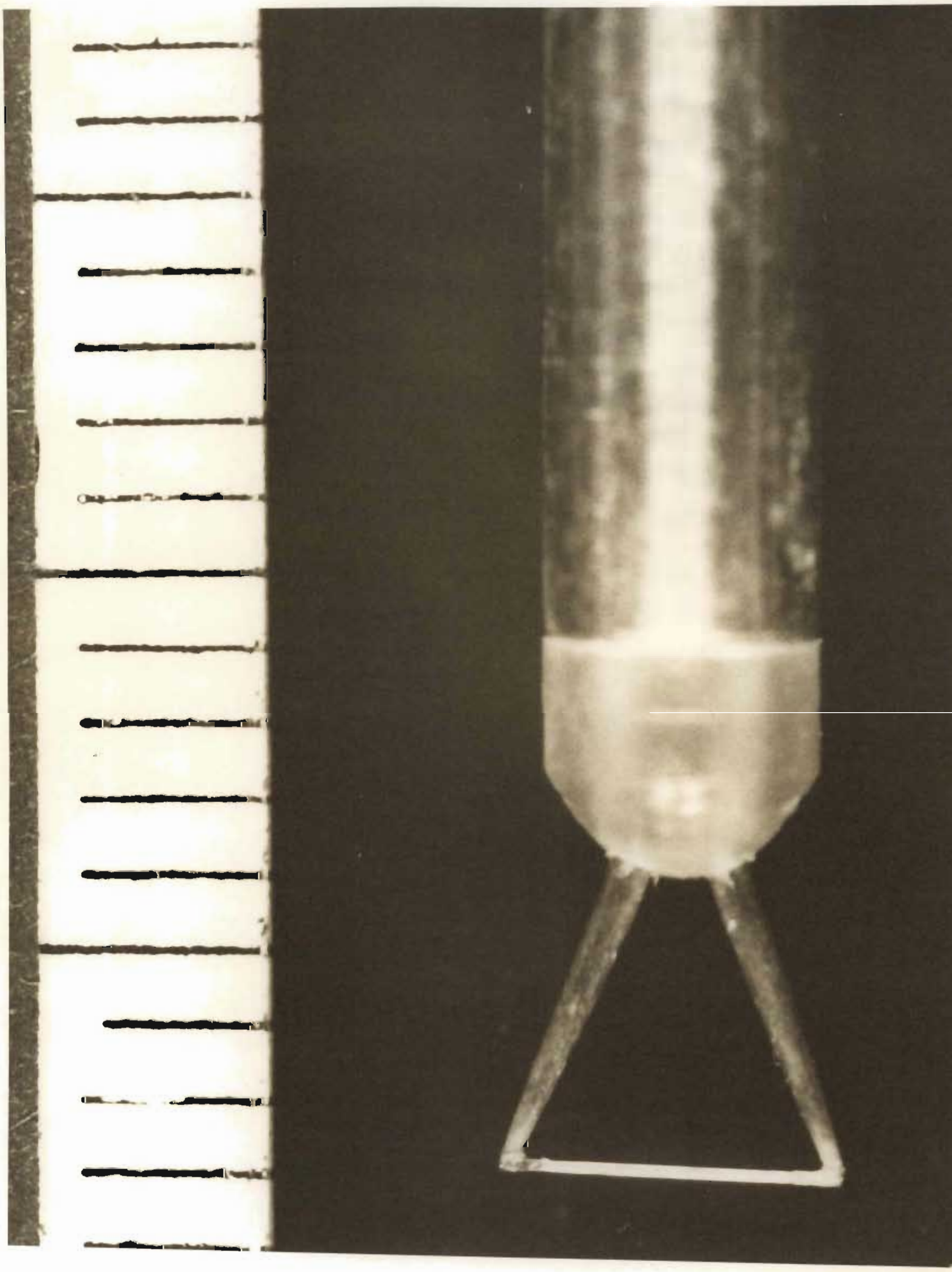

4.5.1 RECORDING AND PLAYBACK

The output from the hot film probe circuit was suitably offset, amplified and frequency modulated before being recorded on a magnetic drum.

The recording drum was 10 inches long and had a diameter of 7 inches. It was coated with magnetic oxide and hence its surface was capable of storing digitalised information. Recording heads similar to those used in conventional magnetic tape recorders were arranged in groups of eight around the drum with a very small clearance from its surface. Each group of recording heads was capable of recording and reading from its associated track an eight binary-number. This corresponded to a resolution of 1 in 256. Each track could accommodate 1024 numbers (bits) and a total of 32 tracks were available.

The input signal is digitalised by means of a 9.5 MHz crystal clock signal to be counted for a period proportional to the incoming voltage. Thus the maximum allowable input voltage (3 volts) corresponded to a count of 256. The state of the binary counters is then written onto the drum by the appropriate group of recording heads in the correct position of the track. The binaries are reset before the cycle is repeated. The minimum cycle time was 100μ seconds. A "bit select" feature allowed one to pinpoint a particular bit on the drum. On playback the number in the appropriate bit is read and transferred to an output register from which it is fed to an I.B.M. punch machine.

4.5.2 CALIBRATION

The conventional way of calibrating Anemometer probes is to experimentally obtain the Anemometer output for one known velocity and use these values to evaluate C_A in the equation :

$$\frac{U}{C_A} = \left(\frac{I^2}{I_o^2} - 1\right)^2$$

where : C_A - constant

I_o - Anemometer Output at zero fluid velocity

I - Anemometer Output

This method was however found to be wholly inaccurate for the velocity range of interest and the probe was calibrated directly from 0 to 0.3 feet per second. For this purpose a trolley running along two parallel rails above a long and narrow calibration tank was constructed. The tank was filled with water and the probe stem was attached to the trolley such that the probe itself was about six inches below the surface. The trolley, fitted with roller bearing wheels, was then pulled along the rails with a piece of string at a constant speed and the time taken for the probe to travel 17 inches through the water was measured with a stopwatch whilst the probe output was recorded. The speed was varied by attaching the string to take-up pulleys of various sizes; these pulleys were fixed on a shaft which was driven by an electric motor through a wormgear and sprockets and chain type reduction. A photograph of this calibration equipment is shown on page 46 , whilst the calibration curve is found on page 47.

The anemometer output at zero fluid velocity was checked before and after the run and the equipment was calibrated immediately afterwards in order to reduce the chance of instrument drift.

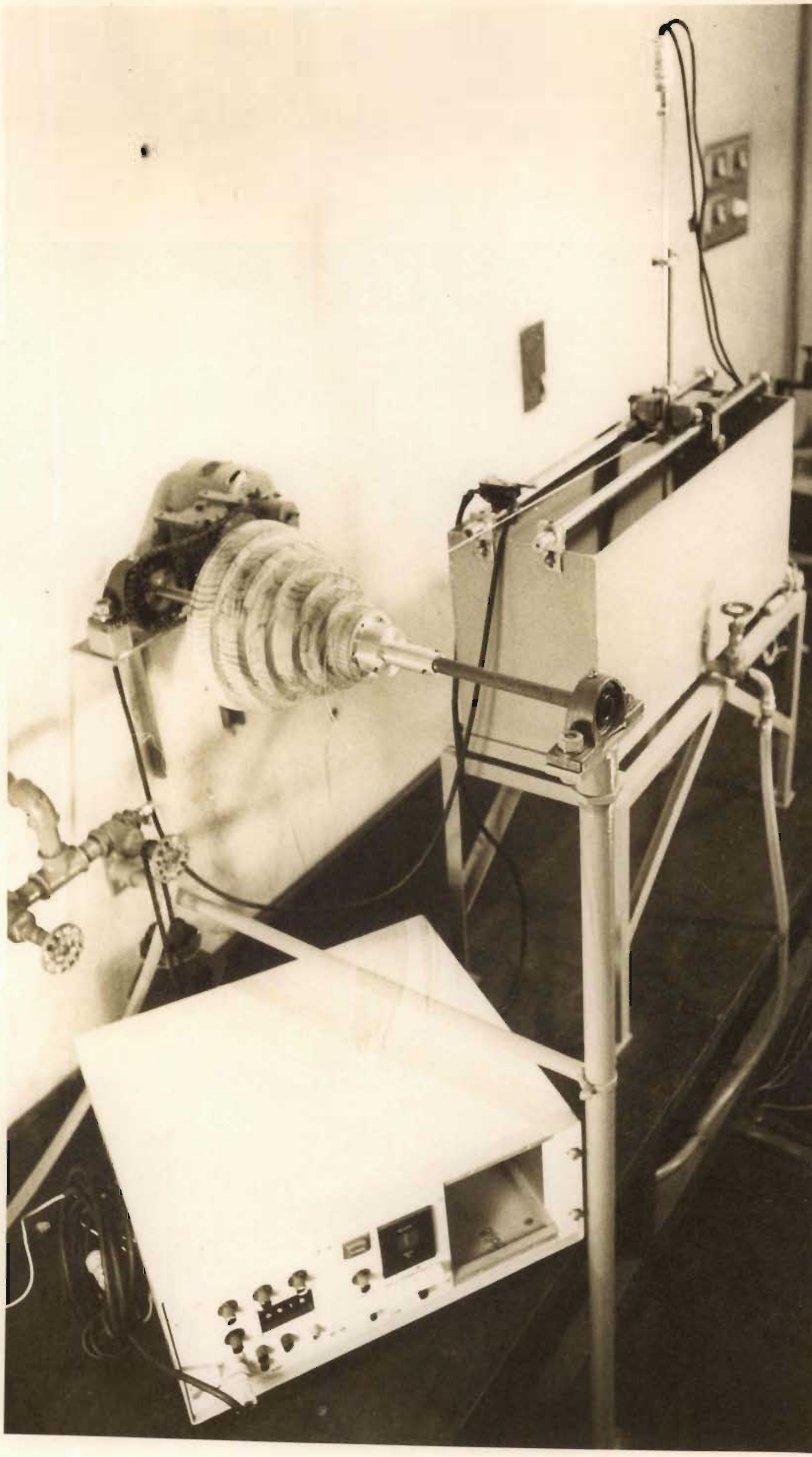

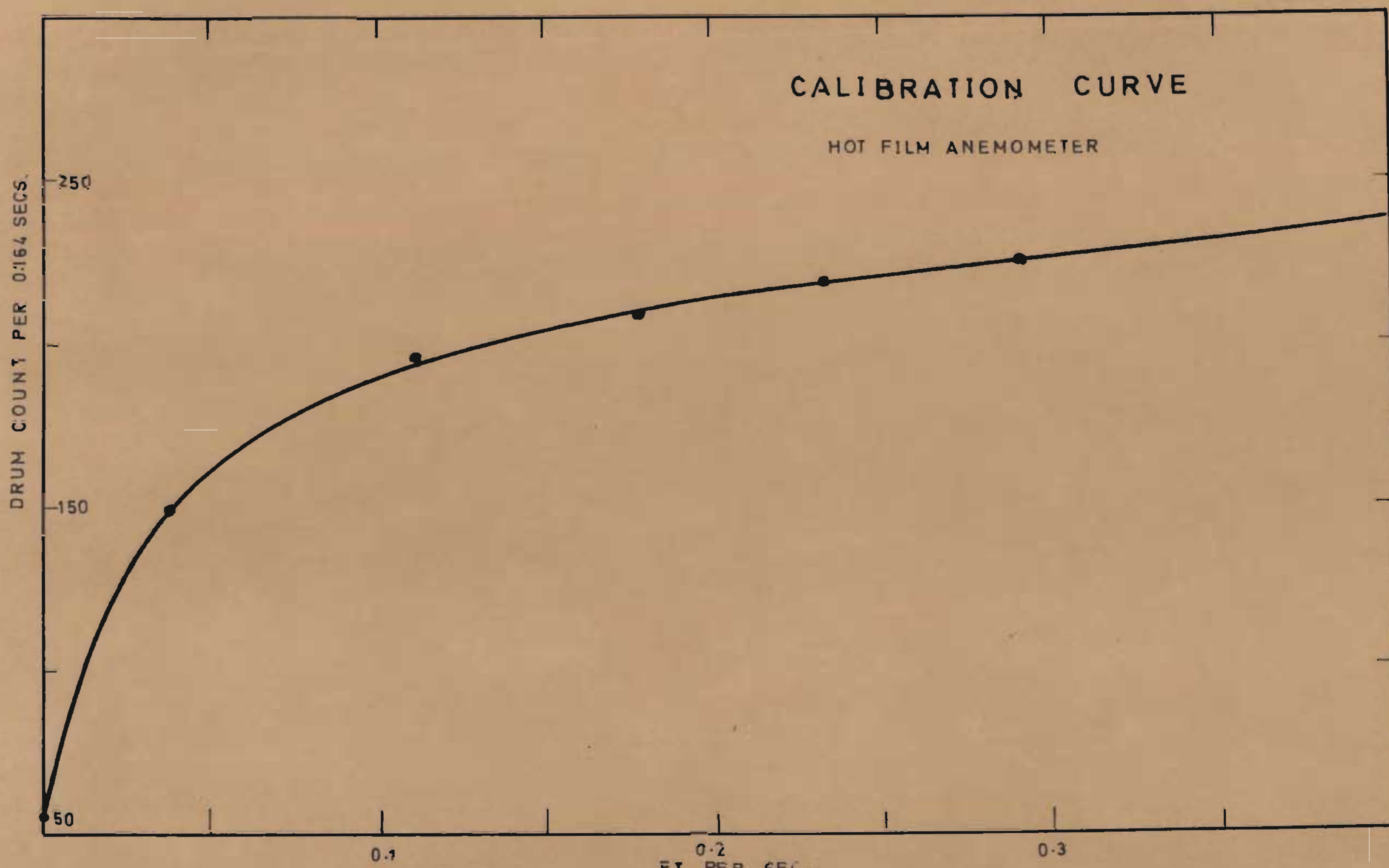
CALIBRATION CURVE
HOT FILM ANEMOMETER
DRUM COUNT PER 0·164 SECS.
250
150
50
0·1
0·2
0·3
FT PER SEC.

FIG. 4·4

CHAPTER V

TESTING OF CONTINUOUS STATE SPACE FLOW MODEL

5.1 GENERAL

The usual procedure adopted when testing a theoretical model of a physical phenomenon is to obtain experimental data of the phenomenon itself or of one closely related to it in order to:

Firstly, assess the extent to which the model is capable of describing the data and

Secondly, interpret the physical significance, if any, of the model parameters.

If the phenomenon has a random character, the model parameters describing it must of necessity be statistical in nature. Hence the experimental procedure must be such that adequate estimates of statistical quantities are obtained. Such experiments are usually not only time-consuming but also costly, as automatic recording and data processing equipment is essential.

In order to limit the experimental effort of this investigation it was decided to explore only a small region of the tank with a fixed point of tracer injection and constant water flow rate.

5.1.1 POSITION OF PROBES

From the basic assumptions of the flow model it is clear that the model cannot hold near the free surface or in the region of the weirs at the far end of the tank. Consequently probe positions were chosen such that these regions, as well as stagnant pockets, were avoided. It necessarily as severe in other physical situations where the flow model may be applied (for example : dispersion in the atmosphere.)

5.1.2 THROUGHPUT AND WITHDRAWAL FLOW RATES

In order to minimise the number of stagnant regions the two outlet weirs were adjusted so that the amounts withdrawn from the surface and bottom of the tank were equal. It was anticipated that the flow model would lend itself to an extension whereby a particle sedimentation process is superimposed on the flow pattern and for this reason a suitable throughput of fifty litres per minute was used.

5.2 EXPERIMENTAL DESIGN CONSIDERATIONS

5.2.1 INTRODUCTION

Two statistical quantities were estimated experimentally :

Firstly, the mean response to a rectangular input pulse of known width at pairs of points, situated downstream from the point of injection; this time-dependent response could be compared directly with predictions of the continuous state model (Chapter III) through equations 3.25 and 3.41.

Secondly, the concentration crosscorrelation between pairs of points for a time stationary tracer source function Q(t); the corresponding model predictions are given by Equations 3.37 and 3.44.

5.2.2. THE MEAN RESPONSE EXPERIMENT

A number of parameters controlling this experiment must be chosen such that adequate estimates of the mean response curves may be made. They are pulse width, pulse frequency, run length and sampling interval.

5.2.2.1 WIDTH OF INPUT PULSE

The importance of tailoring the exciting tracer signal in flow characterisation work has been realised for a considerable time (14, 15). The essential feature of this concept is that the frequency content of the signal exciting the system should adequately span the frequency response curve of the system itself. Figure 5.1 (page 51) illustrates how bandwidth and power of the rectangular pulse vary as a function of pulse width. It is interesting to note that for a given pulse amplitude the bandwidth can only be extended at the expense of power. The pulse width is chosen such that the Power Spectral Density is concentrated over the frequency range of interest.

In the present investigation the system is stochastic in nature and its filtering action will vary randomly. A useful measure of the average filtering action may be obtained by computing a Bode plot from the Mean Response curves. (16)

$$H(w) = \frac{G_o(w)}{G_i(w)}$$

where,

$H(w)$ - Bode plot amplitude

$G_i(w)$ - Frequency Content of normalised first pulse

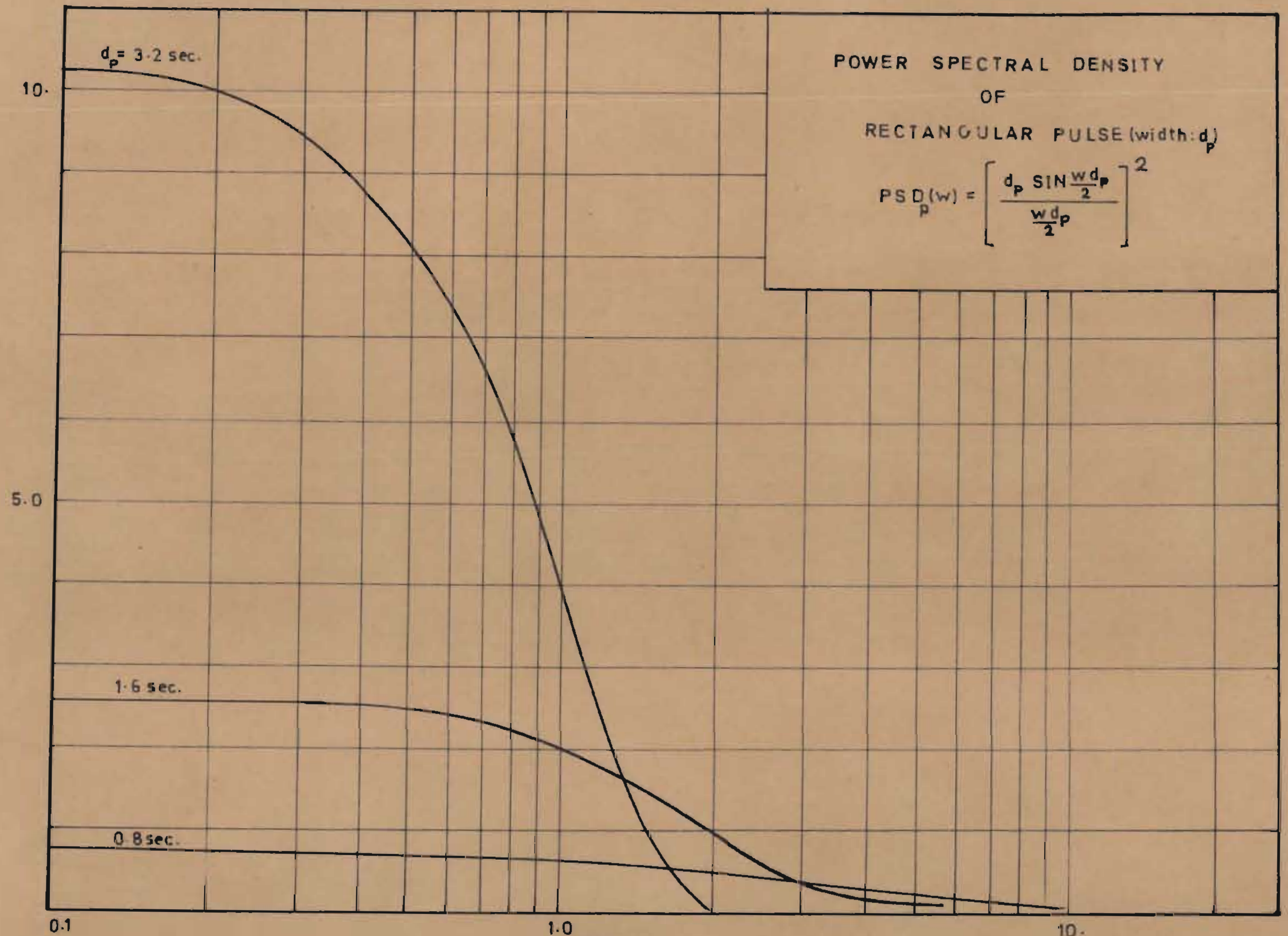
POWER SPECTRAL DENSITY
OF
RECTANGULAR PULSE (width: d_p)
$PSD_p(w) = \left[\frac{d_p \ SIN \frac{w d_p}{2}}{\frac{w d_p}{2}} \right]^2$
d_p = 3·2 sec.
1·6 sec.
0·8 sec.
10·
5·0
0.1
1·0
10·

FIG. 5·1

$G_o(w)$ - Frequency Content of normalised second pulse

$G_i(w)$ and $G_o(w)$ were calculated using the trapezoidal rule of numerical integration on the Fourier Transform of the Mean Response curves. (16)

From the Bode plot (Figure 5.2) it can be seen that frequencies higher than about 1.5 radians per second are completely filtered out by the system and that the frequency range of interest lies between o.2 and 1.5 radians per second.

A second method of obtaining a suitable input pulse width is to examine the Power Spectral Density of the velocity fluctuations themselves. This function may be calculated from the following expression : (17)

$$PSD_{U'}(w) = \frac{2\sigma_o^2 \beta}{\beta^2 + w^2} \qquad 5.1$$

where,

σ_o^2 - variance of velocity fluctuations.

β - flow model parameter

w - frequency in radians per second

Figure 5.3 shows the normalised Power Spectral Density plotted versus frequency; the value for β was obtained from the Hot Film measurements (See Chapter Vl). It can be seen that the frequency at which the normalised PSD has dropped to a value of 0.6 is about 0.4 radians per second.

It is interesting to note the effect of frequency of velocity fluctuations at constant σ_o^2 on the dispersive power of the system. If we focus our attention on a particular fluid particle and note its velocity at two instants of time separated by an interval τ , the

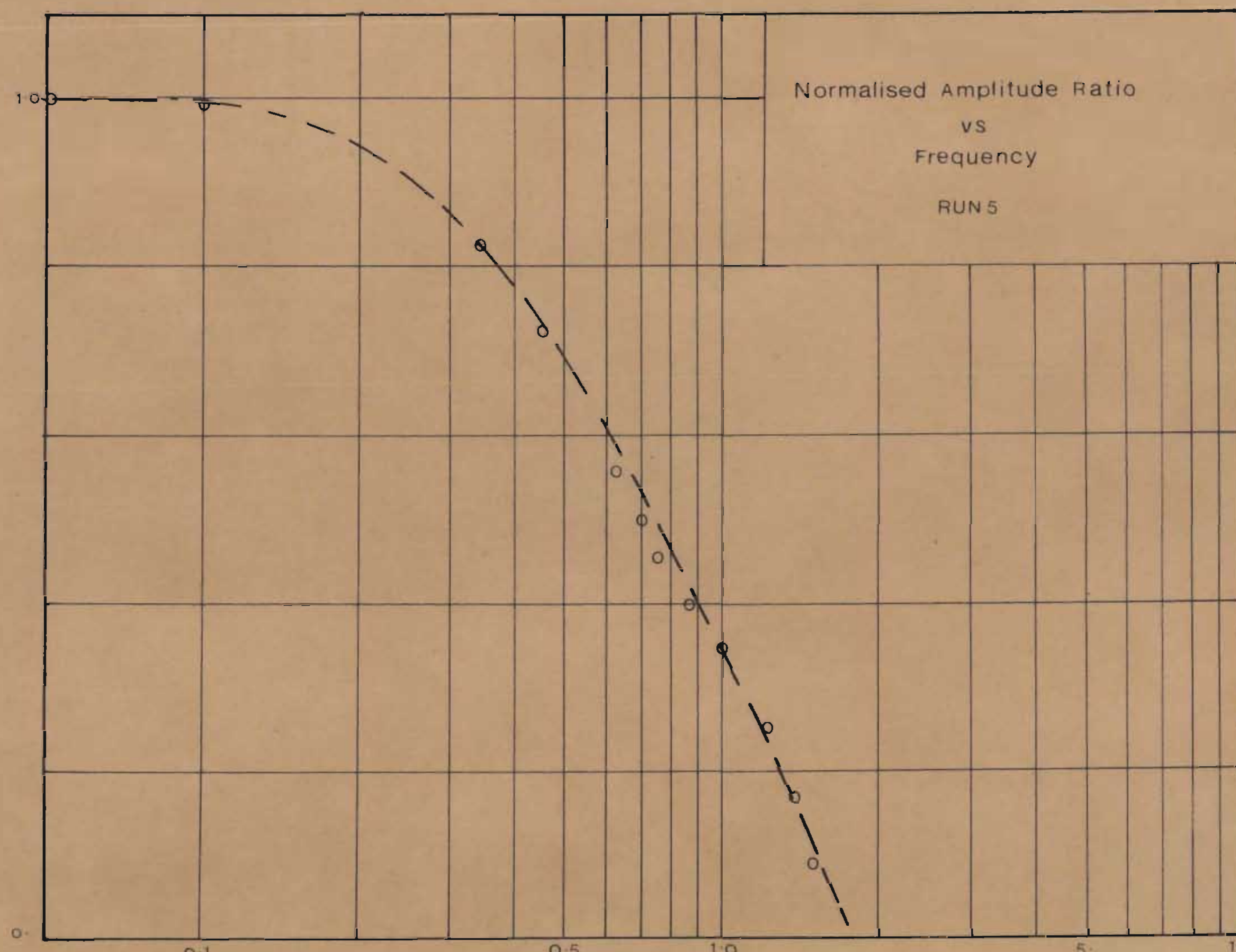
Normalised Amplitude Ratio
vs
Frequency
RUN 5
1·0
0·
0·1
0·5
1·0
5·
10

FIGURE 5·2

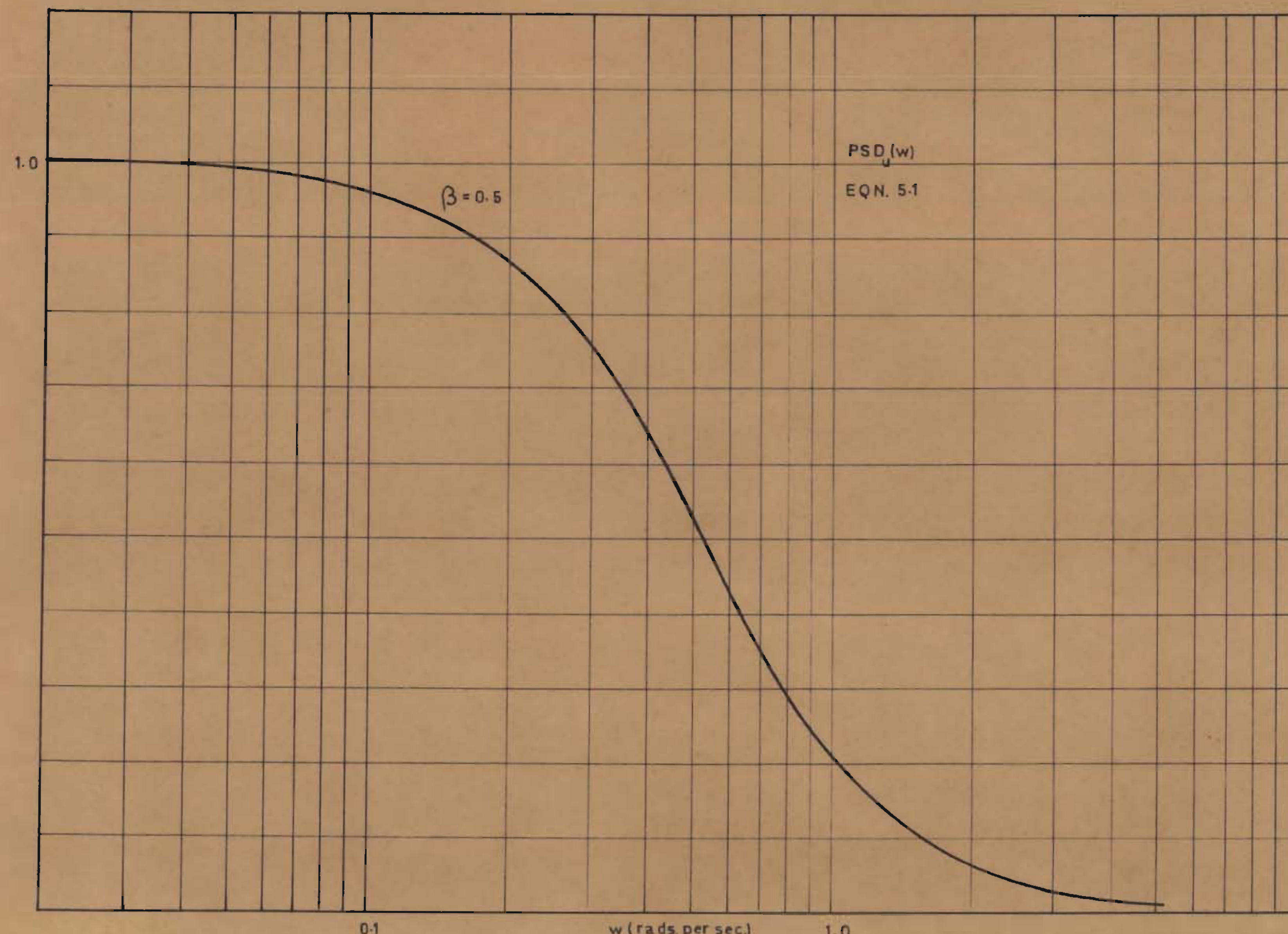

FIG. 5·3

correlation between the two values of velocity, when averaged over a large number of fluid particles, $R(\tau)$, will be higher when the particle's velocity changes slowly than when it undergoes fast fluctuations in velocity. The influence of this effect on dispersion may best be illustrated by considering the case of fully developed turbulent flow. The dispersive power of the system may then be characterised by an Eddy Diffusion Coefficient E: (7)

$$E = \tfrac{1}{2}\sigma_0^2 \int_0^\infty R_N(\tau)\, d\tau \qquad 5.2$$

and the response to a Dirac becomes :

$$\overline{X^2} = 2Et \qquad 5.3$$

From the above it may be seen that if fluid particles undergo slow changes in velocity - i.e. the presence of eddies which persist for a considerable period of time - the $R_N(\tau)$ versus curve will drop off less sharply and hence the value of E and $\overline{X^2}$ will increase.

In the present model a low value for parameter β gives rise to a slow decay of the $R(\tau)$ versus τ curve. (See Equations 3.3).

The variance of the response to a Dirac in this case is given by : (See Equation 3.17)

$$\sigma_1^2(t) = \frac{2\sigma_0^2}{\beta^2}\{\exp(-\beta t) - 1 + \beta t\} \qquad 5.4$$

An examination of Equation 5.4 shows that the value of this variance (σ_1^2) increases with a decrease in β.

In general, the presence of eddies which persist for a considerable period of time have a dominant effect on the dispersive power of the system. This must be borne in mind when deciding on a suitable input signal on the basis of a power spectrum of velocity fluctuations.

A pulse width of 1.6 seconds was used throughout.

5.2.2.2 PULSE FREQUENCY

It is well known that the estimate of a statistical quantity of a stochastic process is improved when the number of realisations is increased. A high pulse frequency is therefore desirable. On the other hand in order to compute a mean pulse from such an ensemble it is important that each realisation can be uniquely identified. Hence the pulse frequency must be low enough to prevent merging of individual pulses as they travel through the system.

Intervals of 9.6, 12.8 and 14.4 seconds between successive input pulses were used. A typical set of successive realisations is shown in Figures 5.4.

5.2.2.3 RUN LENGTH

In order to obtain an accurate estimate of the Mean Response curve, the duration of the run must be long enough to incorporate the effect of all possible realisations of the underlying velocity process.

A practical way of ensuring that even the least frequent realisations have been adequately included is to compute the mean response for a number of run lengths and to note the time at which the shape of the curve no longer changes significantly. Mean response curves were computed for a number of run lengths and are plotted in Figure 5.5. It can be seen that the shortest allowable run length is about twenty minutes.

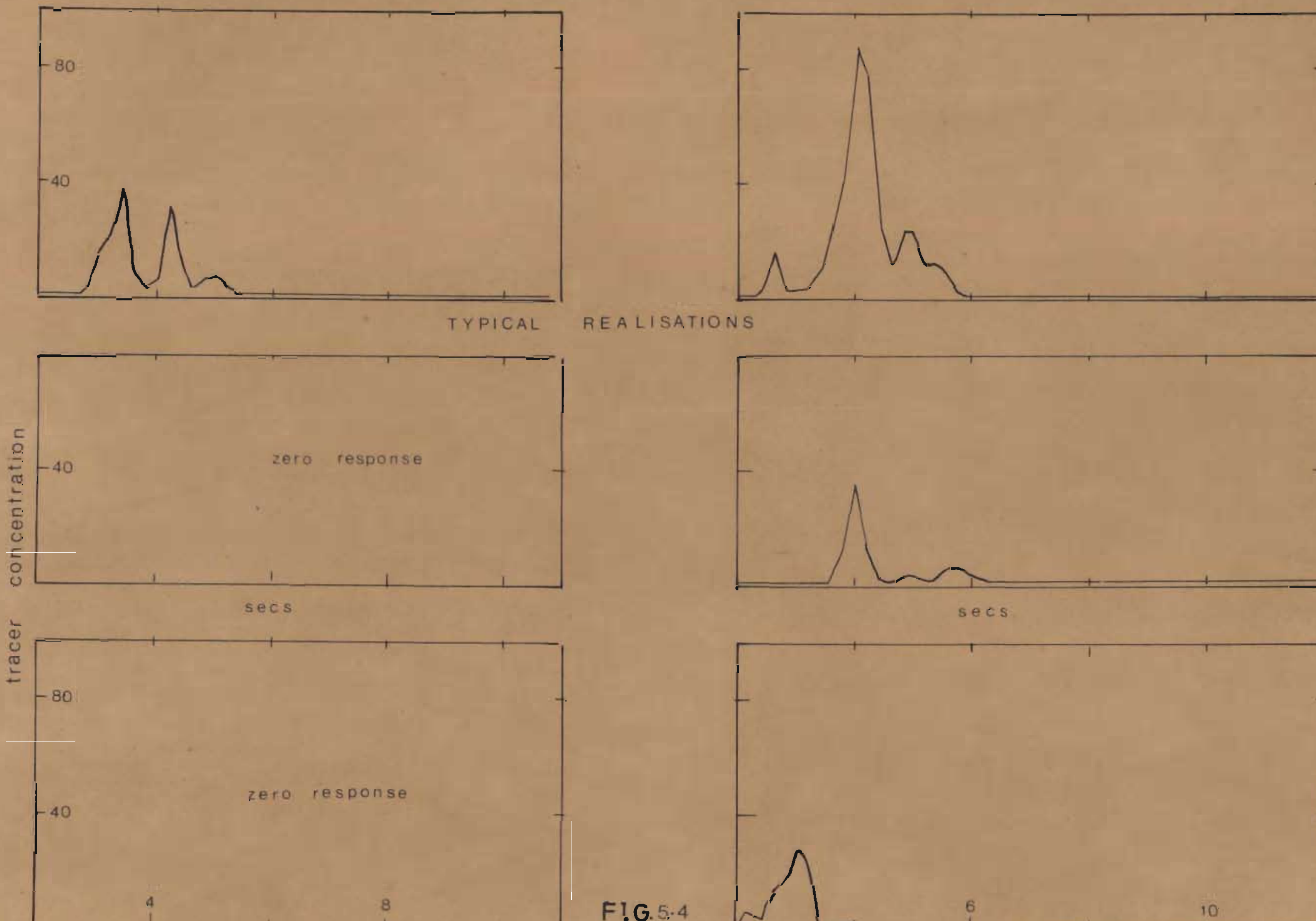

TYPICAL REALISATIONS

FIG. 5.4

MEAN RESPONSE CURVES

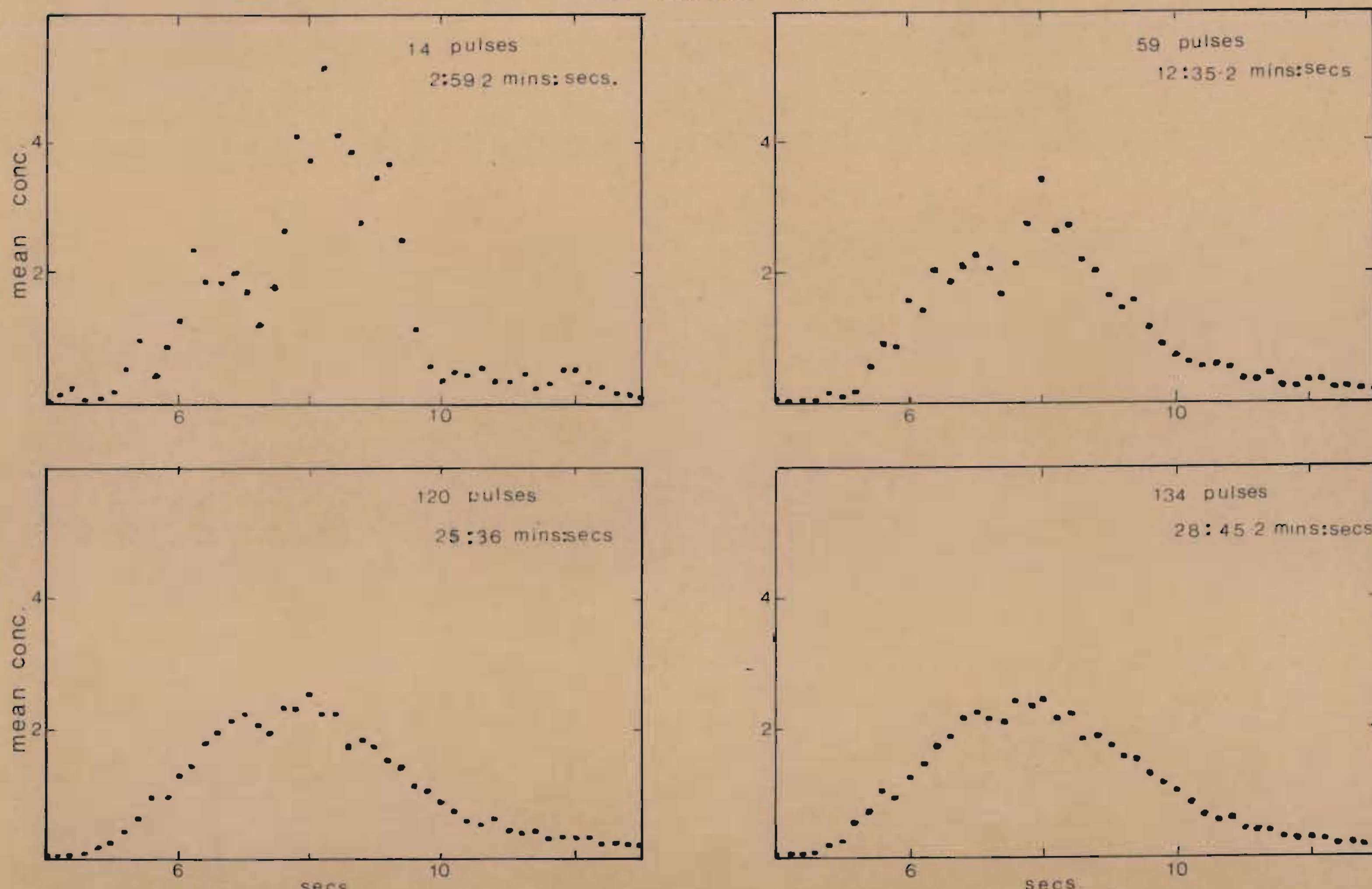

FIG. 5.5

5.2.2.4 SAMPLING INTERVAL

A sampling interval of 0.2 seconds was used throughout; from the Bode plot (Figure 5.2) it can be seen to be sufficiently small for the frequency range of interest. Experimentally it was the smallest interval available and was chosen in order to obtain maximum resolution of the experimental curves.

5.2.2.5 COMPUTATION OF MEAN RESPONSE CURVE

The Mean Response Curve at each monitoring station was calculated by averaging over the ensemble of realisations.

$$\mu_{ex}(\tau) = \frac{1}{N} \sum_{i=0}^{i=N-1} C(iP+\tau) \qquad 5.5$$

Mean concentration values $\mu_{ex}(\tau)$ were computed for values of τ ranging from zero to P at 0.2 seconds intervals.

P = period of input pulse train.

N = total number of pulses.

5.2.3 THE CROSSCORRELATION EXPERIMENT

In order to obtain experimental estimates of the crosscorrelation between the tracer concentration at two points in a time-stationary concentration space a suitable tracer source function Q(t) must be used. The following requirements must be satisfied:

Firstly, it must be a time-stationary function and hence have a constant mean and mean square.

Secondly, its power spectral density must be suitably tailored to the frequency response of the system.

Thirdly, it must have a known autocorrelation, so that the theoretical expression for the crosscorrelation may be computed and compared with experimental estimates.

Fourthly, the function must be conveniently realisable experimentally.

A Pseudo-Random Binary Test Signal was used for $Q(t)$, as it admirably conformed to the above requirements.

5.2.3.1 PSEUDO-RANDOM BINARY TEST SIGNAL (18)

It is a two-valued periodic function having instantaneous amplitude changes only at discrete instants of time separated by a constant interval, the switching time d. A switch need not necessarily take place at every allowable instant and the switching times are generated in such a way as to give the signal several useful properties. If the two allowable amplitudes are zero and q, the mean and mean square taken over any integral number of periods will be $\frac{1}{2}q$ and $\frac{1}{4}q^2$ respectively and are independent of the choice of the first interval. Furthermore, the autocorrelation function $R_Q(\tau)$ has the same period T_p and is defined as follows:

$$R_Q(\tau) = \tfrac{1}{4}q^2\{1 - \frac{N_p+1}{N_p}\frac{|\tau|}{d}\} \quad ; \quad -d \leq \tau \leq d$$

5.6

$$R_Q(\tau) = -\frac{\frac{1}{4}q^2}{N_p} \quad ; \quad d < |\tau| < (N_p-1)d$$

where,

$$N_p = \frac{T_p}{d} = \text{Number of intervals in P.R.B.S.}$$

The Power Spectral Density function of a time-stationary, random signal may be obtained from its autocorrelation as follows : (15)

$$PSD_Q(w_i) = 2\int_0^{\infty} R_Q(\tau)\ \cos(w_i\tau)\ d\tau \qquad 5.7$$

$$= \tfrac{1}{4}q^2\ \frac{(N_p + 1)}{N_p}\ d\ \left(\frac{\sin\{\frac{w_i d}{2}\}}{\frac{w_i d}{2}}\right)^2$$

where,

$$w_i = \frac{2\pi i}{N_p d} \qquad ; \qquad i = 1,2,3,....$$

as N tends to infinity,

$$PSD_Q(w) = \tfrac{1}{4}q^2 d\ \left(\frac{\sin\{\frac{wd}{2}\}}{\frac{wd}{2}}\right)^2 \qquad 5.8$$

Figure 5.6 shows a number of Power Spectral Density functions for various values of d. The similarity between this plot and that of Figure 5.1 is obvious and a decision time of 1.6 seconds was used for reasons discussed in section 5.2.1.1

5.2.3.2 GENERATION OF PSEUDO-RANDOM BINARY SIGNALS

The generation of P.R.B. signals based on the properties of digital filters, is discussed by Briggs et al. (18). A bit shift register circuit is ideally suited to accurately and automatically operate a solenoid valve in the tracer injection line according to a P.R.B. pattern. A photograph of the P.R.B. generator is shown on page 63 . Figure 5.7 shows the relevant logic circuit.

Each register of the circuit may be thought of to contain either 1 or 0. They are connected in series

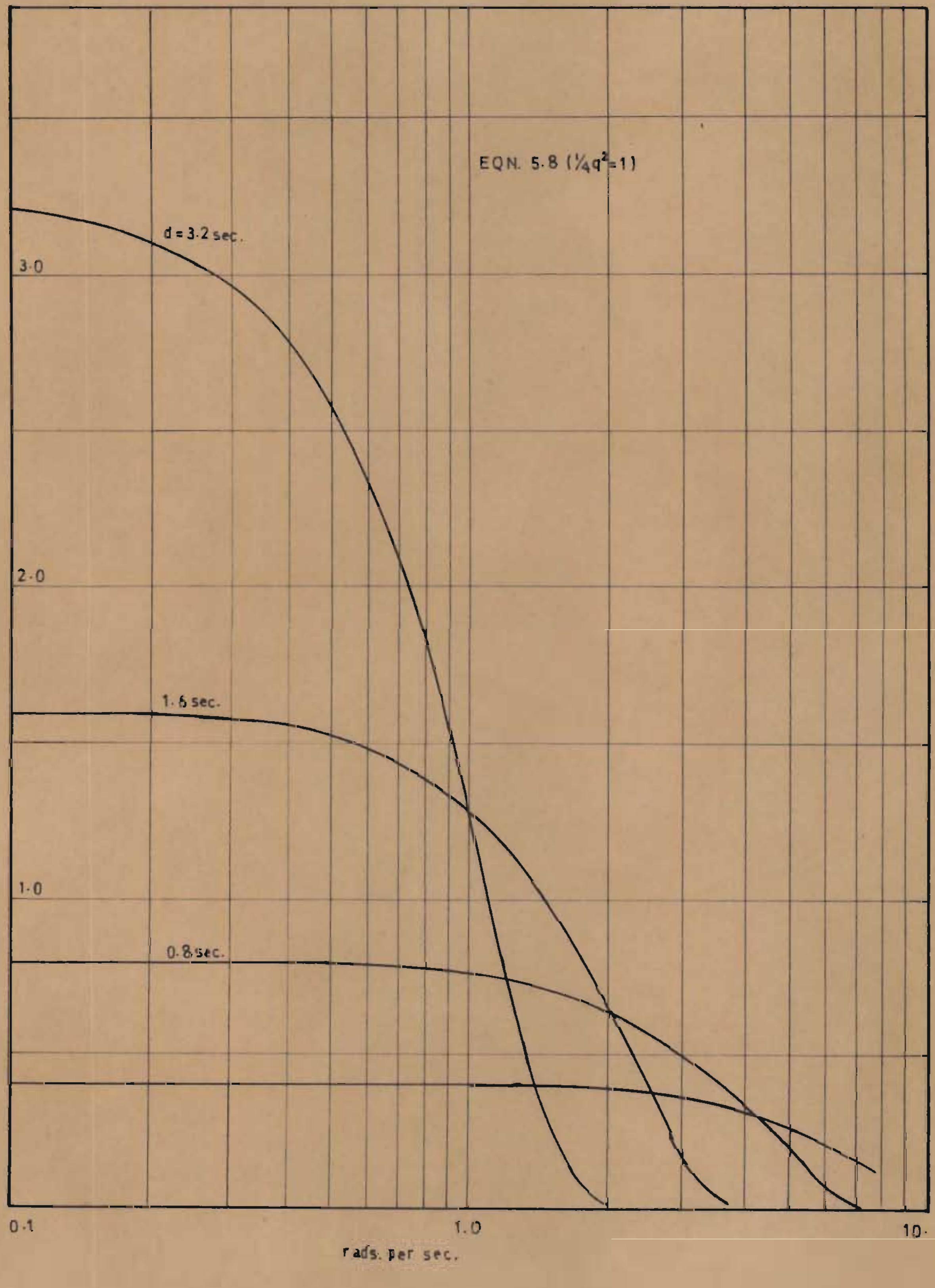

POWER SPECTRAL DENSITY OF P.R.B.S.

FIG. 5.6

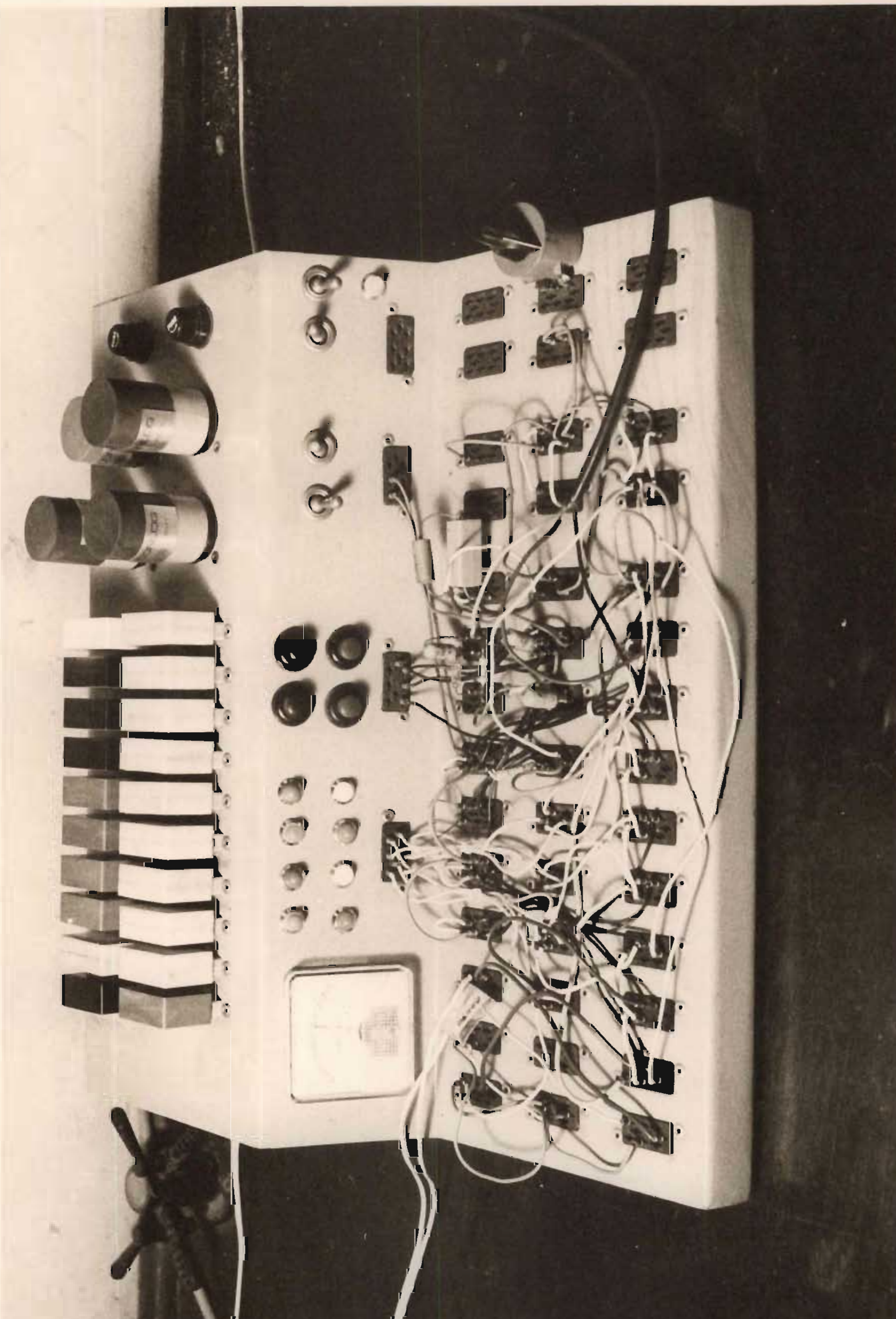

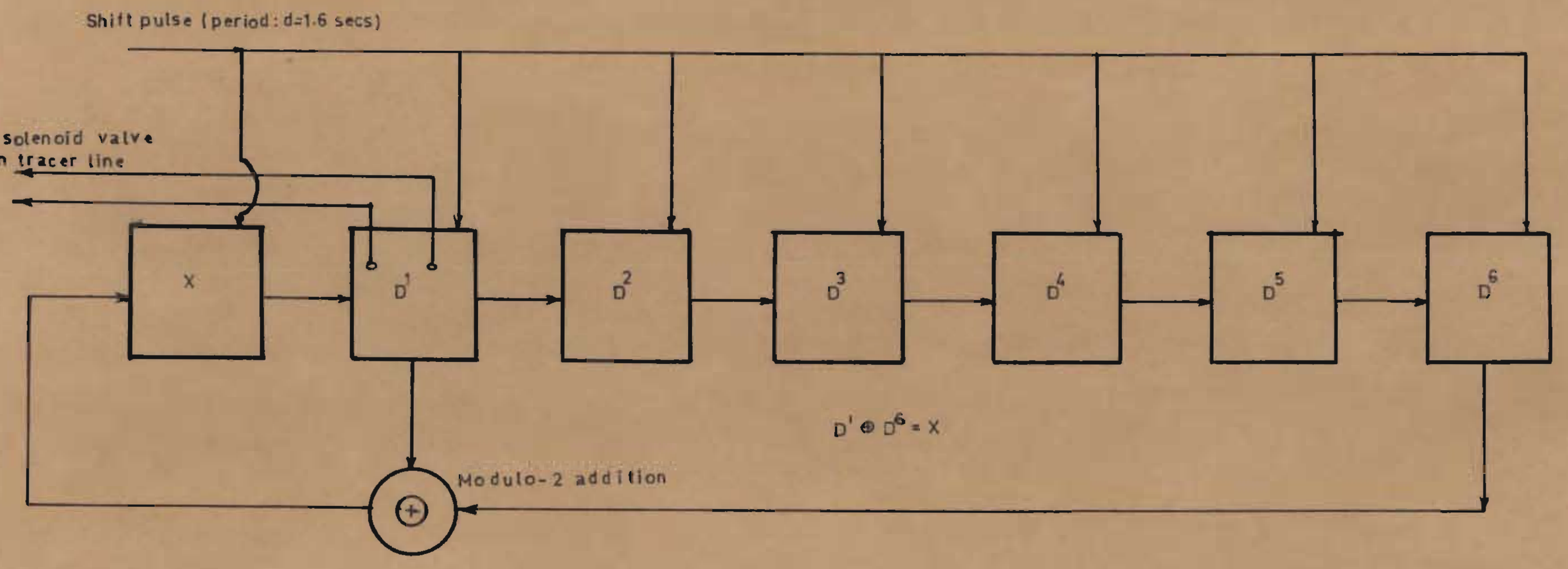

SHIFT REGISTER CIRCUIT TO GENERATE P.R.B. SEQUENCE.

FIG. 5·7

and during a shift of the circuit the contents of each register is passed onto the next one. Furthermore, Modulo-2 addition between registers is performed by adding circuits, connected in such a way that the desired P.R.B. signal is generated. Shifting occurs instantaneously and d is controlled by the period of an externally applied shift pulse. The sequence is started by ensuring that all registers contain 1 and that a 0 is inserted into the first register with the first shift pulse.

The choice of a particular P.R.B.S. was not important and the same sequence was used for all runs. It had a period of 63 d seconds and was generated by the circuit shown on page 64 .

5.2.3.3 NUMBER OF PERIODS AND SAMPLING INTERVAL

The run length and hence the number of periods used in the crosscorrelation experiment was made as long as was experimentally feasible. Similarly the shortest available sampling interval (0.2 second) was used.

Experimental details for all runs are tabulated on page 68.

5.2.3.4 COMPUTATION OF EXPERIMENTAL CROSSCORRELATIONS

A typical concentration versus time curve together with the P.R.B.S. is shown on page 66 .

Experimental crosscorrelations were calculated according to:

$$\Phi_{ex}(\tau) = \sum_{i=1}^{n} C_1(t_i)C_2(t_i+\tau) - \bar{c}_{ex,1}\bar{c}_{ex,2} \qquad 5.9$$

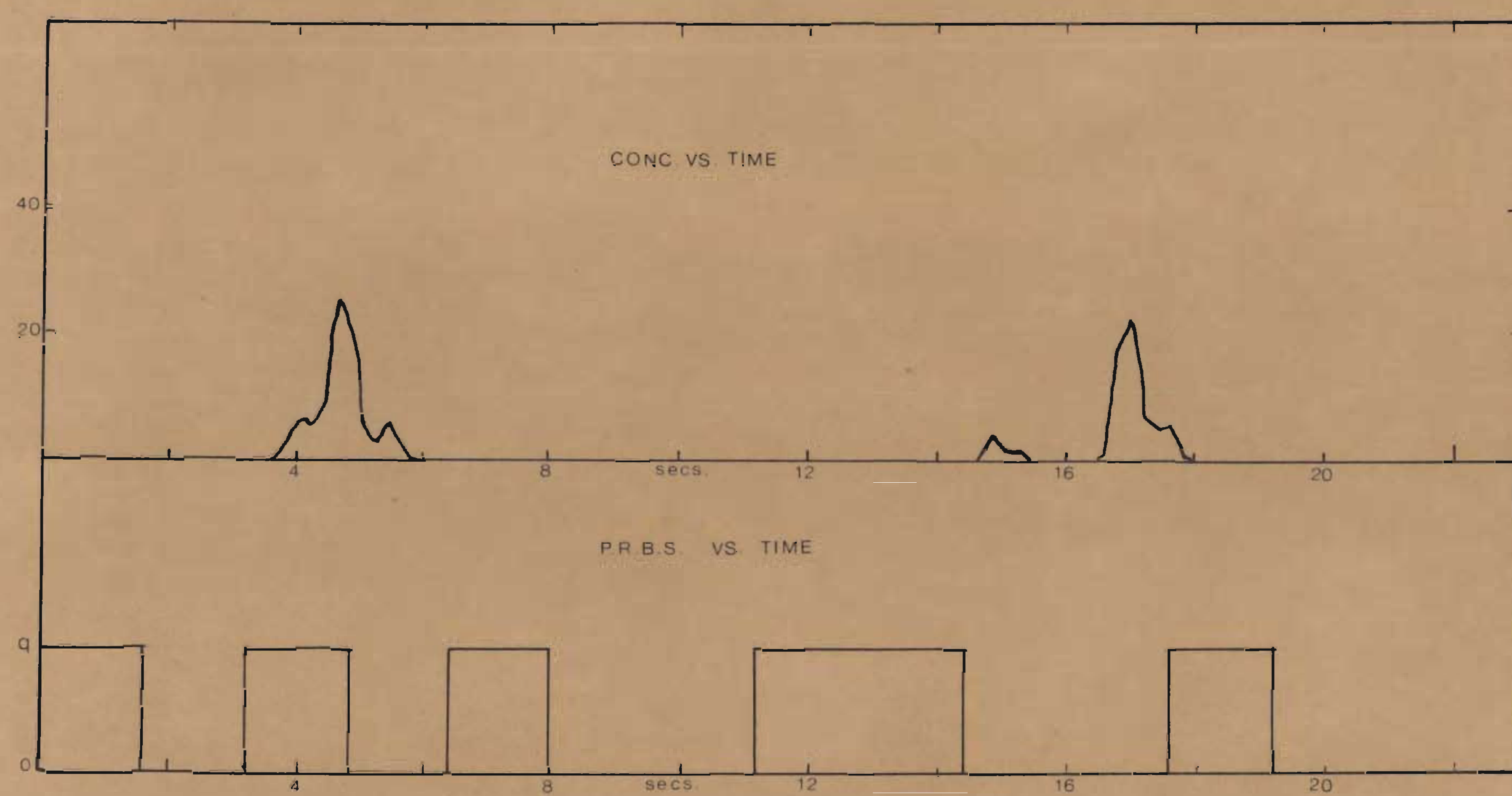
CONC. VS. TIME
40
20
4
8
secs.
12
16
20
P.R.B.S. VS. TIME
q
0
4
8
secs.
12
16
20

FIG. 5·8

where,

$C_1(t_i)$ = tracer concentration at point x_1, y_1 and time $t = i\Delta t$.

$C_2(t_i)$ = tracer concentration at point x_2, y_2 and time $t = i\Delta t$

n = number of readings correlated.

$\bar{c}_{ex,1}$ = mean tracer concentration at point x_1, y_1 over time interval from $t = 0$ to $t = n\Delta t$

$\bar{c}_{ex,2}$ = mean tracer concentration at point x_2, y_2 over time interval from $t = \tau$ to $t = n\Delta t + \tau$

Δt sampling interval

Experimental crosscorrelations were computed for two ranges of the lag τ, since the model predicted a distinct difference for the two cases. The first range extended from $\tau = 0$ to $\tau = 20$ seconds; the second range extended from $\tau = T_p$ to $\tau = T_p + 20$.secs.

	Run 1	Run 2	Run 3	Run 4	Run 5	Run 6	Run 7	Run 8	Run 9	Run 10
<u>MEAN RESPONSE</u>										
No. of observations	8169	9759	9655	7971	8590	7692	10059	7926	10099	10484
No. of pulses	170	203	150	124	134	106	139	123	157	163
Duration of run minutes:seconds	27:10	32:28.8	32:00	24:47.2	28:35.2	25:26.4	33:11.6	26:14.4	33:29.6	34:46.4
<u>CROSSCORRELATION</u>										
No. of observations	-	-	-	-	9820	9852	-	10332	8145	8108
P.R.B. Signal										
No. of decisions	-	-	-	-	63	63	-	63	63	63
Dec. interval (sec)	-	-	-	-	1.6	1.6	-	1.6	1.6	1.6
No. of Periods correlated	-	-	-	-	18	17	-	19	14	15;14
Duration of run minutes:seconds	-	-	-	-	32:44.4	32:50.4	-	34:26.4	27:9.0	27:1.6
<u>COORDINATES (FT)</u>										
1st/upper station										
x_1	0.5	0.6667	0.6667	0.8333	0.25	0.25	0.25	0.25	0.25	0.25
y_1	0.1667	0.1667	0.1667	0.1667	0.0	0.0	0.0	0.0442	-0.0442	0.0917
2nd/lower station										
x_2	0.5	0.6667	0.6667	0.8333	0.6667	0.9167	1.25	0.6667	0.6667	0.6667
Y_2	-0.1667	-0.1667	-0.1667	-0.1667	0.0	0.0	0.0	0.1175	-0.1175	0.2417

5.2.3.5 EVALUATION OF THEORETICAL CROSSCORRELATION

In order to allow for resistance and capacitance effects in the tracer injection line the square pulses of the Pseudo Random Binary input signal are assumed to have passed through a first order filter with time constant T_c before entering the tank. The Autocorrelation of the tracer input function may then be shown to have the following form: (19)

$$R_{Qf}(\tau) = \frac{N_p+1}{N_p}\,\frac{T_c}{d}\,\frac{\cosh\{d/T_c -1\}}{1-\exp\{-N_p d/T_c\}}\,\exp\{-\tau/T_c\} - \frac{1}{N_p} - J \qquad 5.1o$$

where :

d = decision time for P.R.B.S.

N_p = number of decisions in P.R.B.S.

T_c = time constant of first order filter

J = 0, $|\tau| > d$

$J = \frac{N_p+1}{N_p}\,\frac{\sinh\{d-\tau/T_c\}}{d/T_c} - (1-\tau/d)$, $|\tau| < d$

The model predictions of the crosscorrelation were obtained by performing the double integration of Equation 3.44 numerically. The region of integration extending from minus infinity to τ for both variables of integration θ_1 and θ_2 was divided up into a matrix of equal rectangles. The contribution of each rectangle was evaluated using Simpson's Rule. This procedure was carried out column by column, starting with the rectangle containing the upper limits τ,τ . Integration in the vertical direction was stopped when the contribution of a rectangle was less than one per cent of the total of its column computed so far. (Fig 5.9) Similarly, the contribution of the last column was less than one per cent of the total integral. The size of the rectangle was chosen such that the value of the integral did not change significantly when a smaller rectangle was used.

The computation was carried out on an I.B.M. 1130 machine and proved to be very time consuming.

The model predicts a considerable difference in amplitude for the two ranges of the lag (See Section 5.2.3.4 and Figure 6.12). This is due to the fact that for small lags the covariance between $W(t,\tau_1)$ and $W(t+\tau,\tau_2)$ (Equation 3.35) is large in the same region of the θ_1-, θ_2 - plane, where most of the probability mass is found. This is shown in Figure 5.9 for lag $\tau = 4.0$ seconds.

Figure 5.10 illustrates that for large lags ($\tau = T_p + 4$ seconds) the crosscorrelation region in the θ_1-, θ_2 - plane containing most of the probability mass maintains the same position relative to the point (τ, τ) as in Figure 5.9. The covariance $r(\tau,\theta_1;\tau,\theta_2)$ however, is very small in this region giving rise to weaker crosscorrelations.

5.3 HOT FILM ANEMOMETER MEASUREMENTS

5.3.1 GENERAL

In order to establish a physical significance for the flow model parameters and at the same time obtain an independent estimate of their values, the water velocity was measured directly by means of a Hot Film Anemometer.

From preliminary calibration experiments (See Section 4.5.2) it was found that throughout the velocity range of interest the Hot Film Anemometer had no

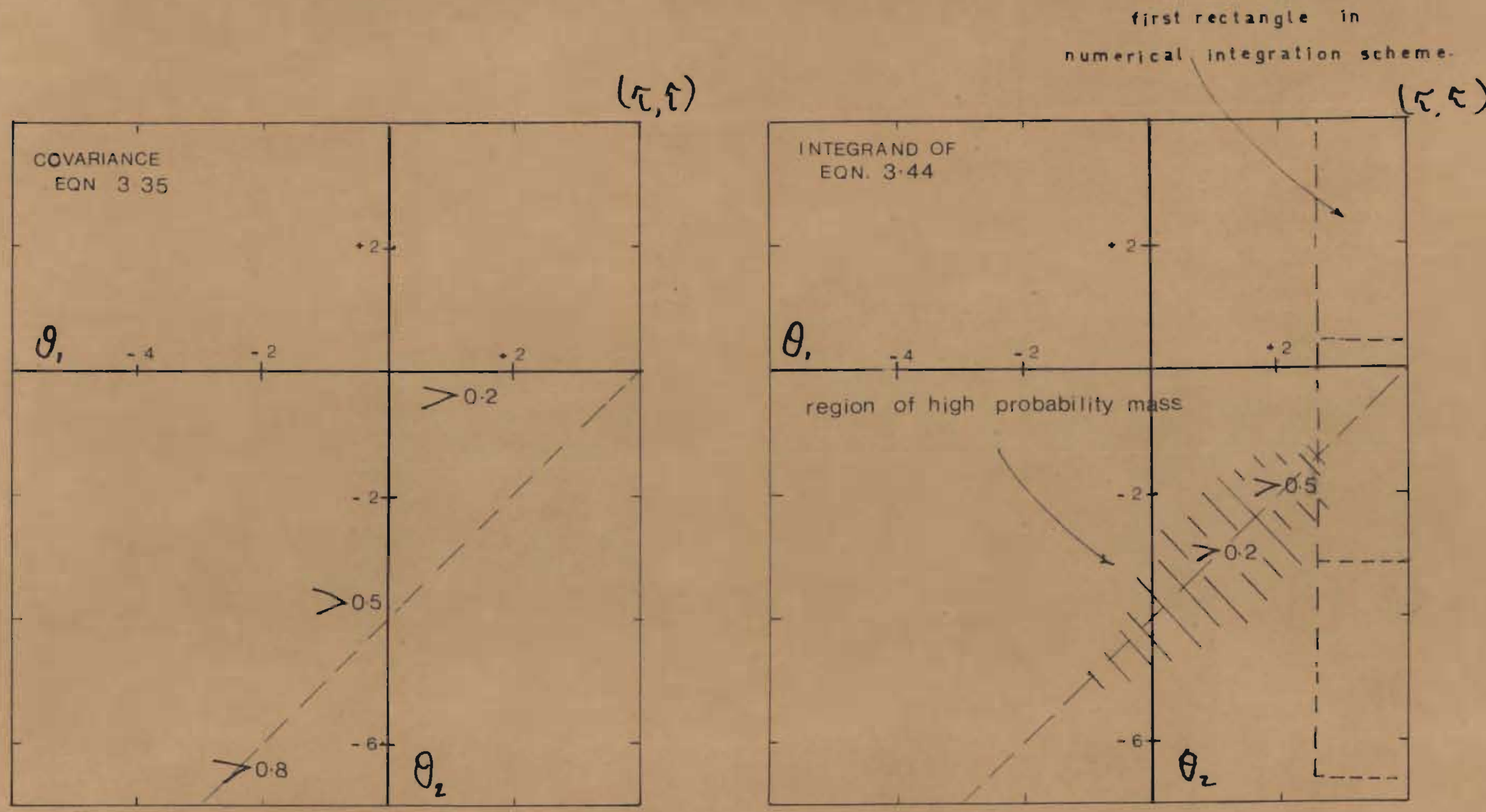
COVARIANCE
EQN 3 35
(τ,τ)
θ_1
θ_2
+2
-2
-4
-6
>0·2
>0·5
>0·8
INTEGRAND OF
EQN. 3·44
first rectangle in
numerical integration scheme.
region of high probability mass
(τ,τ)
θ_1
θ_2
>0·5
>0·2

FIG. 5·9

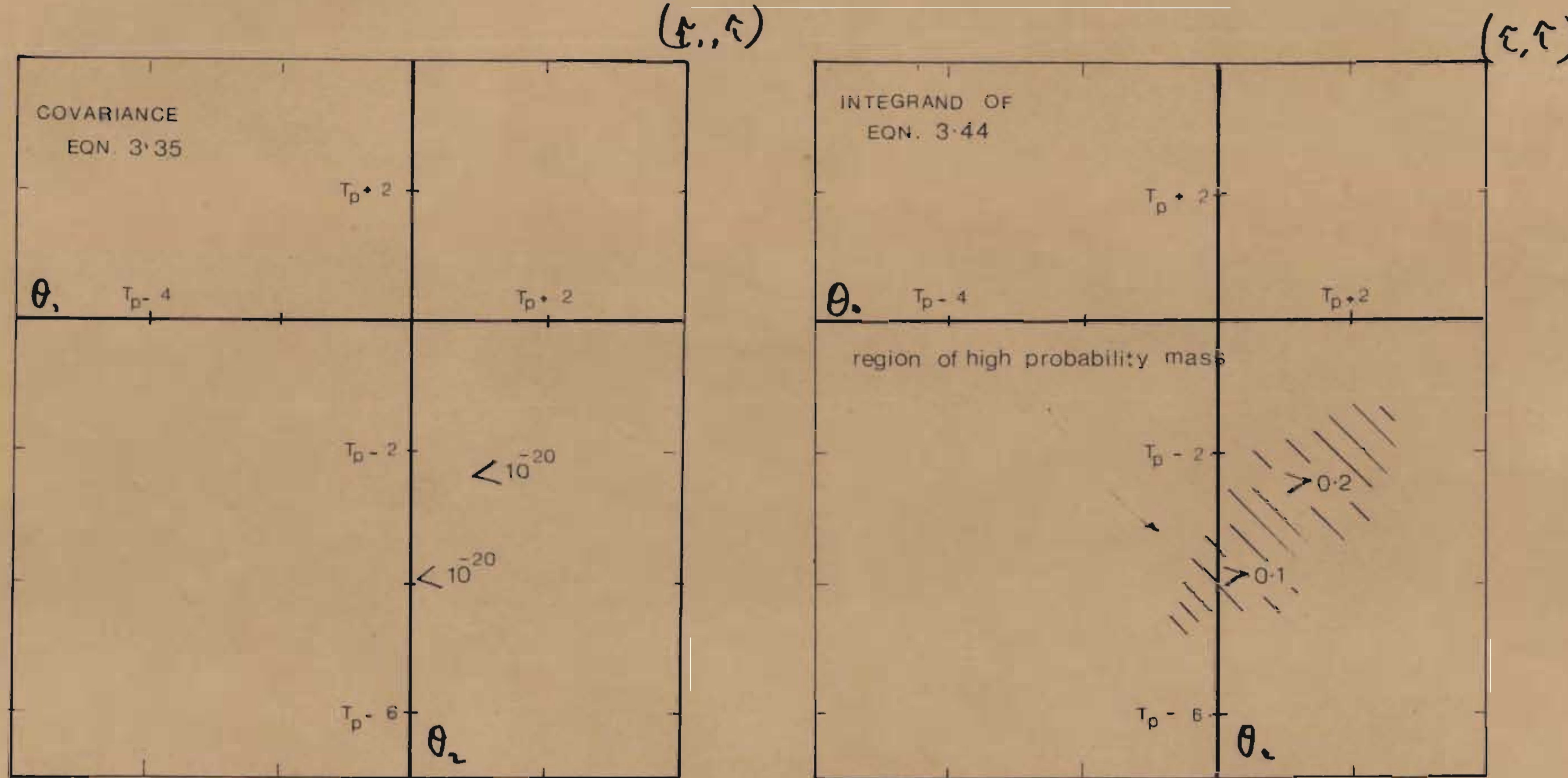
(τ_1, $\hat{\tau}$)
COVARIANCE
EQN. 3·35
$T_p + 2$
θ_1
$T_p - 4$
$T_p + 2$
$T_p - 2$
$< 10^{-20}$
$< 10^{-20}$
$T_p - 6$
θ_2
(τ, $\hat{\tau}$)
INTEGRAND OF
EQN. 3·44
$T_p + 2$
θ_1
$T_p - 4$
$T_p + 2$
region of high probability mass
$T_p - 2$
$> 0·2$
$> 0·1$
$T_p - 6$
θ_2

FIG. 5·10

directional sensitivity for the two directions at right angles to the axis of the probe. Furthermore by rotating the probe from a position at right angles to the direction of flow to a position where the axis of the probe was parallel to the direction of flow the response varied by only 20%. It was therefore decided to place the probe such that its axis was at right angles to both the X-and-Y directions. Its response was then interpreted as the vector sum of the instantaneous velocity components $U_x(t)$ and $U_y(t)$:

$$V(t) = \{U_x^2(t) + U_y^2(t)\}^{\frac{1}{2}} \tag{5.11}$$

The probe was situated at the same depth as the tip of the tracer injection line and 5 inches further downstream at the centre of the tank. (Figure 6.1). The Anemometer signal was sampled every 0.167 seconds for a total period of some 55 minutes.

Two statistical quantities of V(t) were computed, namely :

$f(v)$ = distribution density function of V(t)

$R_{v^2}(\tau)$ = autocorrelation of $V^2(t)$

It is clearly impossible to obtain estimates for the flow parameters of the individual components from a knowledge of the statistics of V(t).

Making the assumptions :

$$\sigma_{ox}^2 = \sigma_{oy}^2 = \sigma_o^2 \quad ; \quad \beta_x = \beta_y = \beta \; ; \; R_{ox} = R_{oy} = R_o(\tau)$$

the two parameters σ_o^2 and β may be determined as shown in the following two sections.

5.3.2 DISTRIBUTION DENSITY FUNCTION

It can be shown (20) that, if $U_x(t)$ and $U_y(t)$ are independent and normal, then $V(t)$ will have a Rayleigh distribution density function of the following form :

$$f(v) = \frac{v}{\sigma_o^2} \exp\left[-\left(\frac{(v^2 + \bar{u}_x^2 + \bar{u}_y^2)}{2\sigma_o^2}\right)\right] I_o\left[\frac{v\{\bar{u}_x^2 + \bar{u}_y^2\}^{\frac{1}{2}}}{\sigma_o^2}\right] \qquad 5.12$$

where,

$I_o(z)$ = Modified Bessel Function of zero order

$$= \sum_{i=o}^{\infty} \frac{z^{2i}}{2^{2i}(i!)^2}$$

5.3.3 AUTOCORRELATION OF $V^2(t)$

The autocorrelation is defined as :

$$R_{v^2}(\tau) = E\{V^2(t)V^2(t+\tau)\} \qquad 5.13$$

Substituting Equations 5.11 and 3.1 in Equation 5.13 yields :

$$R_{v^2}(\tau) = E\{\left[\left(U'_x(t)+\bar{u}_x\right)^2 + \left(U'_y(t)+\bar{u}_y\right)^2\right] \left[\left(U'_x(t+\tau)+\bar{u}_x\right)^2 + \left(U'_y(t+\tau)+\bar{u}_y\right)^2\right]\} \qquad 5.14$$

Remembering that $U'_x(t)$ and $U'_y(t)$ are assumed to be independent Equation 5.14 may be written as :

$$\begin{aligned} R_{v^2}(\tau) = {} & E\{U'^2_x(t)U'^2_x(t+\tau)\} + E\{U'^2_y(t)U'^2_y(t+\tau)\} \\ & + 4\bar{u}_x^2 E\{U'_x(t)U'_x(t+\tau)\} + 4\bar{u}_y^2 E\{U'(t)U'_y(t+\tau)\} \qquad 5.15 \\ & + 2\bar{u}_x^2 E\{U'^2_x(t)\} + 2\bar{u}_y^2 E\{U'^2_y(t)\} + \bar{u}_x^4 + \bar{u}_y^4 \end{aligned}$$

Since $U_x'(t)$ is a time-stationary random process with zero mean and Normal probability density function we may write :

$$E\{U_x'^2(t)U_x'^2(t+\tau)\} = \int_{-\infty}^{\infty}\int_{-\infty}^{\infty} u_{x1}^2 u_{x2}^2 f\{u_{x1}u_{x2},(\tau,\sigma_o^2,\beta)\}du_{x1}du_{x2} \quad 5.16$$

where,

$f\{u_{x1},u_{x2},(\tau,\sigma_o^2,\beta)\}$ = joint Normal distribution density function for $U_x'(t)$ and $U_x'(t+\tau)$.

The integrated result of Equation 5.16 may be conveniently obtained by making use of a property of the characteristic function $K(\xi_1,\xi_2,\tau)$: (21)

$$K(\xi_1,\xi_2,\tau) = \int_{-\infty}^{\infty}\int_{-\infty}^{\infty} f\{u_{x1},u_{x2},(\tau,\sigma_o^2,\beta)\} \exp(i\xi_1 u_{x1}) \exp(i\xi_2 u_{x2})\, du_{x1}\, du_{x2} \quad 5.17$$

$$= \exp\{-\tfrac{1}{2}\sigma_o^2(\xi_1^2 + \xi_2^2 + 2R_o(\tau)\xi_1\xi_2)\}$$

Expressions for the moments are obtained by differentiating the Characteristic Function an appropriate number of times and then equating ξ_1 and ξ_2 to zero.

Hence :

$$E\{U_x'^2(t)U_x'^2(t+\tau)\} = \frac{\partial^2}{\partial\xi_2^2}\left[\frac{\partial^2}{\partial\xi_1^2}\{K(\xi_1,\xi_2,\tau)\}\right] \quad 5.18$$

Carrying out the differentiation in Equation 5.18 and equating ξ_1 and ξ_2 to zero yields :

$$E\{U_x'^2(t)U_x'^2(t+\tau)\} = \left(\frac{2R_o^2(\tau)}{(\sigma_o^2)^2} + 1\right)(\sigma_o^2)^2 \quad 5.19$$

Similarly,

$$E\{U_y'^2(t)U_y'^2(t+\tau)\} = \left(\frac{2R_o^2(\tau)}{(\sigma_o^2)^2} + 1\right)(\sigma_o^2)^2 \qquad 5.19$$

Substituting Equations 3.3, 5.19 in Equation 5.15 and combining terms not containing τ yields :

$$\begin{aligned} E\{V^2(t)V^2(t+\tau)\} &= 4R_o^2(\tau) + 4R_o(\tau)(\bar{u}_x^2 + \bar{u}_y^2) \\ &\quad + \left(E\{U_x^2(t)\} + E\{U_y^2(t)\}\right)^2 \\ &= 4R_o^2(\tau) + 4R_o(\tau)(\bar{u}_x^2 + \bar{u}_y^2) \\ &\quad + \left(2\sigma_o^2 + \bar{u}_x^2 + \bar{u}_y^2\right)^2 \qquad 5.20 \end{aligned}$$

5.3.4. COMPUTATION OF EXPERIMENTAL DISTRIBUTION DENSITY f(v) AND AUTOCORRELATION $R_{v^2}(\tau)$ CURVES.

Experimental readings from the recording drum were converted to velocities using the calibration curve shown in Figure 4.4. Thus a digitalised record (interval Δt) of V(t) was obtained.

A frequency histogram of velocities was then constructed and the distribution density of V(t) was calculated from the following equation :

$$f\left\{\frac{v_i+v_{i+1}}{2}\right\} = \frac{F_i + F_{i+1}}{2N_v(v_{i+1} - v_i)} \qquad 5.21$$

(See Figure 6.22)

Where,

F_i = Frequency of occurrence of velocity v_i

N_v = Total number of velocity readings.

The autocorrelation of $V^2(t)$ was computed as follows:

$$R_{v^2}(\tau) = \frac{1}{N_c} \sum_{i=1}^{N_c} V^2(t_i)V^2(t_i+\tau) - (\overline{v^2})^2 \qquad 5.22$$

for values of τ from 0 to 100 Δt at intervals of

$\Delta t = 0.167$ secs.

(See Figure 6.23)

where,

N_c = Number of readings correlated.

$$\overline{v^2} = \frac{1}{N_c} \sum_{i=1}^{N_c} V^2(t_i)$$

5.4 ESTIMATION OF PARAMETERS

5.4.1 INTRODUCTION

In order to estimate parameters from the available experimental data it was found necessary to assume that :

$$\beta_x = \beta_y = \beta$$

$$\sigma^2_{ox} = \sigma^2_{oy} = \sigma^2_o$$

and hence 5.21

$$R_{ox}(\tau) = R_{oy}(\tau) = R_o(\tau)$$

$$\sigma^2_{1x}(t,\tau) = \sigma^2_{1y}(t,\tau) = \sigma^2_1(t,\tau)$$

From tracer experiments two statistical quantities were estimated, namely :

The Mean Response at pairs of points to a rectangular input pulse. One set of runs involved probe positions vertically one above the other, whilst in a second set of runsthe two probes were placed such that they were in a straight line with the point of injection. Model predictions of Mean Response curves have the following form :

Without molecular diffusion

$$\mu(x,y,t) = \int_o^t \frac{q(\tau)}{2\pi\sigma_1^2} \exp-\left(\frac{(x - m_{1x})^2 + (y - m_{1y})^2}{2\sigma_1^2}\right) d\tau \qquad 5.22$$

With molecular diffusion

$$\mu(x,y,t) = \int_o^t \frac{q(\tau)}{4\pi\{\frac{1}{2}\sigma_1^2 + D(t-\tau)\}} \exp\left(\frac{-1}{2D(t-\tau)\sigma_1^2}\left(\frac{-\frac{1}{4}}{\frac{1}{2}\sigma_1^2 + D(t-\tau)}\right.\right.$$
$$\left[\{\sigma_1^2 x + D(t-\tau)2m_{1x}\}^2 + \{\sigma_1^2 y + D(t-\tau)2m_{1y}\}^2\right]$$
$$\left.\left. + \tfrac{1}{2}\sigma_1^2(x^2 + y^2) + D(t-\tau)(m_{1x}^2 + m_{1y}^2)\right)\right) d\tau \qquad 5.23$$

The second statistical quantity estimated from tracer experiments was the concentration crosscorrelation between two points. The tracer input function was a Pseudo-Random Binary Sequence, which is time-stationary and periodic. The sequence is assumed to have passed through a first order filter before entering the tank. (Equation 5.10). The model prediction of the cross-correlation for the case involving molecular diffusion was used to estimate parameters. (Equation 3.44).

Hot Film Anemometer data yielded estimates of two statistical quantities :

Firstly, the Probability Distribution Density for V(t) : f(v)

where, $$V(t) = \{U_x^2(t) + U_y^2(t)\}^{\frac{1}{2}} \tag{5.25}$$

$$f(v) = \frac{v}{\sigma_o^2} \exp\left[-\frac{(v^2 + \bar{u}_x^2 + \bar{u}_y^2)}{2\sigma_o^2}\right] I_o\left\{\frac{v(\bar{u}_x^2 + \bar{u}_y^2)^{\frac{1}{2}}}{\sigma_o^2}\right\} \tag{5.26}$$

where,

$$I_o(z) = \sum_{i=o}^{\infty} \frac{z^{2i}}{2^{2i}\,(i!)^2}$$

Secondly, the autocorrelation of $V^2(t)$; this quantity was compared with the following expression:

$$\begin{aligned} R_{V^2}(\tau) &= 4R_o^2(\tau) + 4R_o(\tau)(\bar{u}_x^2 + \bar{u}_y^2) \\ &\quad + \{2\sigma_o^2 + \bar{u}_x^2 + \bar{u}_y^2\}^2 \end{aligned} \tag{5.27}$$

The following parameters were estimated :

$\bar{u}_x$ = X-component of the mean velocity

$\bar{u}_y$ = Y-component of the mean velocity

σ_o^2 = Variance of velocity fluctuations

β = Flowscale parameter

q = Tracer source strength.

5.4.2 PARAMETERS FROM TRACER EXPERIMENTS

Parameters were estimated from Mean Response curves using a non-linear regression technique based on a least squares criterion. (22) The application of this technique requires that the shape of the function should be sensitive to small changes in the values of the parameters and that the parameters are not correlated among themselves. It was found however, that both model predictions (Equations 3.25 and 3.40) were insensitive to β and this parameter could therefore not be estimated from the Mean Response Experiment.

In order to facilitate the estimation of the four remaining parameters a new parameter α was introduced. This parameter arises when the equation underlying the random process of velocity fluctuations is assumed to have the following form : (Ornstein-Uehlenbeck process, 23)

$$\frac{dU'(t)}{dt} + \beta U'(t) = \beta N_\alpha(t) \qquad 5.28$$

where,

$N_\alpha(t)$ = random process with White Noise properties, whose Power Spectral Density equals α.

It can be shown (Appendix 6) that this equation satisfies the properties assumed for $U'(t)$ and that :

$$\alpha = \frac{2\sigma_o^2}{\beta} \qquad \text{(See Section 3.1)} \qquad 5.29$$

Keeping the value of β fixed it was then possible to estimate parameters $\bar{u}_x$, $\bar{u}_y$, α and q by regression for particular probe positions. The effect of probe positions and the numerical results of the parameters are discussed in

Chapter VI.

It was found that the strength of the theoretical crosscorrelation was sensitive to the value of β. However, due to the complexity of this expression and limited computer facilities no attempt at regressing crosscorrelation data was made. Instead, a value of β was estimated by matching peak heights of experimental and theoretical crosscorrelations, using an iterative procedure. A value of β was assumed and the remaining parameters were obtained by regressing on a number of Mean Response curves (see table - on page 68). A new value of β was then obtained from crosscorrelations by matching peak heights, using average values for the parameters obtained by regression. Mean Response regressions were then repeated.

This procedure yielded a value of $\beta = 0.3$; this value together with a set of average values for the remaining four parameters gave reasonable correspondence between theoretical and experimental crosscorrelations (Figures 6.12, 6.15 and 6.18).

If

$\mu_{ex}(t_i) =$ experimental mean concentration,

and the first and last value of the Mean Response curve occur at times t_o and t_n respectively, then the nonlinear regression technique seeks to minimise the following function :

$$SOS = \sum_{t_i=t_o}^{t_i=t_n} \{\mu_{ex}(t_i) - \mu(x,y,t_i)\}^2 \qquad 5.30$$

where, $\mu(x,y,t)$ is given by Equations 5.22 and 5.23. The method involves evaluations of $\mu(x,y,t)$ as well as its derivatives with respect to the parameters for values of t_i from t_o to t_n. Simpson's rule of numerical integration was used.

It was found necessary to slightly modify this technique when applied to both Mean Response curves simultaneously. In this case two pulses contribute to the sum of squared errors :

$$SOS = SOS_{(1st\ pulse)} + SOS_{(2nd\ pulse)} \qquad 5.31$$

In order to prevent a bias towards the pulse with larger amplitudes i.e. the pulse measured closer to the point of injection, the contribution of the smaller pulse was increased with a correction factor. Smooth curves (24) through the experimental points were computed with the aid of a digital filter and the ratio of the variance of the larger pulse to that of the smaller pulse was considered to be a suitable correction factor. (Page 88).

The rectangular input pulse (amplitude q) was assumed to have passed through a first order filter with a time constant of 0.01 seconds before entering the tank (see Section 5.2.3.5).

Hence :

$$q(t) = q\left[1 - \exp(-100t)\right] \qquad ; 0 < t \leq 1.6$$

$$q(t) = q\left[\exp\{-100(t-1.6)\} - \exp\{-100t\}\right]; \quad t > 1.6$$

5.23

5.4.3. PARAMETERS FROM THE HOT FILM EXPERIMENT

The statistical quantities calculated from a direct measurement of the instantaneous velocity at a point provided an independent measurement of the following parameters :

σ_o^2 = variance of velocity fluctuations

β = flow scale parameter

$\bar{u}_x^2 + \bar{u}_y^2$ = sum of squares of mean velocity components.

Best fit values of parameters

$$\sigma_o^2 \text{ and } \{\bar{u}_x^2 + \bar{u}_y^2\}$$

were obtained by regressing the experimental distribution density function of V(t) using Equation 5.26.

The Autocorrelation of $V^2(t)$ may be conveniently split into two parts; firstly,

A transient part, where its value is strongly dependent on the lag τ, secondly,

$R_{V^2}(\tau)$ for large values of τ. From Equation 5.27 it may be seen that this value tends to $\{2\sigma_o^2 + \bar{u}_x^2 + \bar{u}_y^2\}^2$

Parameters σ_o^2 and β were estimated from the transient part of the experimental $R_{V^2}(\tau)$ curve by regression using τ- dependent terms of Equation 5.27.

CHAPTER VI

RESULTS AND DISCUSSION

6.1 TRACER EXPERIMENTS

The tracer experiments may be conveniently divided into three groups according to the positions of the monitoring stations relative to the point of injection. Figure 6.1 shows the positions of the two probes for each run. It will be noted that the point of injection was fairly closely situated to the inlet duct and was kept in the same position for all runs. Furthermore, it can be seen that the region of the tank explored was relatively small. (See Figure 4.1)

In each case the results are compared with the continuous state flow model including the effect of molecular diffusion. A value of 0.1×10^{-7} ft.^{2} per second was used for the molecular diffusion coefficient.

6.1.1. GROUP 1.

In the first group the probe positions are vertically above one another and equidistant from the point of injection (Figure 6.1). For each of the first three runs parameters $\bar{u}_x$, $\bar{u}_y$, α and q were evaluated by regressing on both Mean Response curves simultaneously using Equation 5.23. Figures 6.2, 6.3 and 6.4 show that the model can adequately describe Mean Response curves for these positions. The flow parameters $\bar{u}_x$, $\bar{u}_y$, and α remain reasonably constant, whilst the agreement between the measured source strength and the value for q obtained by regression is fair. (See table - on Page 88).

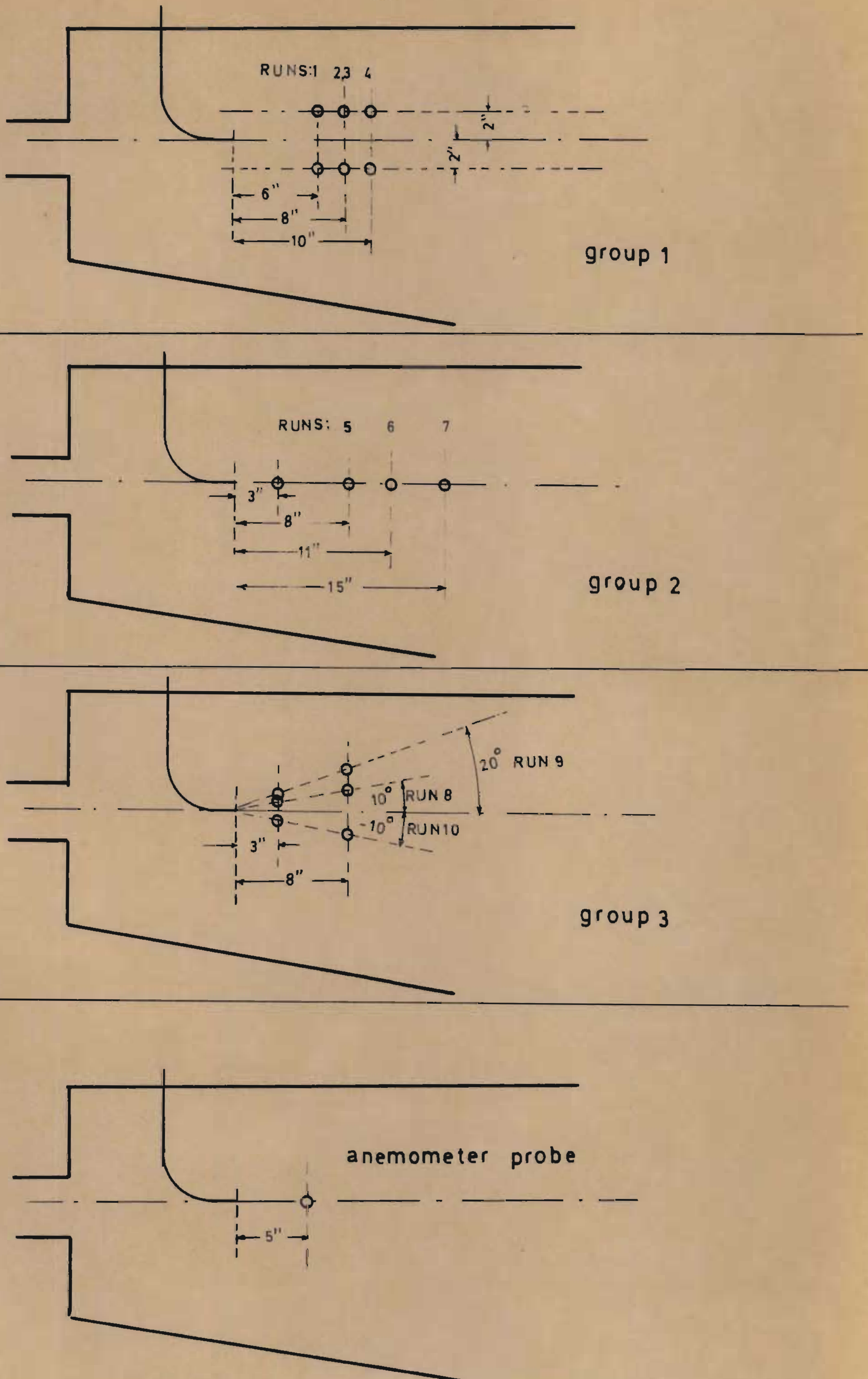

RUNS:1 2,3 4
6"
8"
10"
2"
2"
group 1
RUNS: 5 6 7
3"
8"
11"
15"
group 2
20° RUN 9
10° RUN 8
10° RUN10
3"
8"
group 3
anemometer probe
5"

FIG.6.1

Figure 6.5 shows the Mean Response curves for Run 4 together with their model predictions. The prediction for the lower station is clearly inadequate; this may be attributed to the fact that its position lies in a region with different flow characteristics. This is confirmed by a comparison of the parameter values obtained from regressions on each Mean Response curve individually. (Figures 6.6 and 6.7).

The model predicts zero crosscorrelations and this fact was confirmed experimentally.

6.1.2. GROUP 2.

The second group of tracer experiments was carried out with the probe positions along the X-axis. The first probe was kept at a distance of three inches from the point of injection, whilst the second probe was placed at a number of positions further downstream (Figure 6.1).

The Mean Response curves for these positions contain very little information concerning $\bar{u}_y$, the Y-component of the mean velocity, since both probes have the same Y-coordinate. Parameters $\bar{u}_x$, α and q were again evaluated by regressing on both Mean Response curves simultaneously. An average value of $\bar{u}_y$ obtained from the first group of tracer experiments was used in these regressions.

From Figures 6.8 and 6.9 it can be seen that the model is capable of describing the experimental Mean Response curves and that the values of the flow parameters are in good agreement with each other and with those of group I. There is, however, a considerable difference in amplitude between the theoretical and experimental curves for the second station of Run 6. An examination of the parameters obtained from an individual regression of this pulse (Figure 6.10) shows an excessively high source strength q and good agreement for the flow parameters. Hence, even though the fit is excellent, little reliance can be placed on the estimation of the source strength from a single pulse regression. Figure 6.11 shows a comparison of the experimental Mean Response curves for Run 7 with those predicted by the model, using average parameter values obtained from previous regressions. Noting the large difference in amplitude and spread between the two pulses the model prediction is considered to be very good.

Figures 6.12 and 6.13 show comparisons of predicted and experimental concentration crosscorrelations. The values of the parameters are the same as those used to predict Mean Response curves. The effect of correlation between $W(t,\tau_1)$ and $W(t+\tau,\tau_2)$ is clearly illustrated by the higher amplitudes obtained for small values of the lag τ. (see Section 5.2.3.5)

6.1.3. GROUP 3.

The third group of runs was carried out with the probes positioned such that they were on straight lines radiating from the point of injection at angles of 10^o, 20^o, and -10^o with the X-axis.

Parameters obtained from a regression on both Mean Response curves of Run 8 are in good agreement with those of groups 2 and 3 (Figure 6.14), whilst Figure 6.15 shows

PARAMETER VALUES OBTAINED FROM TWO-PULSE REGRESSIONS.

	RUN 1	RUN 2	RUN 3	RUN 5	RUN 6	RUN 8	Parameter values used in MODEL PREDICTIONS.	
$\bar{u}_x$	0.093	0.097	0.0973	0.092	0.090	0.094	0.096	ft./sec.
$\bar{u}_y$	0.0113	0.0117	0.0091	*(0.011)	(0.011)	(0.011)	0.011	ft./sec.
α	0.00557	0.0048	0.0073	0.00545	0.00597	0.0067	0.006	ft^2./sec.
σ_o^2	0.000836	0.00072	0.0011	0.000818	0.000896	0.00102	0.0009	ft^2./sec^2.
β	(0.3)	(0.3)	(0.3)	(0.3)	(0.3)	(0.3)	0.3	sec^{-1}.
q	0.182	0.197	0.314	0.24	0.303	0.295	0.3	** -
$q_{measd.}$	0.247	0.247	0.3	0.3	0.3	0.3	-	-
correction factor	7.0	2.5	1.7	20.0	5.0	14.0	-	

*( ) value kept constant in regression for remaining parameters.

**see Appendix 7.

satisfactory model predictions for the concentration crosscorrelations. Runs 9 and 10, however, show some discrepancy between the predicted and experimental curves. (Figures 6.16, 6.17, 6.18 and 6.19); it may be attributed to the fact that probes were situated at points with different flow characteristics. This is especially true for the second probe position of Run 10 which was observed to experience occasional intervals of near stagnancy. (Figure 6.1). All predicted curves are based on the same set of parameters.

6.1.4 EFFECT OF MOLECULAR DIFFUSION

In order to investigate the effect of molecular diffusion parameter values obtained from regressions on Mean Response curves using Equation 5.23 (with molecular diffusion) may be compared with those using Equation 5.22 (no molecular diffusion). From Figures 6.20 and 6.21 it can be seen that the simpler model without molecular diffusion is equally capable of describing Mean Response curves. Furthermore an examination of the table below shows that the values of the parameters obtained by regression are practically identical for the two cases.

	WITH MOL. DIFFUSION			NO MOL. DIFFUSION			
	Run 1	Run 2	Run 8	Run 1	Run 2	Run 8	
$\bar{u}_x$	0.093	0.097	0.094	0.093	0.097	0.094	ft/sec
$\bar{u}_y$	0.0113	0.0117	(0.011)	0.0113	0.0116	(0.011)	ft/sec
α	0.00557	0.0048	0.00677	0.00556	0.0048	0.00676	ft^2/sec
β	(0.3)	(0.3)	(0.3)	(0.3)	(0.3)	(0.3)	sec^{-1}
q	0.182	0.197	0.295	0.182	0.197	0.295	*

(*see Appendix 7)

The molecular diffusivity is a measure of the power associated with molecular vibrations and its value (o.1 x $10^{-7} ft^2/s$ may be compared directly with the power of the velocity fluctuations given by Equation 5.1. The values differ by a factor of the order of 10^6 and it is therefore not surprising that molecular diffusion has a negligible effect on dispersion. This is likely to be true for all liquid flow systems with a similar flow structure, since molecular diffusivities do not vary a great deal from liquid to liquid. In gas flow systems, however, molecular diffusion will play a more important role, as diffusivity values are of the order of 10^5 times greater.

The following table shows parameter values obtained by regression on a single Mean Response curve (Run 4, second station) for a number of values of molecular diffusivity.

Mol.Dif.	$\bar{u}_x$	$\bar{u}_y$	α	β	q	SOS
0.1×10^{-7}	0.106	0.011	0.00766	0.3	0.329	0.689
0.1×10^{-4}	0.106	0.011	0.00763	0.3	0.329	0.693
0.1×10^{-2}	0.106	0.011	0.00432	0.3	0.326	0.778

It can be seen that the value of α decreases as D increases in order to accommodate the same amount of spread.

6.2. HOT FILM ANEMOMETER RESULTS

Figures 6.22 and 6.23 show the results obtained from the Hot Film Anemometer experiment. The value of

$\{\bar{u}_x^2 + \bar{u}_y^2\}^{\frac{1}{2}}$ from a regression of the distribution density function of V(t) was used in the estimation of from the Autocorrelation of $V^2(t)$. (Figure 6.23).

The table below shows a comparison of parameters $\{\overline{u_x^2} + \overline{u_y^2}\}^{\frac{1}{2}}$, α , σ_0^2 and β for the various methods of parameter estimation.

	α	σ_0^2	β	$\{\overline{u_x^2} + \overline{u_y^2}\}^{\frac{1}{2}}$
tracer experiments	0.006	0.0009	0.3	0.0961
distribution density $f(v)$	-	0.00314	-	0.115
autocorrelation $R_{v^2}(\tau)$	0.0196	0.00532	0.544	0.115
	0.0251	0.00633	0.505	0.0961

It can be seen that, whereas there is reasonable agreement for the values of $(\overline{u}_x^2 + \overline{u}_y^2)^{\frac{1}{2}}$ and β obtained from tracer experiments and Hot Film Anemometer data, parameter estimations of α (and hence σ_0^2) for the two methods differ widely. A number of reasons may be suggested :

The model only accounts for velocity fluctuations in the X-and Y- directions, whereas the Hot Film probe is affected by all three velocity components.

As mentioned earlier (Section 5.2.2.1) low frequency velocity fluctuations have a dominant effect on dispersion. It was shown that dispersion is related to the area under the $R_0(\tau)$ versus τ curve rather than to the variance of the velocity fluctuations. This may be further demonstrated by a consideration of the case where the velocity fluctuations $\{U'(t)\}$ have White Noise properties (Wiener process, 25). The variance of position $\overline{X}^2(t)$ is then given by:

$$\overline{X}^2(t) = \alpha_w t$$

where,

α_w = Power Spectral Density of $U'(t)$

whereas, the variance of the velocity fluctuations themselves is infinite.

In order to show that the addition of a low power, high frequency Ornstein-Uehlenbeck velocity process has a negligible effect on dispersion, but makes a noticeable difference to the variance of the velocity fluctuations, we assume :

$$U'(t) = U_1'(t) + U_2'(t) \qquad 6.1$$

and

$$\frac{dU_1'(t)}{dt} + \beta_1' U_1'(t) = \beta_1' N_{\alpha_1'}$$

$$6.2$$

$$\frac{dU_2'(t)}{dt} + \beta_2' U_2'(t) = \beta_2' N_{\alpha_2'}$$

(see Appendix 6)

where,

$$\beta_2' > \beta_1' \quad \text{and} \quad \alpha_2' < \alpha_1' \qquad 6.3$$

If we further assume $U'_1(t)$ and $U'_2(t)$ to be uncorrelated, the autocorrelation of $U'(t)$ becomes :

$$R_o(\tau) = \frac{\alpha_1'\beta_1'}{2}\exp(-\beta_1'|\tau|) + \frac{\alpha_2'\beta_2'}{2}\exp(-\beta_2'|\tau|) \qquad 6.4$$

$$\sigma_o^2 = \frac{\alpha_1'\beta_1'}{2} + \frac{\alpha_2'\beta_2'}{2} \qquad 6.5$$

(see Equations 3.3, 5.29)

Similarly, the variance of the mean response to a Dirac input is :

$$\sigma_1^2(t) = \frac{\alpha_1'}{\beta_1'}\{\exp(-\beta_1't) - 1 + \beta_1't\} + \frac{\alpha_2'}{\beta_2'}\{\exp(-\beta_2't) - 1 + \beta_2't\} \qquad 6.6$$

The contribution from the velocity U_2' to the total variance measured with high frequency response Anemometer equipment is dominated by the product $\alpha_2'\beta_2'$ as can be seen from Equation 6.4; however its contribution to tracer dispersion is dominated by the ratio $\frac{\alpha_2'}{\beta_2'}$. Bearing in mind the inequalities 6.3 it can be seen that

if $\alpha_2'\beta_2' \doteq \alpha_1'\beta_1'$ then $\frac{\alpha_2'}{\beta_2'} \ll \frac{\alpha_1'}{\beta_1'}$

Thus the low-power high-frequency process U_2' has no effect on the measured dispersion but a large effect on the measured variance of the total velocity process.

If it is assumed that parameters obtained from tracer experiments are estimates of α_1' , β_1' i.e. parameters of the velocity process which has a dominant effect on dispersion, we may write :

Variance of $U_2'(t)$ = σ_o^2 (Hot Film Anemometer)

$- \sigma_o^2$ (tracer expts.)

The lack of fit of the distribution density function f(v) (Figure 6.22) indicates a weakness in the assumptions that velocity fluctuation components are normally distributed and that their statistical parameters σ_0^2 and β are equal.

In conclusion the results show that :

Firstly, the continuous state flow model is capable of describing dispersion in a relatively small region of the tank.

Secondly, the tracer experiments were insensitive to molecular diffusion and high frequency velocity fluctuations.

Thirdly, the various methods of parameter estimation yielded reasonably consistent results.

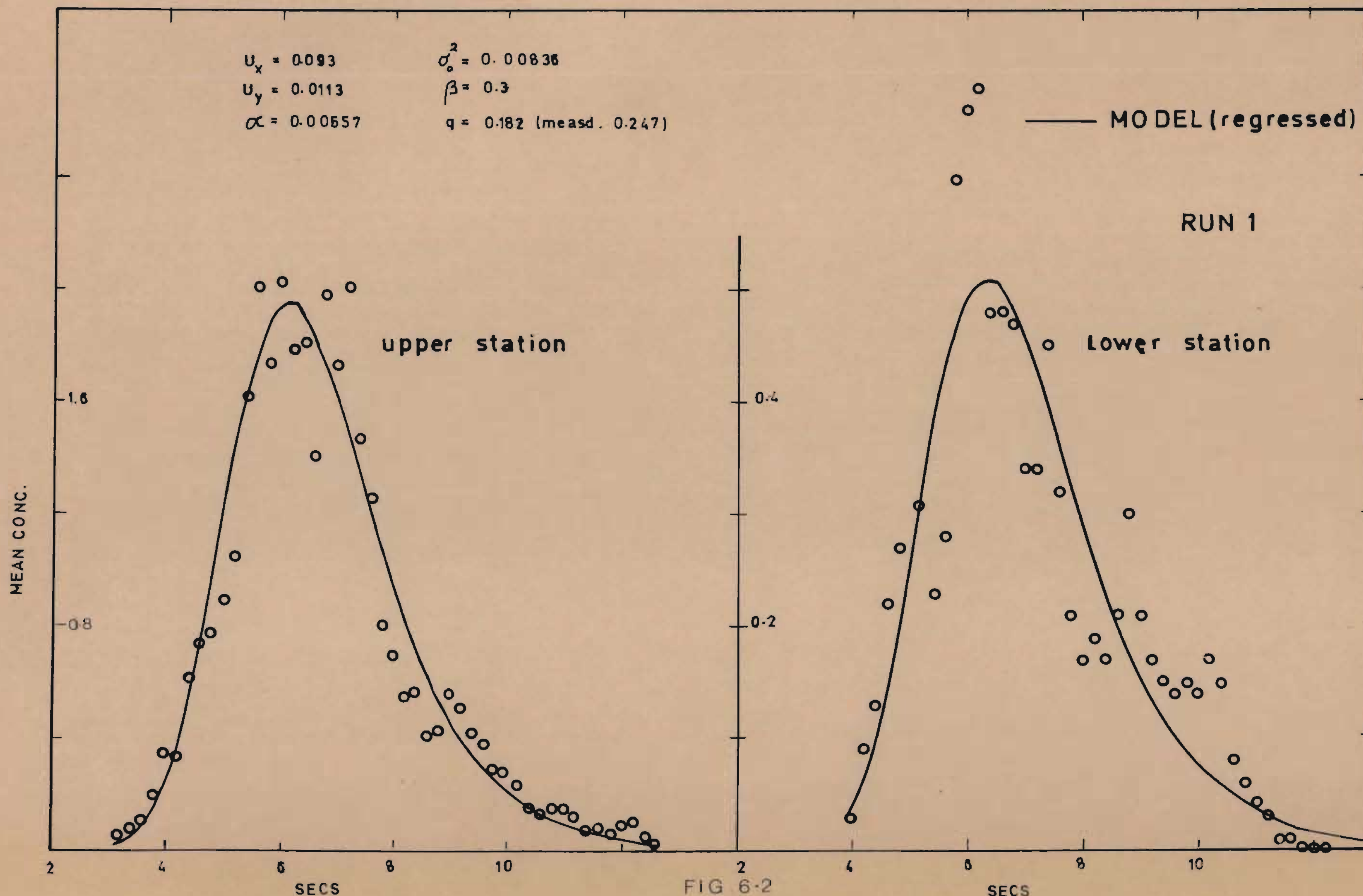

U_x = 0.093
U_y = 0.0113
α = 0.00557
σ_o^2 = 0.00836
β = 0.3
q = 0.182 (measd. 0.247)
MODEL (regressed)
RUN 1
upper station
lower station
MEAN CONC.
1.6
0.8
0.4
0.2
2
4
6
8
10
SECS

FIG 6.2

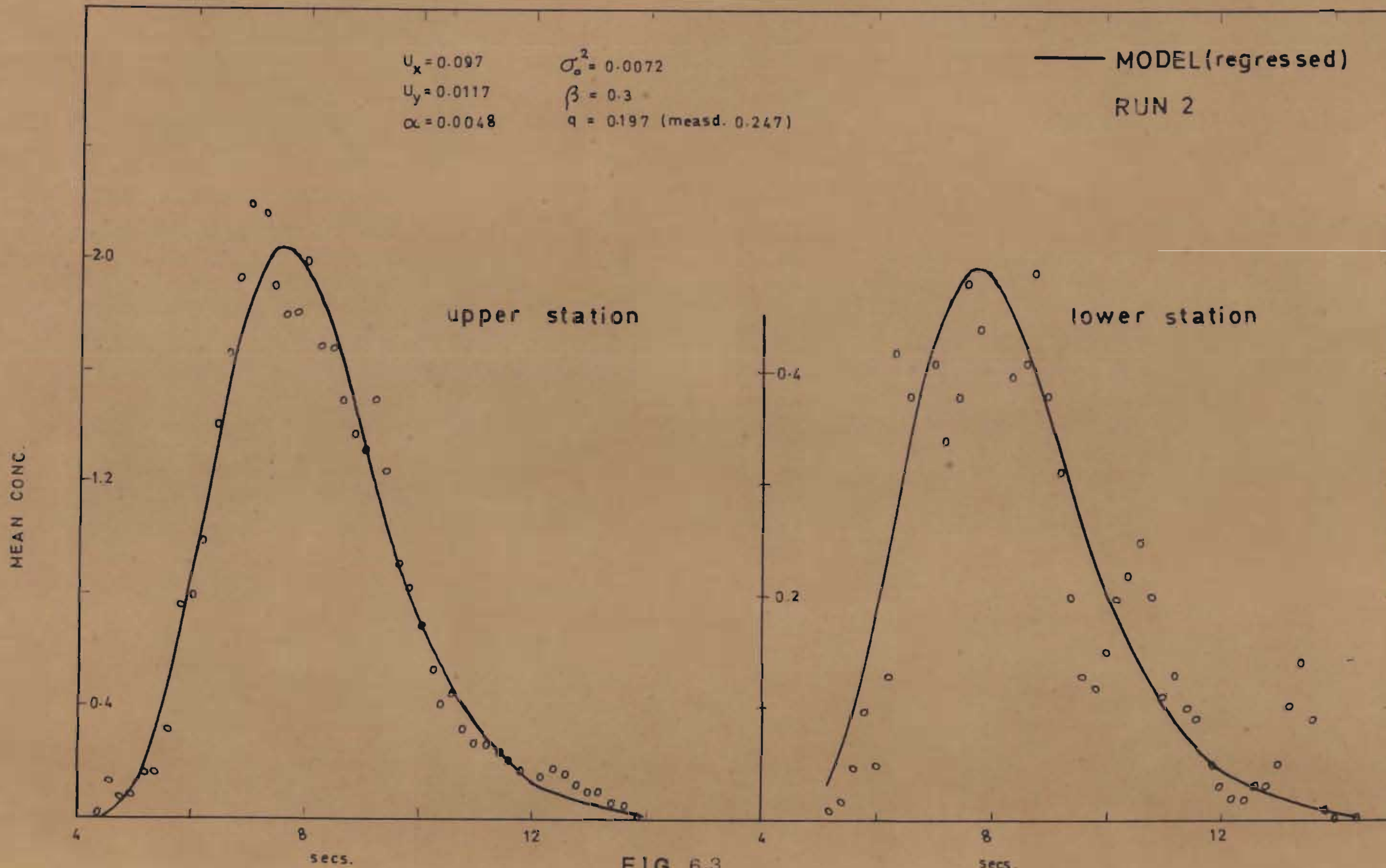

$U_x = 0.097$
$U_y = 0.0117$
$\alpha = 0.0048$
$\sigma_a^2 = 0.0072$
$\beta = 0.3$
q = 0.197 (measd. 0.247)
MODEL (regressed)
RUN 2
upper station
lower station
MEAN CONC.
2.0
1.2
0.4
0.4
0.2
4
8
12
secs.

FIG. 6.3

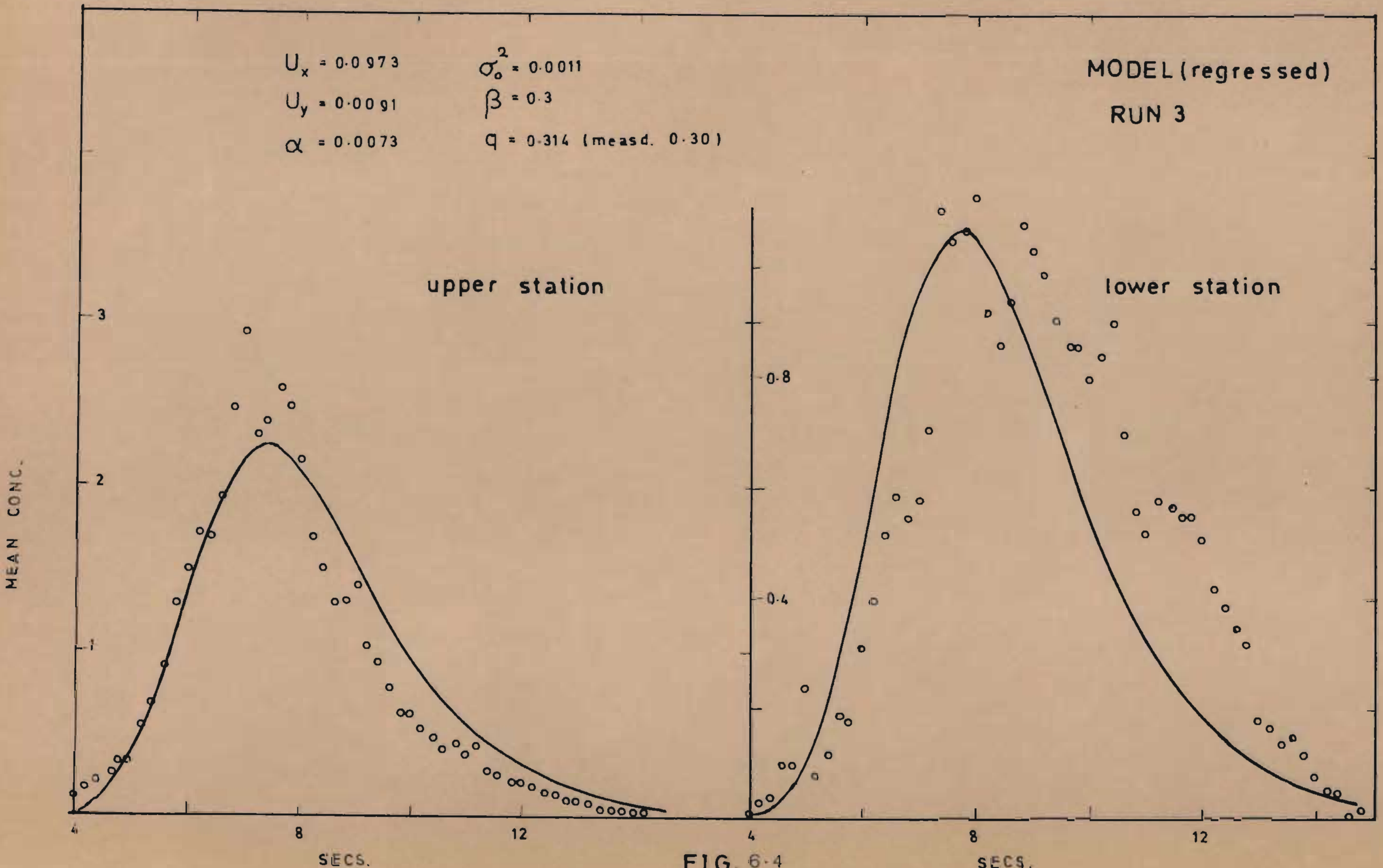

U_x = 0.0973
U_y = 0.0091
α = 0.0073
σ_o^2 = 0.0011
β = 0.3
q = 0.314 (measd. 0.30)
MODEL (regressed)
RUN 3
upper station
lower station
MEAN CONC.
1
2
3
0.4
0.8
4
8
12
SECS.
SECS.

FIG. 6.4

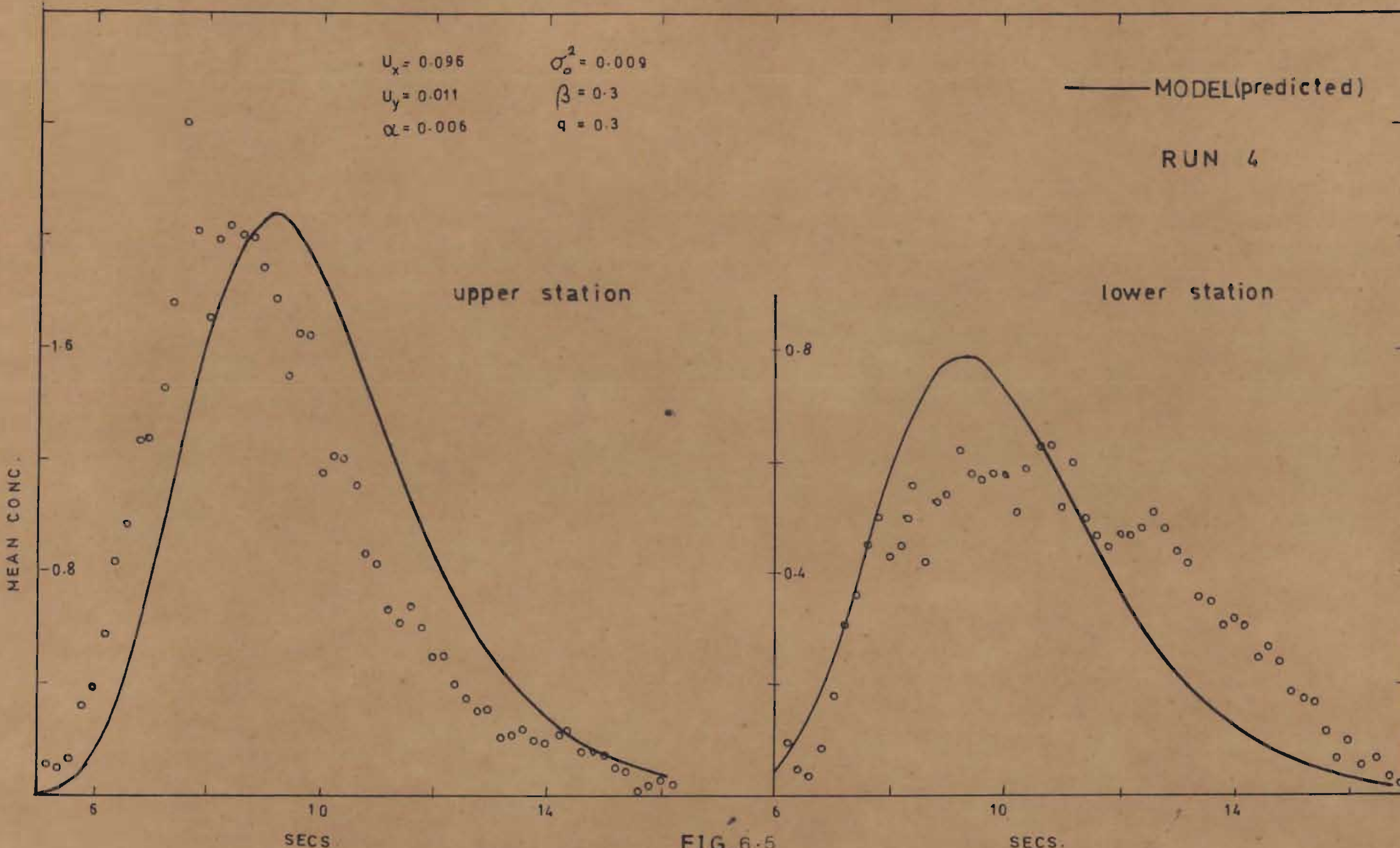

U_x = 0.096
U_y = 0.011
α = 0.006
σ_o^2 = 0.009
β = 0.3
q = 0.3
MODEL(predicted)
RUN 4
upper station
lower station
MEAN CONC.
1.6
0.8
0.8
0.4
6
10
14
SECS
6
10
14
SECS.

FIG. 6.5

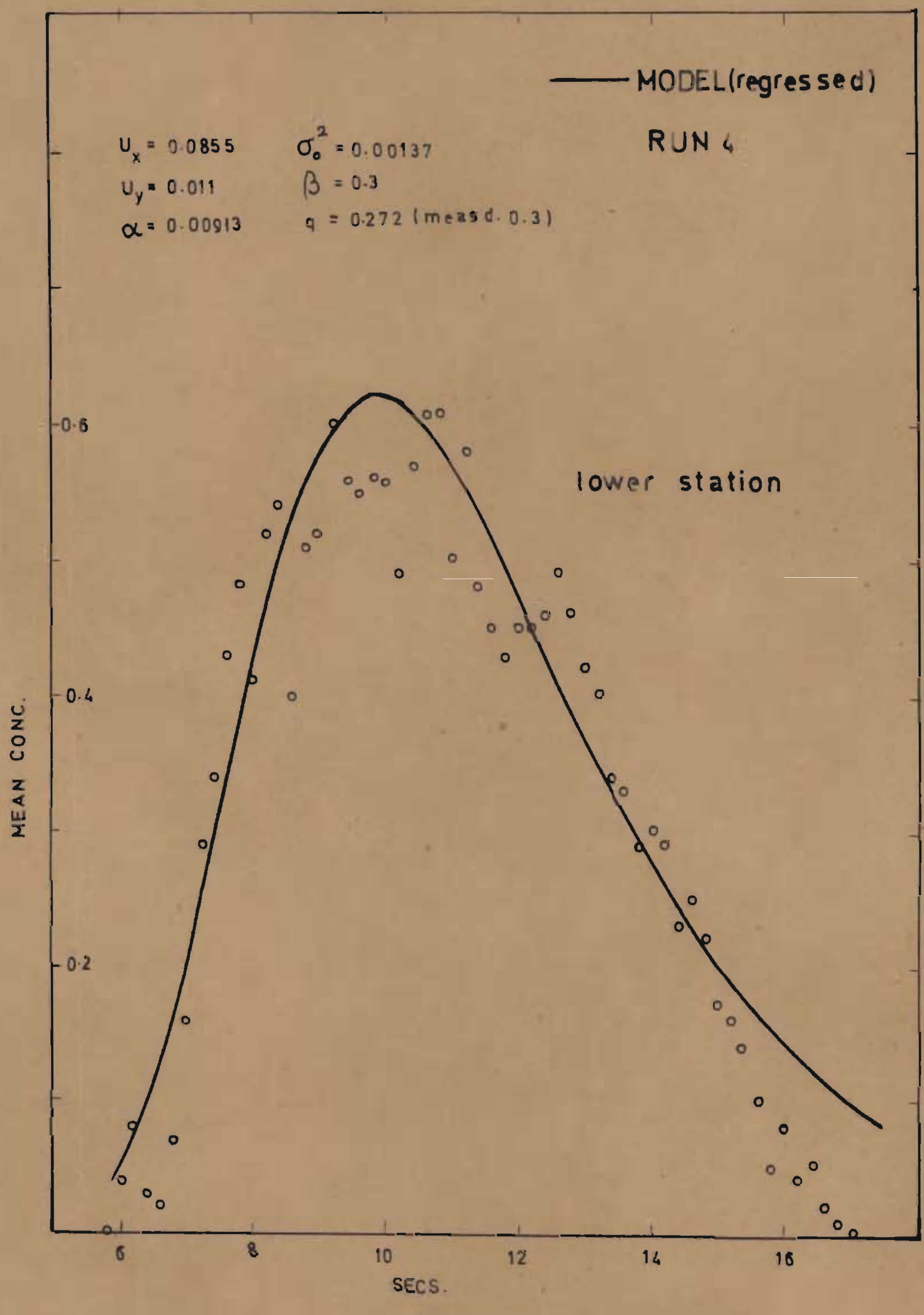
MODEL(regressed)
RUN 4
U_x = 0.0855
U_y = 0.011
α = 0.00913
σ_o^2 = 0.00137
β = 0.3
q = 0.272 (measd. 0.3)
lower station
MEAN CONC.
0.2
0.4
0.6
6
8
10
12
14
16
SECS.

FIG. 6.6

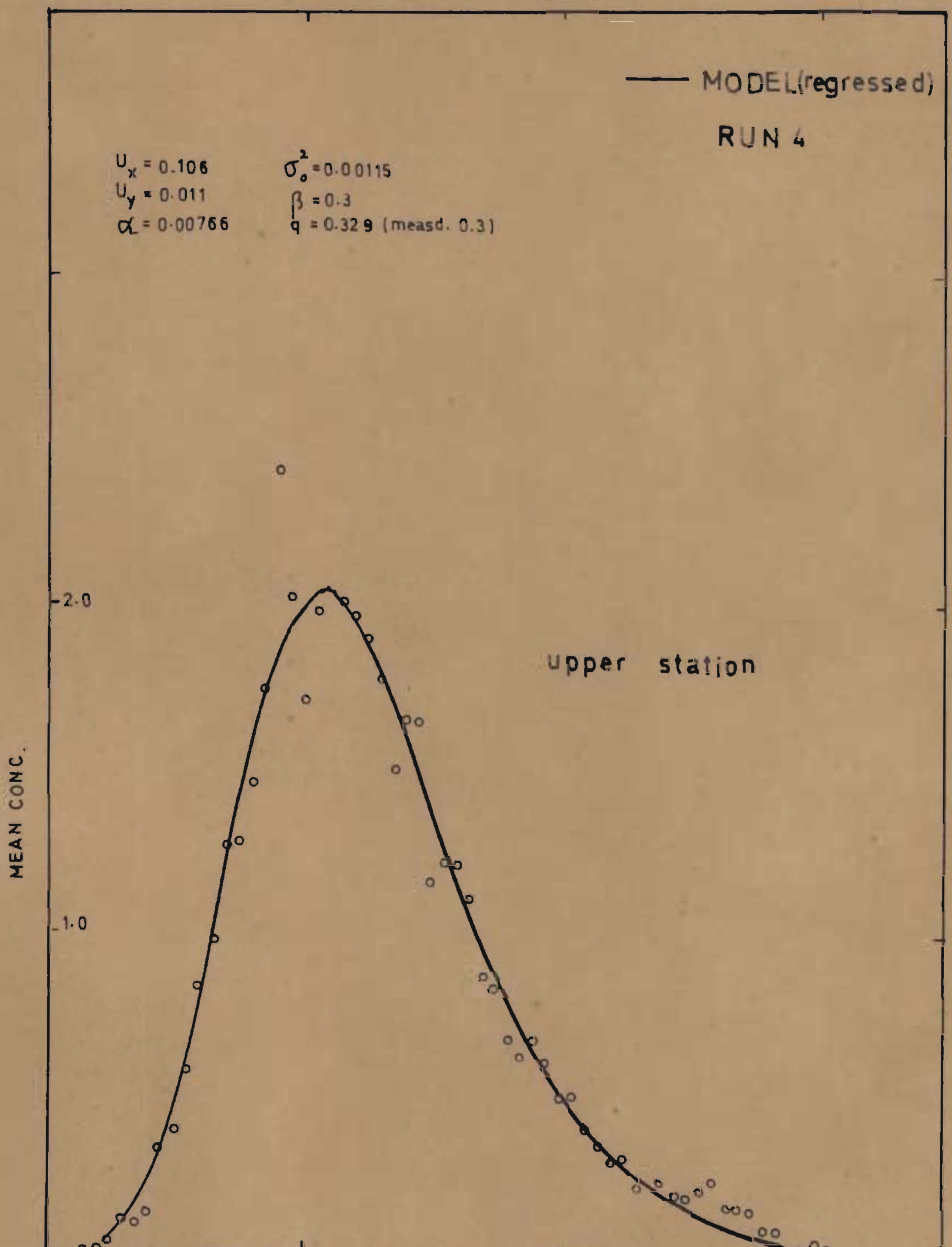
MODEL(regressed)
RUN 4
U_x = 0.106
U_y = 0.011
α = 0.00766
σ_0^2 = 0.00115
β = 0.3
q = 0.329 (measd. 0.3)
upper station
MEAN CONC.
2.0
1.0
4
8
12
16
SECS.

FIG. 6.7

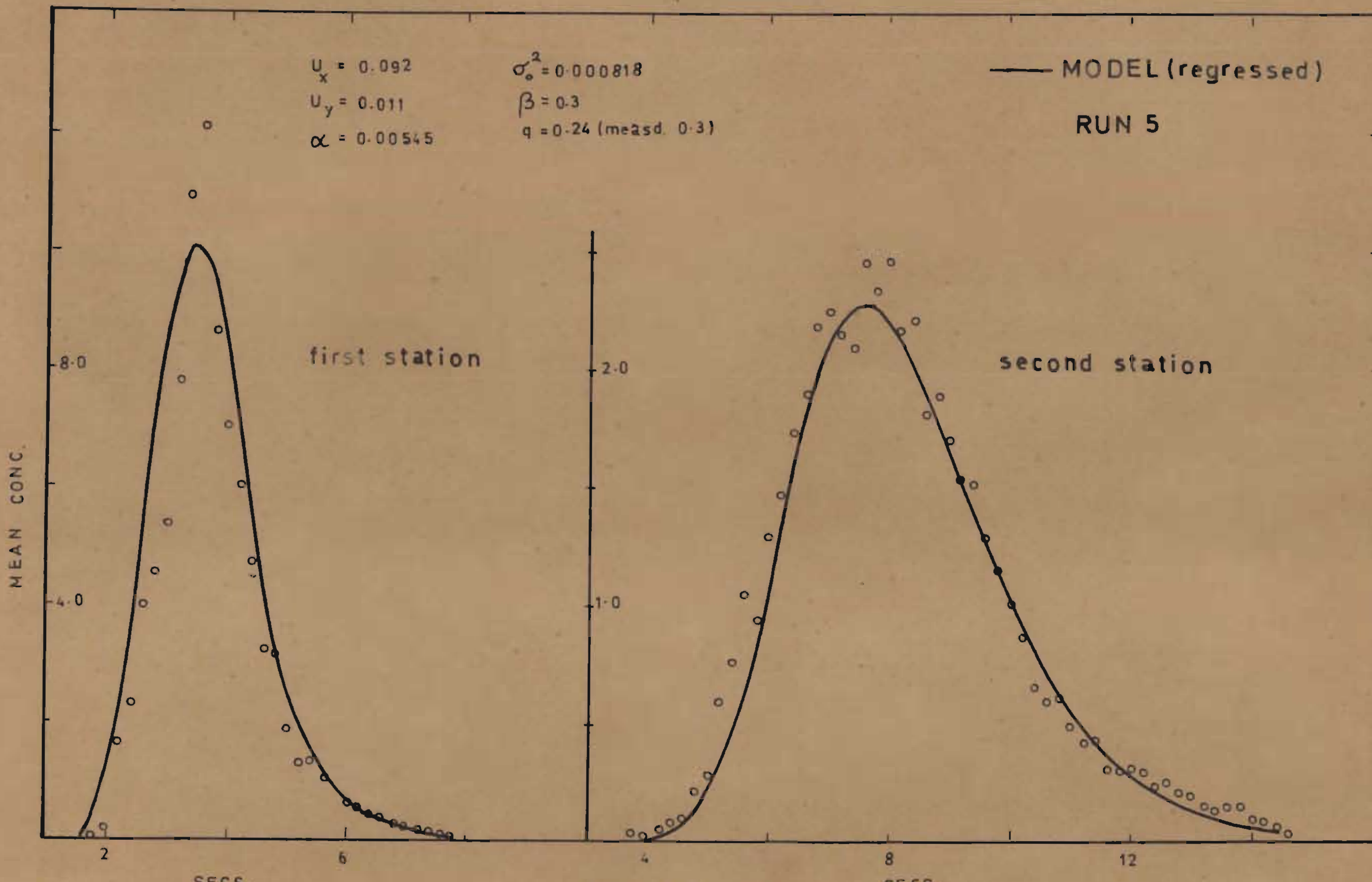

U_x = 0.092
U_y = 0.011
α = 0.00545
σ_o^2 = 0.000818
β = 0.3
q = 0.24 (measd. 0.3)
MODEL (regressed)
RUN 5
MEAN CONC.
8.0
4.0
2.0
1.0
first station
second station
2
6
4
8
12
SECS.
SECS.

FIG. 6.8

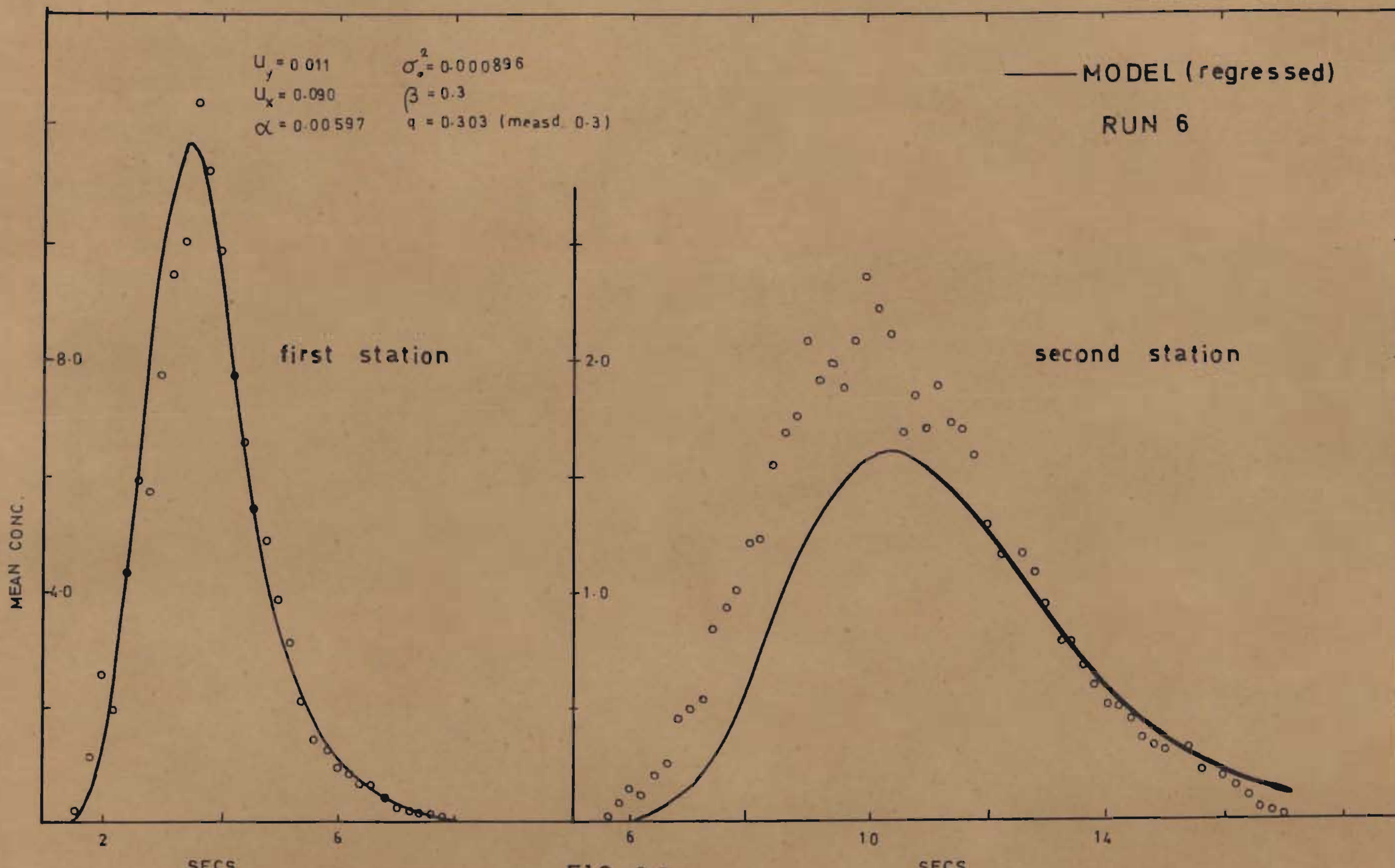

U_y = 0.011
U_x = 0.090
α = 0.00597
σ_o^2 = 0.000896
β = 0.3
q = 0.303 (measd. 0.3)
MODEL (regressed)
RUN 6
first station
second station
MEAN CONC.
8.0
4.0
2.0
1.0
2
6
10
14
SECS.
SECS.

FIG. 6-9

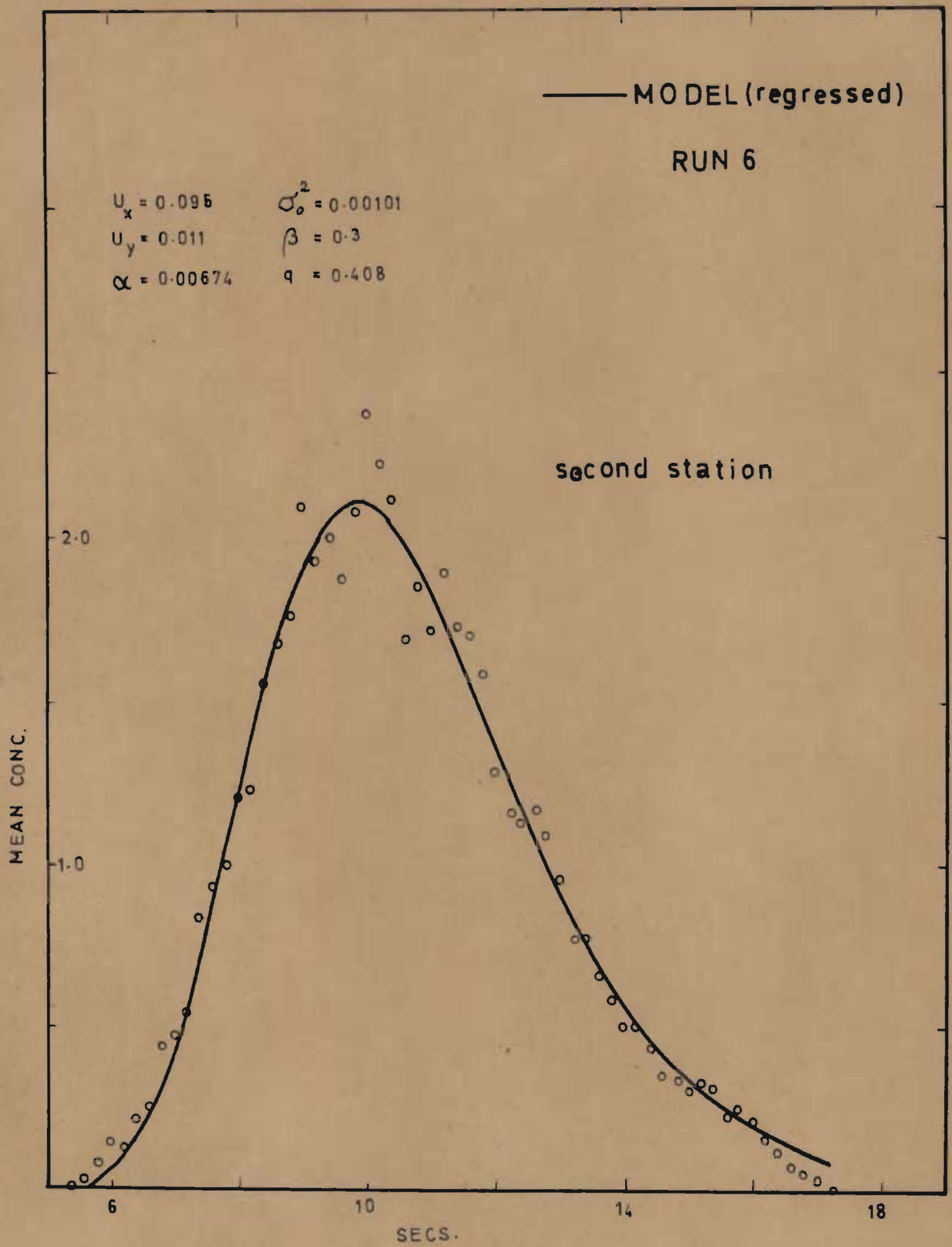
MODEL (regressed)
RUN 6
U_x = 0.095
U_y = 0.011
α = 0.00674
σ_o^2 = 0.00101
β = 0.3
q = 0.408
second station
MEAN CONC.
2.0
1.0
6
10
14
18
SECS.

FIG. 6.10

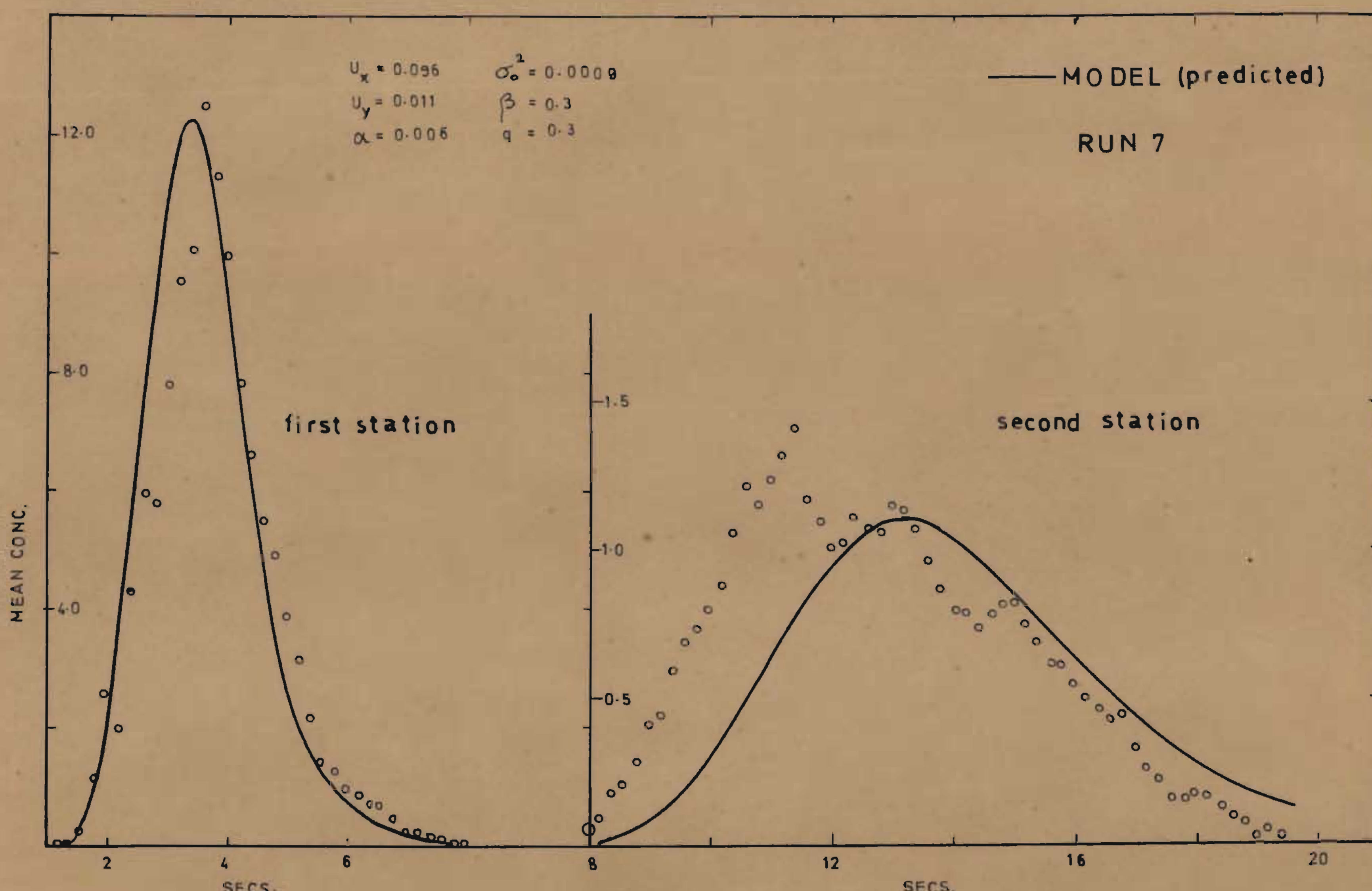
U_x = 0.096
U_y = 0.011
α = 0.006
σ_o^2 = 0.0009
β = 0.3
q = 0.3
MODEL (predicted)
RUN 7
first station
second station
MEAN CONC.
12.0
8.0
4.0
1.5
1.0
0.5
2
4
6
8
12
16
20
SECS.
SECS.

FIG. 6-11

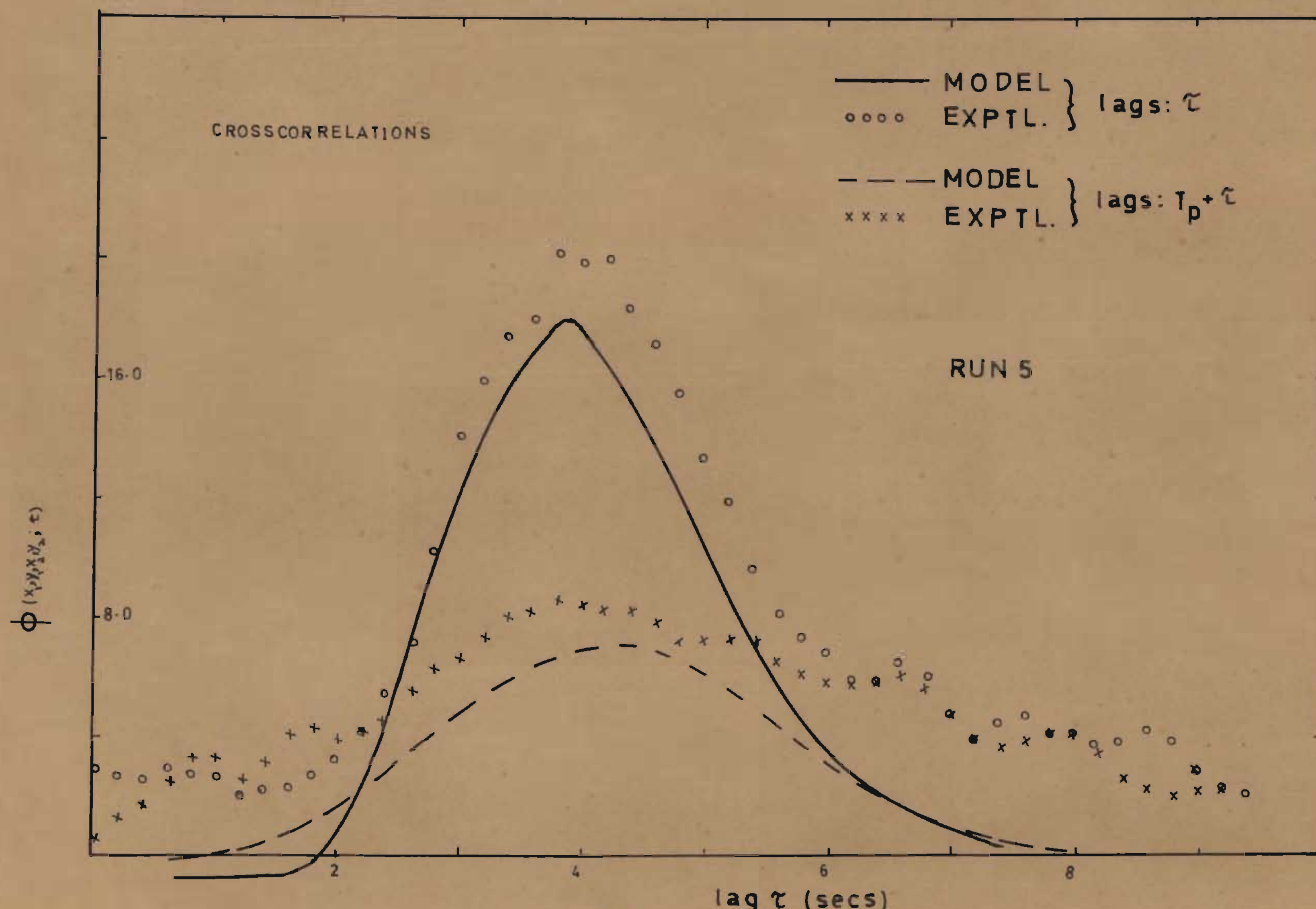
CROSSCORRELATIONS
MODEL
EXPTL.
lags: τ
MODEL
EXPTL.
lags: Tp+τ
RUN 5
16·0
8·0
2
4
6
8
lag τ (secs)

FIG. 6.12

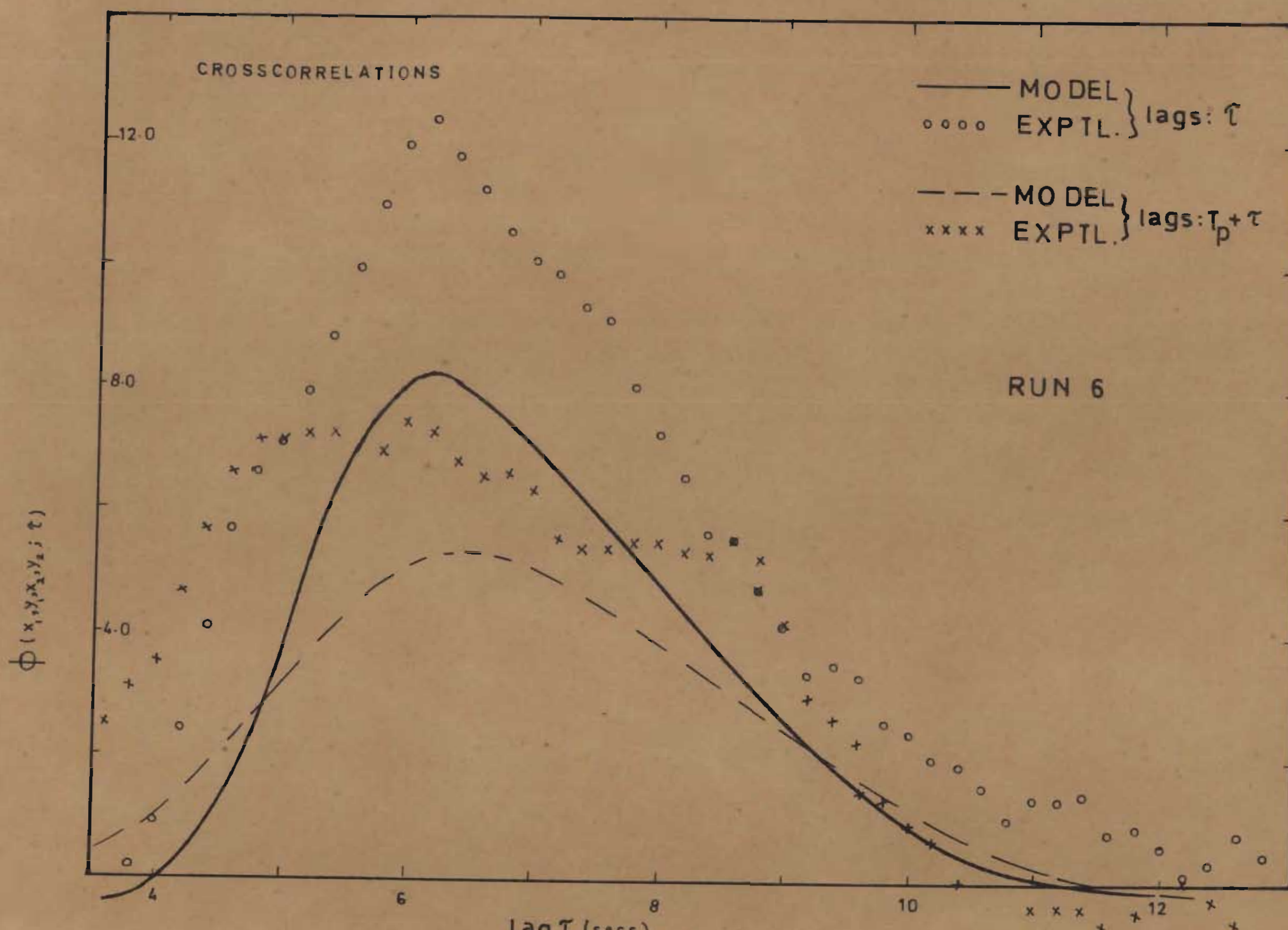
CROSSCORRELATIONS
MODEL
EXPTL.
lags: τ
MODEL
EXPTL.
lags: $T_p + \tau$
RUN 6
12.0
8.0
4.0
4
6
8
10
12
lag τ (secs.)
$\phi(x_1, y_1, x_2, y_2; \tau)$

FIG. 6.13

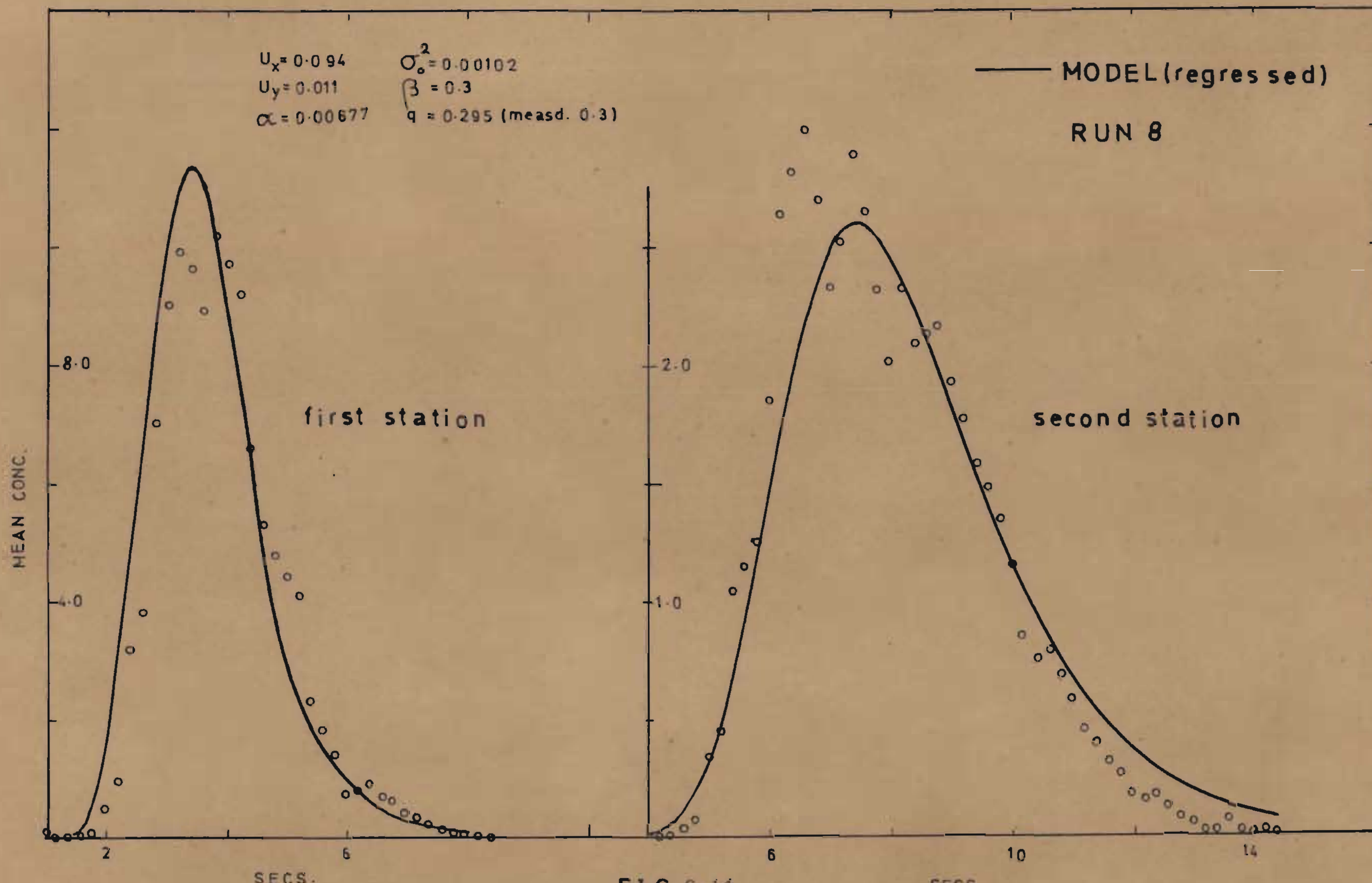

$U_x = 0.094$
$U_y = 0.011$
$\alpha = 0.00677$
$\sigma_o^2 = 0.00102$
$\beta = 0.3$
$q = 0.295$ (measd. 0.3)
MODEL (regressed)
RUN 8
first station
second station
MEAN CONC.
8.0
4.0
2.0
1.0
2
6
10
14
SECS.
SECS.

FIG. 6-14

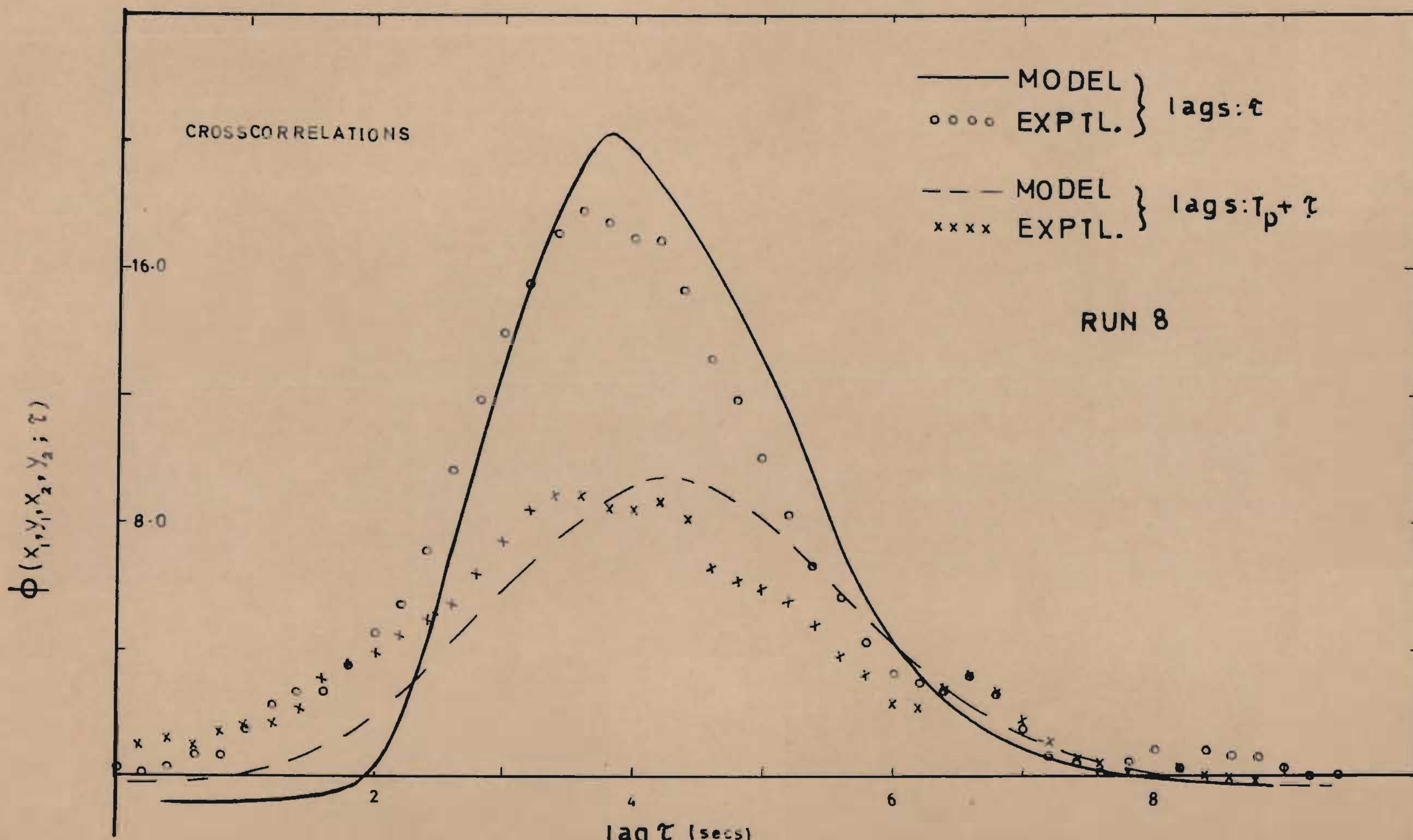

CROSSCORRELATIONS
MODEL
EXPTL.
lags: τ
MODEL
EXPTL.
lags: $T_p + \tau$
RUN 8
16·0
8·0
2
4
6
8
lag τ (secs)
$\phi(x_1, y_1, x_2, y_2; \tau)$

FIG. 6.15

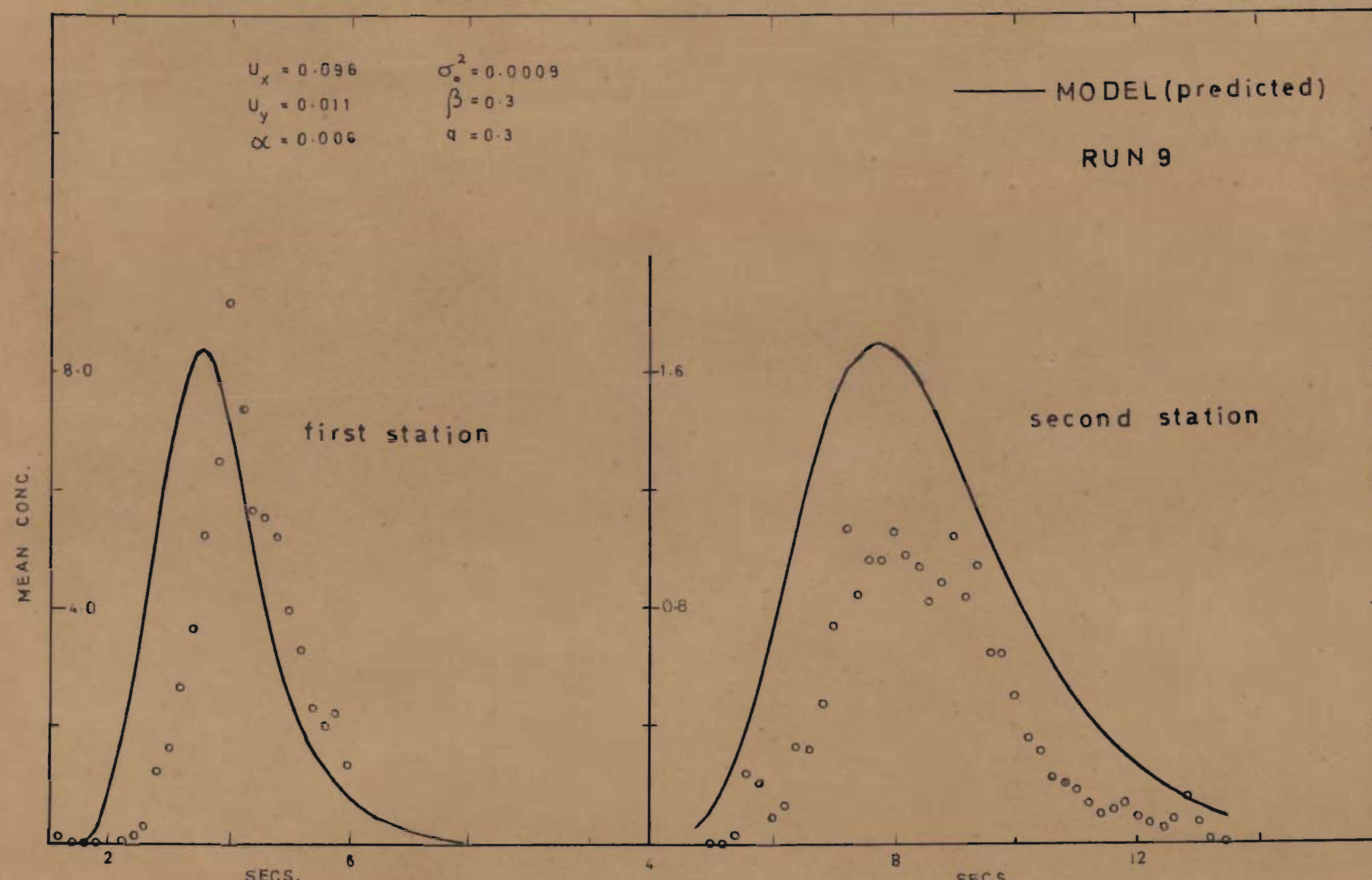

$U_x = 0{\cdot}096$
$U_y = 0{\cdot}011$
$\alpha = 0{\cdot}006$
$\sigma_o^2 = 0{\cdot}0009$
$\beta = 0{\cdot}3$
$q = 0{\cdot}3$
MODEL (predicted)
RUN 9
first station
second station
MEAN CONC.
8·0
4·0
1·6
0·8
2
6
4
8
12
SECS.
SECS.

FIG. 6.16

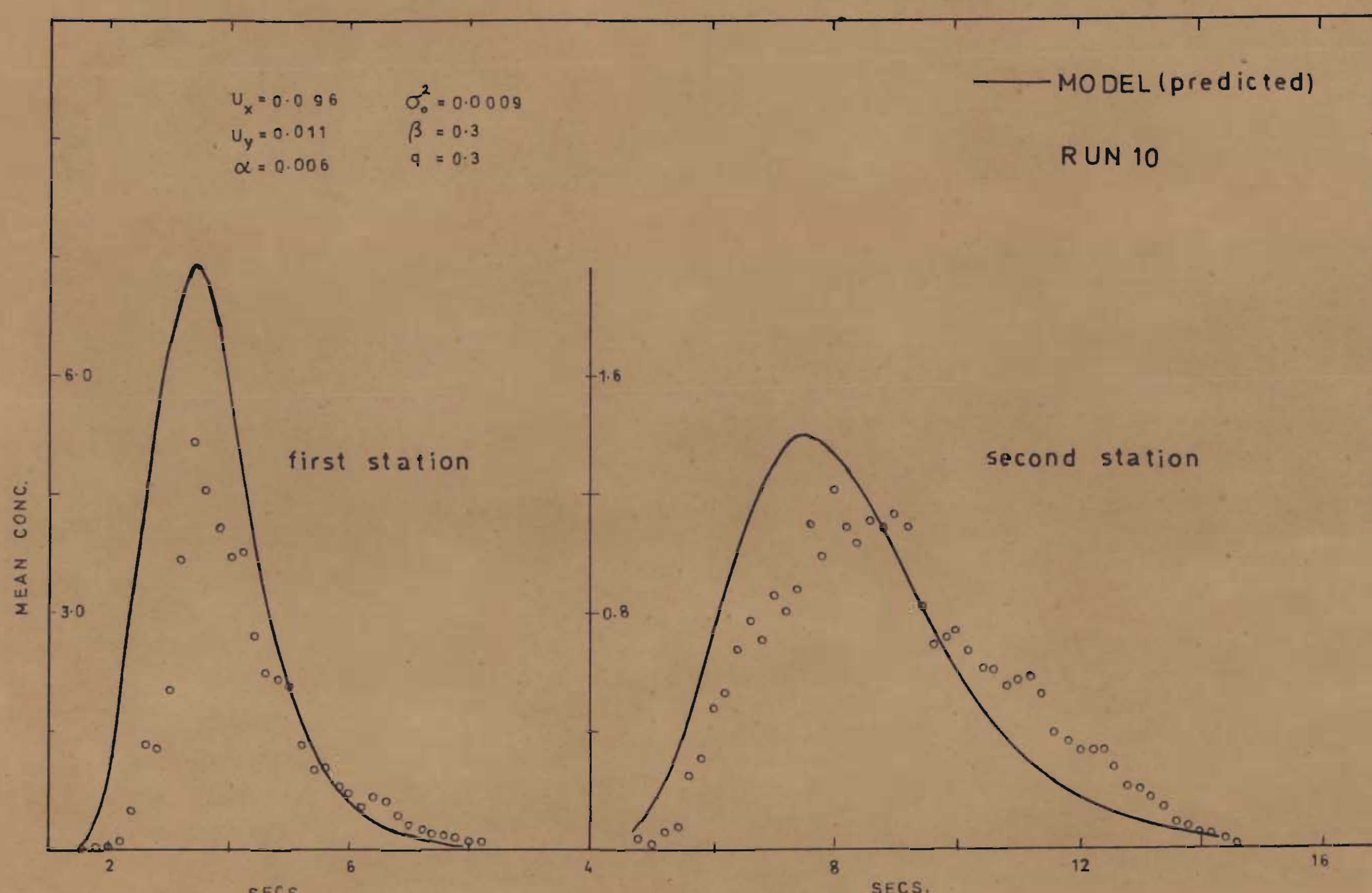

MODEL (predicted)
RUN 10
$U_x = 0{\cdot}0\,96$
$U_y = 0{\cdot}011$
$\alpha = 0{\cdot}006$
$\sigma_o^2 = 0{\cdot}0009$
$\beta = 0{\cdot}3$
$q = 0{\cdot}3$
first station
second station
MEAN CONC.
6·0
3·0
1·6
0·8
2
6
4
8
12
16
SECS.
SECS.

FIG. 6·17

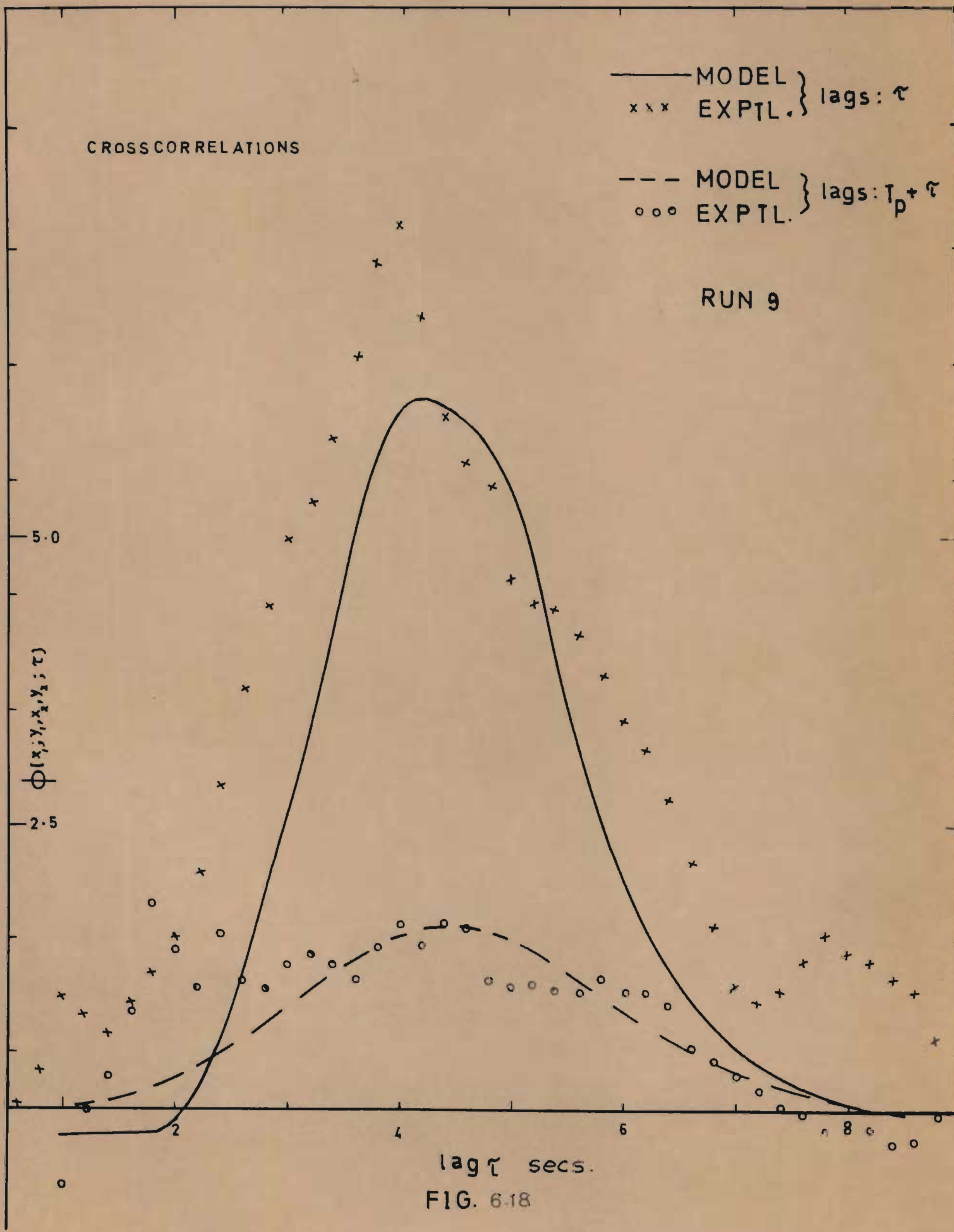
MODEL
EXPTL.
lags : τ
MODEL
EXPTL.
lags : T_p + τ
CROSSCORRELATIONS
RUN 9
5·0
2·5
$\phi(x_1; y_1, x_2, y_2; \tau)$
2
4
6
8
lag τ secs.

FIG. 6.18

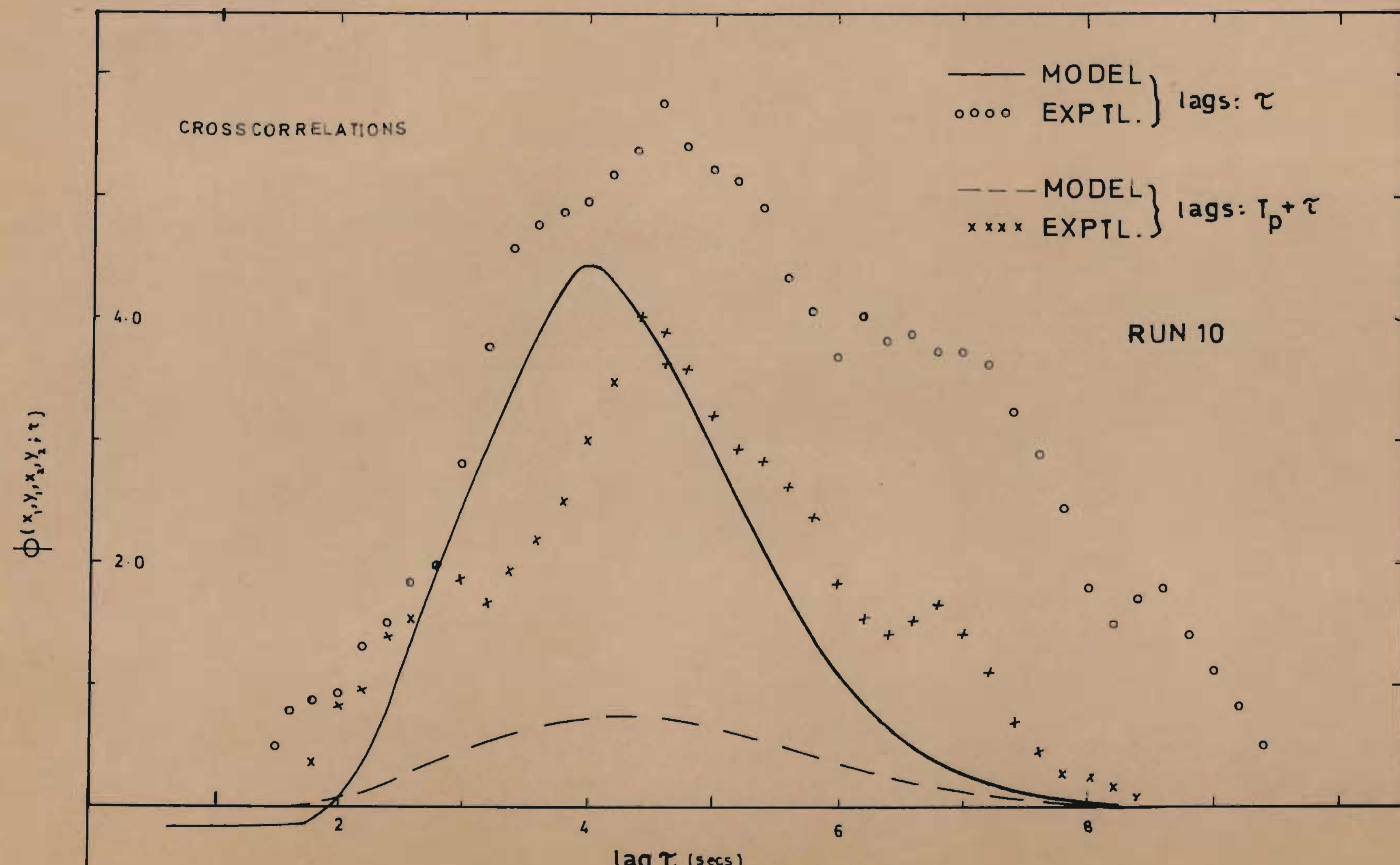
MODEL
EXPTL.
lags: τ
MODEL
EXPTL.
lags: $T_p + \tau$
CROSSCORRELATIONS
RUN 10
4.0
2.0
2
4
6
8
$\phi(x_1, y_1, x_2, y_2; \tau)$
lag τ (secs)

FIG. 6.19

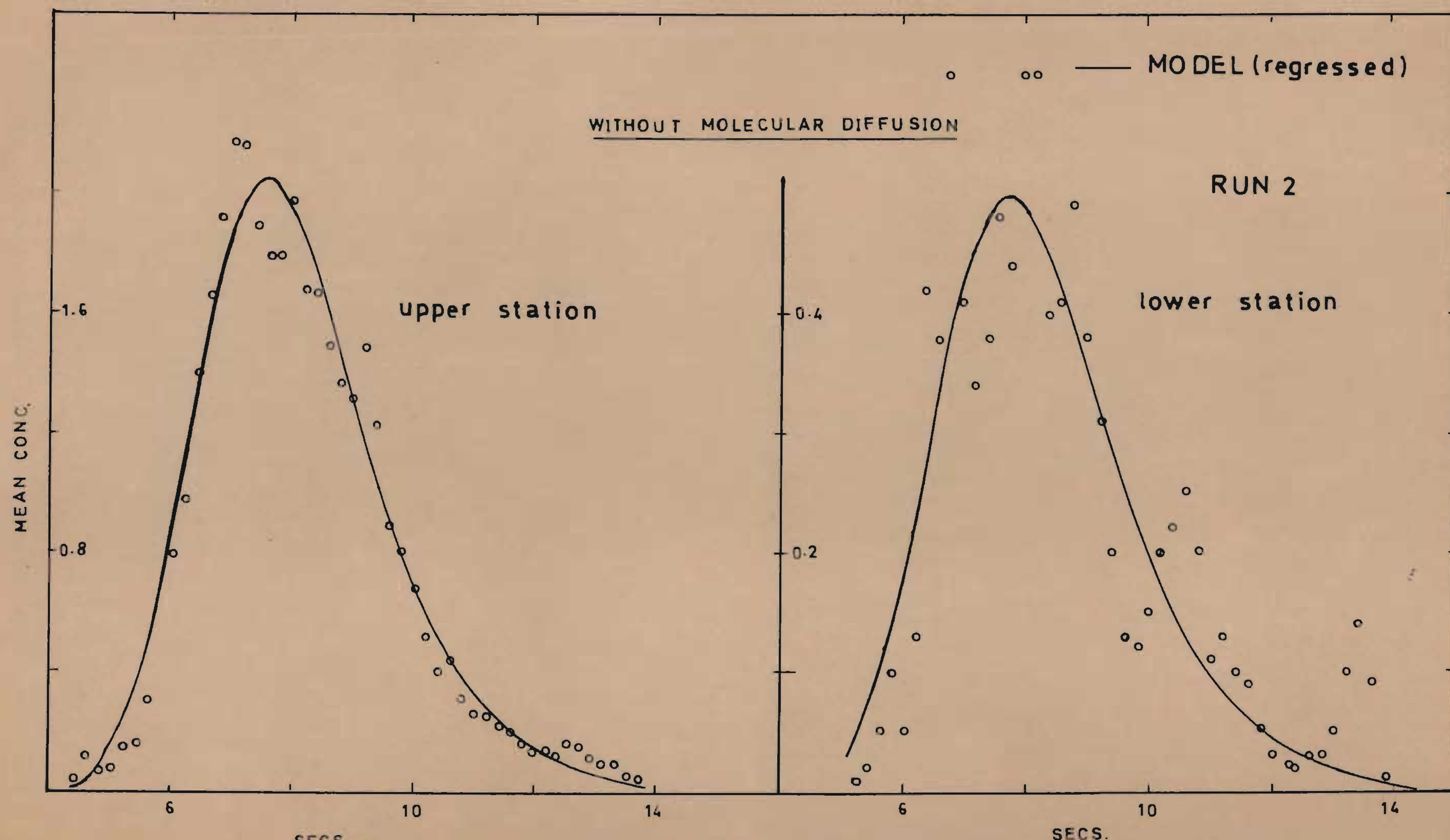
MODEL (regressed)
WITHOUT MOLECULAR DIFFUSION
RUN 2
upper station
lower station
MEAN CONC.
1.6
0.8
0.4
0.2
6
10
14
SECS.
SECS.

FIG. 6.20

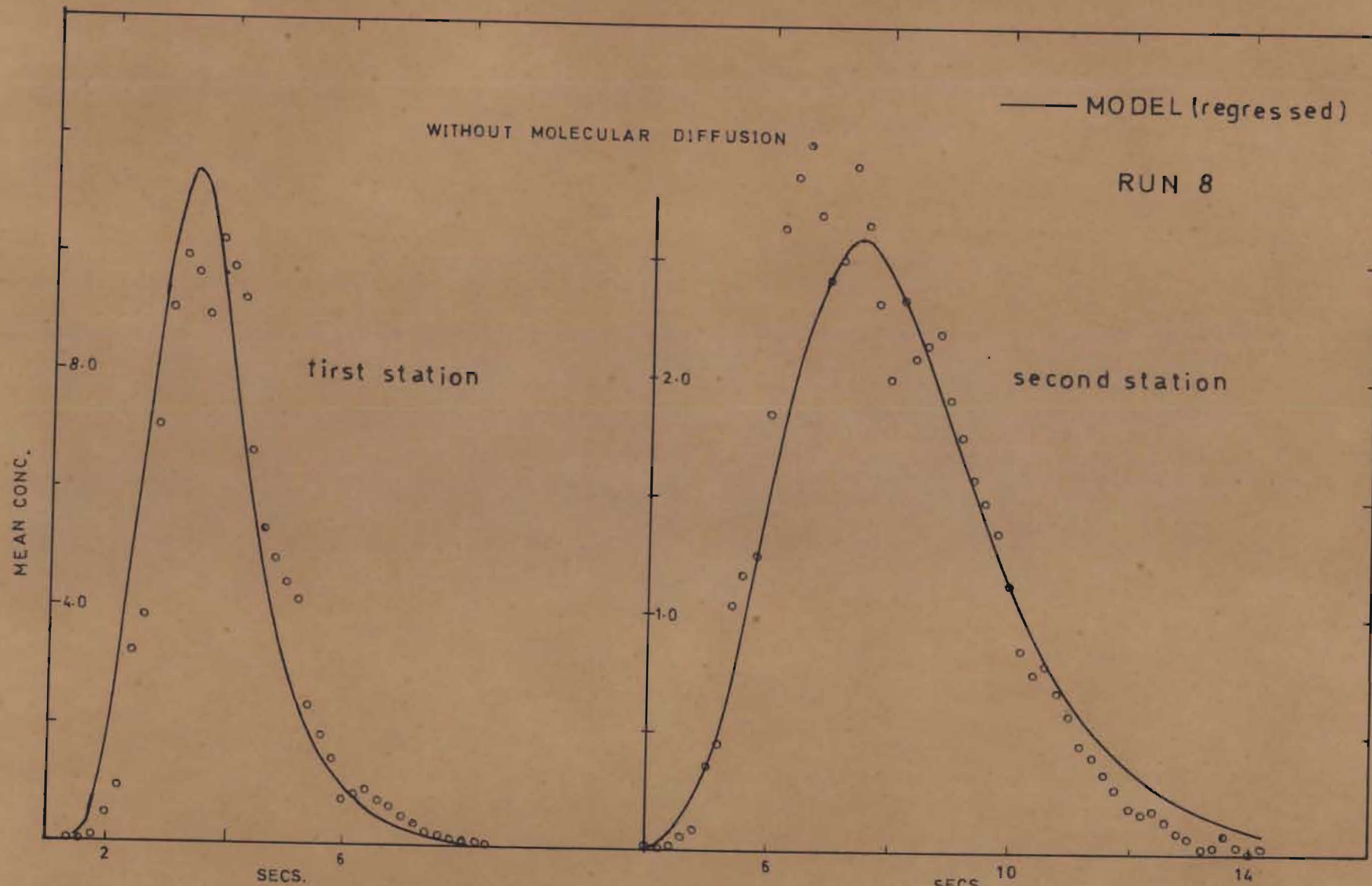
MODEL (regressed)
WITHOUT MOLECULAR DIFFUSION
RUN 8
MEAN CONC.
8.0
4.0
first station
2.0
1.0
second station
2
6
SECS.
6
10
14
SECS.
FIG. 6·21

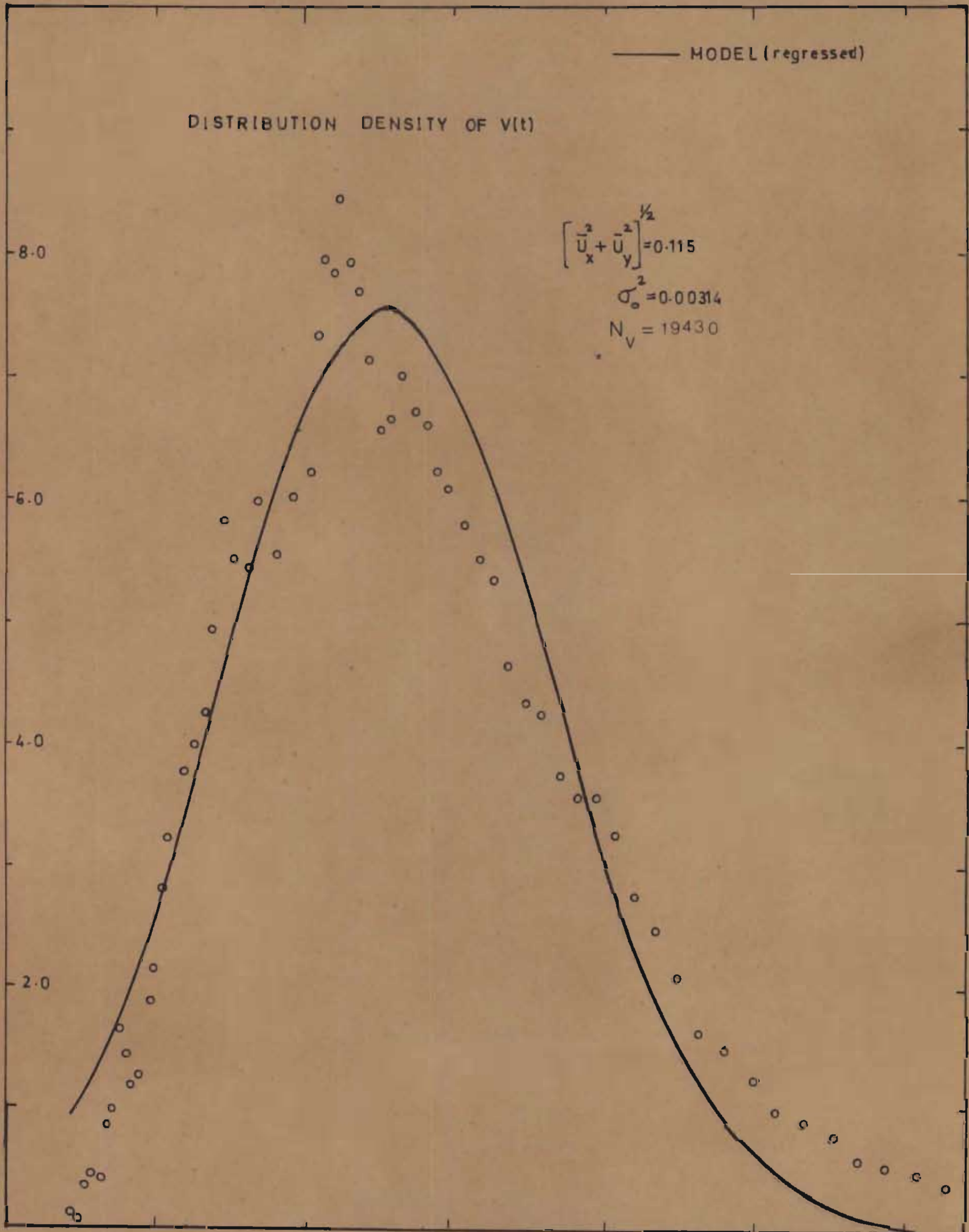
MODEL (regressed)
DISTRIBUTION DENSITY OF V(t)
$\left[\bar{U}_x^2 + \bar{U}_y^2\right]^{1/2} = 0.115$
$\sigma_o^2 = 0.00314$
$N_V = 19430$
8.0
6.0
4.0
2.0
0.1
0.2
0.3
FT. PER SEC.

FIG 6·22

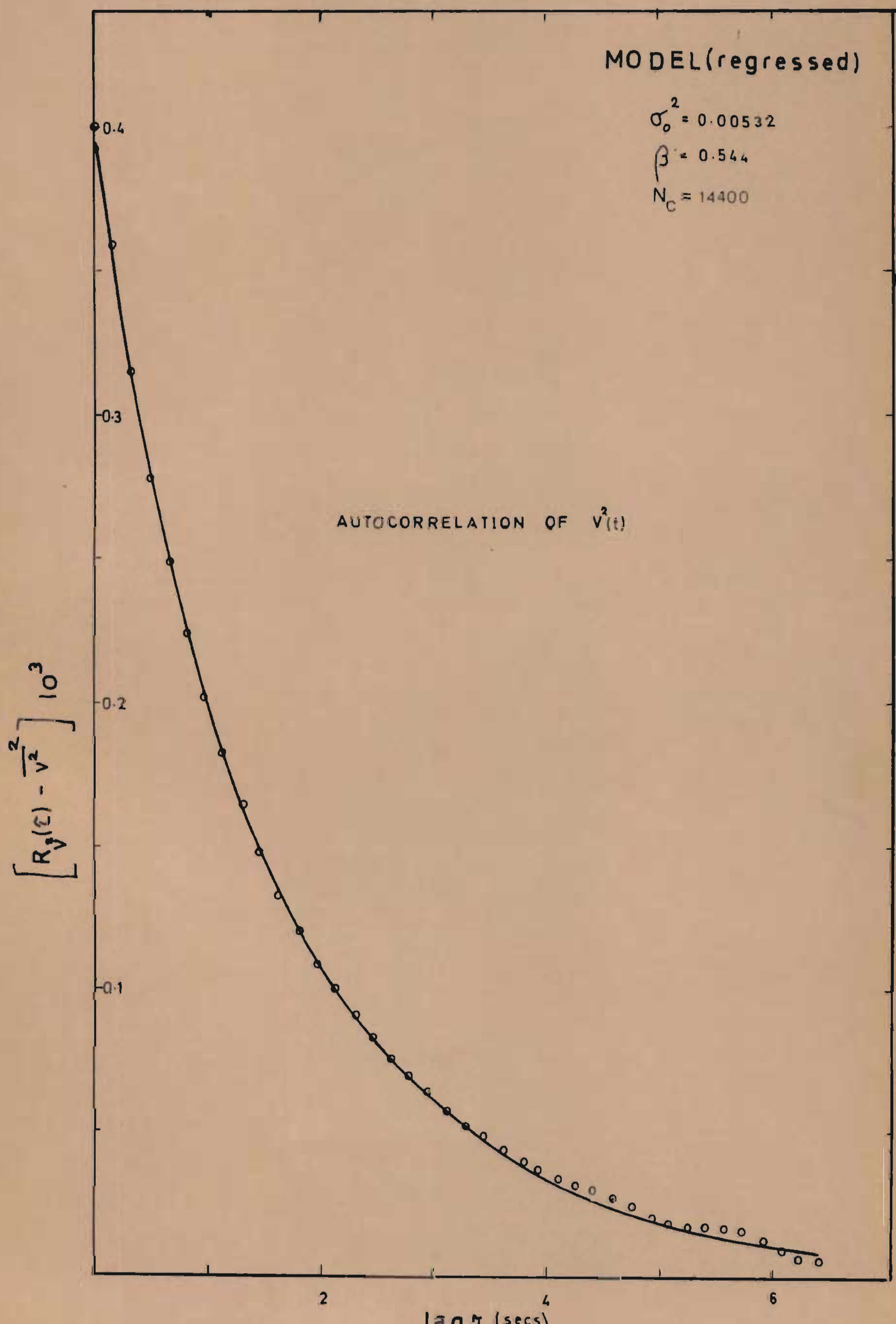
MODEL(regressed)
$\sigma_0^2 = 0.00532$
$\beta = 0.544$
$N_C = 14400$
AUTOCORRELATION OF $V^2(t)$
0.4
0.3
0.2
0.1
$\left[R_{v^2}(\tau) - \overline{v^2}^2\right] 10^3$
2
4
6
lag τ (secs)

FIG. 6-23

BIBLIOGRAPHY

1. Lumley J.L. and Corrsin S. Advances in Geophysics 1959 6 179. Edited by Frenkiel and Sheppard. Acad. Press Inc. N.Y. 1959.
2. Taylor G.I. Proc. London Math. Soc. Ser. 2 1921 20 196.
3. Bharucha-Reid A.T. Probabilistic Methods in Applied Mathematics. Volume 1, P 94. Academic Press 1968.
4. Krambeck F.J., Shinnar R., Katz S. I and EC Fundamentals, 1967 6 276.
5. Taylor G.I. Proc. Roy. Soc. 1935 151 444.
6. Doob J.L. Selected Papers on Noise and Stochastic Processes. Edited by Wax N P. 351.
7. Taylor G.I. Proc Roy. Soc. 1954 223.
8. Cox D.R. and Miller H.D. The Theory of Stochastic Processes. P. 183 Methuen.
9. de Karman T. and Howarth L. Proc Roy. Soc. 1938 164 192.
10. Papoulis A. Probability, Random Variables and Stochastic Processes. Chapter 8. P. 255. McGraw-Hill 1965.
11. King R.P. Chem. Eng. Sc. 1968 23 1035.
12. Doob J.L. Stochastic Processes. Chapters 2, 9. Wiley New York 1953.
13. Doob J.L. J. Appl. Math. 1942 43 357.
14. Dreifke G.E. Sc.D. Thesis, Washington University, 1961, P. 132.

BIBLIOGRAPHY (Continued)

15. Everson R.C. Ph.D. Thesis, University of Natal, South Africa, P. 50.

16. Clements W.C. Schnelle K.B. I and E.C. Proc. Des. and Development 1963 2 2 94.

17. Brown R.G. and Nilsson J.W. Introduction to Linear Systems Analysis. Chapter 12 P. 329.

18. Briggs P., Hammond P. Hughes M. and Plumb G. Proc. Inst. Mech. Eng. 1964 - 1965 79 Part 3H.

19. Roberts P.D. and Davis R.H. Proc. I.E.E., 1966 113 190.

20. Papoulis A. Probability, Random Variables and Stochastic Processes. Chapter 7 P. 196. McGraw-Hill 1965.

21. Middleton D. Statistical Communication Theory. Chapter 7 P. 338.

22. Law V.J. and Bailey R.V. Chem. Eng. Sci. 1963, 18 189.

23. Ornstein L.S. and Uehlenbeck G.E. Selected Papers on Noise and Stochastic Processes. P. 93. Edited by N. Wax. Dover 1954.

24. Bellman, R. Quant. Appl. Maths. 1957 14 353.

25. Papoulis A. Probability, Random Variables and Stochastic Processes. Chapter 14 P. 502. McGraw-Hill 1965.

APPENDIX 1

EDDY DIFFUSION MODEL ** ERROR ESTIMATION

The error incurred by the application of the Eddy Diffusion model to tracer experiments carried out in this work may be estimated as follows :

From Taylor (2):

$$\bar{X}^2(t) = 2\sigma_0^2 \int_0^t \int_0^{\tau_1} R_N(\tau)\, d\tau\, d\tau_1 \qquad 1.A$$

If $R_N(\tau)$ reaches zero at $\tau = t_1$ and $t > t_1$, we may write :

$$\int_0^t \int_0^{\tau_1} R_N(\tau)\, d\tau d\tau_1 = \int_0^t \{\int_0^{t_1} R_N(\tau)\, d\tau + \int_{t_1}^{\tau_1} R_N(\tau)\, d\tau\} d\tau_1$$

$$= At - \int_0^t \int_{\tau_1}^{t_1} R_N(\tau)\, d\tau\, d\tau_1 \qquad 1.B$$

where,

$$A = \int_0^{t_1} R_N(\tau)\, d\tau$$

The last term of Equation 1.B may be split up as follows:

$$\int_0^t \int_{\tau_1}^{t_1} R_N(\tau)\, d\tau d\tau_1 = \int_0^{t_1} \int_{\tau_1}^{t_1} R_N(\tau) d\tau d\tau_1 + \int_{t_1}^{t} \int_{\tau_1}^{t_1} R_N(\tau) d\tau d\tau_1 \qquad 1.C$$

Since the value of τ_1 ranges from t_1 to t and $t > t_1$, the last term of Equation 1.C equals zero. From Equations 3.3 it follows that :

$$R_N(\tau) = \exp\{-\beta|\tau|\} \qquad 1.D$$

Substitution of Equation 1.D in Equation 1.B followed by integration yields :

$$\bar{X}^2(t) = \frac{2\,\sigma_0^2}{\beta}\{ t - \frac{1}{\beta}(1 - \exp{-\beta t_1}) + t_1 \exp(-\beta t_1)\}$$

Since the Eddy Diffusion model implies : (7)

$$\overline{X}^2(t) = 2\sigma_0^2 At = \frac{2\sigma_0^2 t}{\beta}$$

the percentage error becomes :

$$\frac{\left| - \frac{1}{\beta}\{1 - \exp(-\beta t_1)\} + t_1 \exp(-\beta t_1) \right|}{t - \frac{1}{\beta}\{1 - \exp(-\beta t_1)\} + t_1 \exp(-\beta t_1)} \; 100$$

Substitution of the following values in the above expression gives a percentage error of 30%.

$\beta = 0.3$; $t_1 = 8$ secs. (see Figure 6.23) ; $t = 10$ secs.

APPENDIX 2

DERIVATION OF KOLMOGOROV EQUATIONS FOR DISCRETE SPACE MODEL

The transition probability density function $\pi(j,c_2;t_o+\tau|i,c_1;t_o)$ is defined such that $\pi(j,c_2;t_o+\tau|i,c_1;t_o)dc_2$ represents the probability that at time $t_o+\tau$ the flow is in state j and the concentration at x_2,y_2 has a value between c_2 and c_2+dc_2 knowing that at time t_o the flow was in state i and the concentration at the point x_1,y_1 had a value c_1.

If the source strength q(t) is known flow state and concentration form a composite Markov Process and hence we may write the Chapman-kolmogorov equation :

$$\pi(j,c_2;t_o+\tau+\Delta\tau|i,c_1;t_o) =$$

$$\sum_k\int_{-\infty}^{\infty}\pi(j,c_2;t_o+\tau+\Delta\tau|k,c_2-\Delta c;t_o+\tau)\pi(k,c_2-\Delta c;t_o+\tau|i,c_1;t_o)\ d\Delta c \tag{2.A}$$

Assuming first and second order derivatives to exist the integrand of Equation 2.A may be expanded in a closed Taylor series about c_2 :

$$\pi(j,c_2;t_o+\tau+\Delta\tau|i,c_1;t_o) =$$

$$\sum_k\int_{-\infty}^{\infty}\pi(j,c_2+\Delta c;t_o+\tau+\Delta\tau|k,c_2;t_o+\tau)\pi(k,c_2;t_o+\tau|i,c_1;t_o)\ d\Delta c\ -$$

$$\sum_k\int_{-\infty}^{\infty}\frac{\partial}{\partial c_2}\{\pi_1(0)\pi_2(0)\}\Delta c\ d\Delta c\ +\ \sum_k\int_{-\infty}^{\infty}\frac{\partial^2}{\partial c_2^2}\{\pi_1(\theta_{1k})\pi_2(\theta_{2k})\}\frac{\Delta c^2}{2}\ d\Delta c$$

where,

$$\pi_1(\theta_{1k}) = \pi_1(j,c_2+\theta_{1k}\Delta c;t_o+\tau+\Delta\tau|k,c_2;t_o+\tau)$$

$$\pi_2(\theta_{2k}) = \pi_2(k,c_2-\theta_{2k}\Delta c;t_o+\tau|i,c_1;t_o)$$

$$0 \leqslant \theta_{1k},\ \theta_{2k} \leqslant 1$$

Integrating the first term of Equation 2.B and rearranging the second and third terms yields :

$$\pi(j,c_2;t_o+\tau+\Delta\tau|i,c_1;t_o) =$$

$$\sum_k \pi(j;t_o+\tau+\Delta\tau|k,c_2;t_o+\tau)\ \pi(k,c_2;t_o+\tau|i,c_1;t_o) -$$

$$\sum_k \frac{\partial}{\partial c_2}\{\pi_2(0)\int_{-\infty}^{\infty}\Delta c\pi_1(j,c_2+\Delta c;t_o+\tau+\Delta\tau|k,c_2;t_o+\tau)\ d\Delta c\} -$$

$$\sum_k \frac{\partial^2}{\partial c_2^2}\{\int_0^{\infty}\frac{\Delta c^2}{2}\ \pi_1(\theta_{1k})\ \pi_2(\theta_{2k})\ d\Delta c\} \qquad 2.C$$

Since the probability of a change in flow state is independent of concentration and assumed to be time-stationary we may write :

$$\pi(j;t_o+\tau+\Delta\tau|k,c_2t_o+\tau) = \pi(j|\ k:\Delta\tau) \qquad 2.D$$

where,

$$\pi(j|k:\Delta\tau) = \delta_{kj} + \lambda_{kj}\Delta\tau + O(\Delta\tau) \qquad 2.E$$

Furthermore, since the concentration at the point x_2,y_2 and time $t_o+\tau$ has the value c_2 and the flow is in state k, the second term of the RHS of Equation 2.C may be written as : (integral part only)

$$\int_{-\infty}^{\infty}\frac{\partial c_2}{\partial t}\ \Delta\tau\ \pi_1(j,c_2+\Delta c;t_o+\tau+\Delta\tau|k,c_2;t_o+\tau)\ d\Delta c \qquad 2.F$$

provided $\Delta\tau$ is small.

$\frac{\partial c_2}{\partial t}$ is evaluated at time $t_o+\tau$ and flow state k; hence

$$\frac{\partial c_2}{\partial t} = - u_{xk} \frac{\partial c_2}{\partial x} - u_{yk} \frac{\partial c_2}{\partial y} + q(t)\delta(x)\delta(y)$$

$$= \alpha(k,c_2) \qquad 2.G$$

Similarly, the third term of the RHS of Equation 2.C may be written as : (integral part only)

$$\int_{-\infty}^{\infty} \frac{\alpha^2(k,c_2)}{2} \Delta\tau^2 \, \pi_1(\theta_{1k}) \, \pi_2(\theta_{2k}) \, d\Delta c$$

and 2.F becomes :

$$\alpha(k,c_2) \; \Delta\tau$$

Substituting Equations 2.D, 2.E, 2.F and 2.G in Equation 2.C , dividing by $\Delta\tau$ and letting $\Delta\tau \to 0$, yields the following Kolmogorov equation :

$$\frac{\partial \pi}{\partial \tau}(j,c_2;t_o+\tau|i,c_1;t_o) = \sum_k \lambda_{kj} \, \pi(k,c_2;t_o+\tau|i,c_1;t_o)$$

$$- \frac{\partial}{\partial c_2}\{\alpha(j,c_2)\pi(j,c_2;t_o+\tau|i,c_1;t_o)\} \qquad 2.H$$

The Kolmogorov equation associated with $p(j,c;t)$ is obtained by multiplying each term of Equation 2.H by $p(i,c_1;t)$, integrating over all values of c_1 and summing over all possible flow states i.

Writing

$$c = c_2 \quad ; \quad t = \tau + t_o$$

we obtain :

$$\frac{\partial p}{\partial t}(j,c;t) = \sum_k \lambda_{kj} p(k,c;t) - \frac{\partial}{\partial c}\{\alpha(j,c)p(j,c;t)\} \qquad 2.I$$

Similarly, a Kolmogorov equation associated with $p(j,q,c;t)$ may be derived; it has the following form :

$$\frac{\partial p(j,q,c;t)}{\partial t} = \sum_k \lambda_{kj} p(k,q,c;t) - \frac{\partial}{\partial q}\{\alpha_q(j,q)p(j,q,c;t)\}$$
$$- \frac{\partial}{\partial c}\{\alpha_c(j,c)p(j,q,c;t)\} \qquad 2.J$$

where,

$$\alpha_q(j,q) = E\{\frac{dQ(t)}{dt} | Q(t)=q, \text{ flow state } = j\}$$

For the case of a time-stationary random source function $Q(t)$ the following Kolmogorov equation will hold :

$$\frac{\partial \pi(j,q_1,c|i,q:\tau)}{\partial \tau} = \sum_k \lambda_{kj} \pi(k,q_1,c|i,q:\tau)$$
$$- \frac{\partial}{\partial q_1}\{\alpha_{q_1}(j,q_1,c)\ \pi(j,q_1,c|i,q:\tau)\}$$
$$- \frac{\partial}{\partial c}\{\alpha_c(j,q_1,c)\ \pi(j,q_1,c|i,q:\tau)\} \qquad 2.K$$

APPENDIX 3

DERIVATION OF EQUATION 2.30

The partial crosscorrelation is defined as :

$$\Phi_{jqc}(0) = \int_0^\infty\int_0^\infty qc\ p(j,q,c;t)\ dq\ dc \qquad 2.A$$

Differentiating Equation 2.A with respect to t and substituting Equation 2.20 yields :

$$\frac{\partial\Phi_{jqc}(0)}{\partial t} = \int_0^\infty\int_0^\infty qc\ \sum_k \lambda_{kj} p(k,q,c;t)\ dq\ dc -$$

$$\int_0^\infty\int_0^\infty qc\ \frac{\partial}{\partial q}\{\alpha_q(j,q,c;t)p(j,q,c;t)\}\ dq\ dc -$$

$$\int_0^\infty\int_0^\infty qc\ \frac{\partial}{\partial c}\{\alpha_c(j,q,c;t)p(j,q,c;t)\}\ dq\ dc \qquad 2.B$$

Substituting Equation 2.A and integrating by parts :

$$\frac{\partial\Phi_{jqc}(0)}{\partial t} = \sum_k \lambda_{kj}\Phi_{kqc}(0) - \int_0^\infty c \left| q\alpha_q(jqc;t)p(j,q,c;t) \right|_{q=0}^{q=\infty} dc$$

$$+ \int_0^\infty\int_0^\infty c\alpha_q(j,q,c;t)p(j,q,c;t)dqdc - \int_0^\infty q \left| c\alpha_c(j,q,c;t)p(j,q,c;t) \right|_{c=0}^{c=\infty} dq$$

$$+ \int_0^\infty\int_0^\infty q\alpha_c(j,q,c;t)p(j,q,c;t)\ dq\ dc \qquad 2.C$$

where,

$\alpha_q(j,q,c;t)$ and $\alpha_c(j,q,c;t)$ are defined by Equations 2.21 and 2.22.

If Q(t) is obtained from the output of a first order filter (time constant T_c) with input $N_w(t)$, we can write :

$$T_c \frac{dQ(t)}{dt} + Q(t) = N_w(t) \qquad 2.D$$

Since the value of the source strength at time t does not depend on the concentration at point (x,y) at time t, Equation 2.21 becomes :

$$\alpha_q(j,q,c;t) = E\{\frac{dQ(t)}{dt} \mid Q(t) = q, \text{ flow state } = j\}$$

From Equation 2.D it follows that :

$$\alpha_q(j,q,c;t) = \frac{1}{T_c} E\{N_w(t) \mid Q(t) = q\} - \frac{q}{T_c} \qquad 2.E$$

From Equation 2.22 it follows that :

$$\alpha_c(j,q,c;t) = - u_{xj} \frac{\partial c}{\partial x} - u_{yj} \frac{\partial c}{\partial y} + q(t)\delta(x)\delta(y) \qquad 2.F$$

Since $p(j,\infty,c;t) = p(j,q,\infty;t) = 0$, the second and fourth terms of the RHS of Equation 2.C equal zero.

Substituting Equations 2.E and 2.F in Equation 2.C yields :

$$\frac{\partial \Phi_{jqc}(0)}{\partial t} = \sum_k \lambda_{kj} \Phi_{kqc}(0) + \frac{1}{T_c}\int_0^\infty\int_0^\infty c\, E\{N_w(t) \mid Q(t)=q\} p(j,q,c;t)\,dq\,dc$$

$$- \frac{1}{T_c}\int_0^\infty\int_0^\infty cq p(j,q,c;t)\,dq\,dc - u_{xj}\int_0^\infty\int_0^\infty q\frac{\partial c}{\partial x}\, p(j,q,c;t)\,dq\,dc$$

$$- u_{yj}\int_0^\infty\int_0^\infty q\frac{\partial c}{\partial y}\, p(j,q,c;t)\,dq\,dc + \int_0^\infty\int_0^\infty q^2\delta(x)\delta(y)\, p(j,q,c;t)\,dq\,dc \qquad 2.G$$

Consider the last term of Equation 2.G; integrating with respect to c and noting that $p(j,q;t) = p(j;t)p(q;t)$, it may be written as : $R_{qq}(0,t)p(j;t)\delta(x)\delta(y)$ where,

$R_{qq}(\tau,t)$ = Autocorrelation of $Q(t)$

Integrating the second term of the RHS of Equation 2.G with respect to q and substituting Equations 2.14 and 2.A in Equation 2.G for a time-stationary process finally yields

APPENDIX 4

EVALUATION OF COVARIANCE $\rho(t,\tau_1;t+\tau,\tau_2)$

$$\rho(t,\tau_1;t+\tau,\tau_2) = \int_{\tau_2}^{t+\tau}\int_{\tau_1^0}^{t} \sigma^2 \exp\{-\beta(|\theta'-\theta''|)\}d\theta'\, d\theta''$$

case A

$$t+\tau > t > \tau_2 \gtrless \tau_1$$

The region of integration is subdivided and the integral of each part is evaluated separately :

$$\int_{t}^{t+\tau}\int_{\tau_1}^{t} \exp\{-\beta(\theta''-\theta')\}d\theta'\, d\theta'' = -\frac{1}{\beta^2}\Big(\{\exp(-\beta\tau) - 1\}$$

$$- \left[\exp\{-\beta(t+\tau-\tau_1)\} - \exp\{-\beta(t-\tau_1)\}\right]\Big)$$

$$\int_{\tau_2}^{t}\int_{\tau_1}^{\theta''} \exp\{-\beta(\theta''-\theta')\}d\theta'\, d\theta'' = -\frac{1}{\beta^2}\Big(-\beta(t-\tau_2)$$

$$- \left[\exp\{-\beta(t-\tau_1)\} - \exp\{-\beta(\tau_2-\tau_1)\}\right]\Big)$$

$$\int_{\tau_2}^{t}\int_{\theta''}^{t} \exp\{-\beta(\theta'-\theta'')\}d\theta'\, d\theta'' =$$

$$-\frac{1}{\beta^2}\Big(1 - \exp\{-\beta(t-\tau_2)\} - \beta(t-\tau_2)\Big)$$

Adding the three contributions yields :

$$\int_{\tau_2}^{t+\tau}\int_{\tau_1}^{t} \exp\{-\beta(|\theta'-\theta''|)\}d\theta'\, d\theta'' = \frac{1}{\beta^2}\Big(- \exp(-\beta\tau) +$$

$$\exp\{-\beta(t+\tau-\tau_1)\} + 2\beta(t-\tau_2) - \exp\{-\beta(\tau_2-\tau_1)\} + \exp\{-\beta(t-\tau_2)\}\Big)$$

case B

$$t+\tau > t > \tau_1 \gtrless \tau_2$$

The region of integration is subdivided into two parts :

$$\int_{\tau_1}^{t}\int_{\theta'}^{t+\tau} \exp\{-\beta(\theta''-\theta')\}d\theta''\, d\theta' = -\frac{1}{\beta^2}\Big[\exp(-\beta\tau) - \exp\{-\beta(t+\tau-\tau_1)\} - \beta(t-\tau_1)\Big]$$

$$\int_{\tau_1}^{t}\int_{\tau_2}^{\theta'} \exp\{-\beta(\theta'-\theta'')\}d\theta''\, d\theta' = -\frac{1}{\beta^2}\Big[-\beta(t-\tau_1) - \exp\{-\beta(t-\tau_2)\} - \exp\{-\beta(\tau_1-\tau_2)\}\Big]$$

Adding the two contributions yields :

$$\int_{\tau_2}^{t+\tau}\int_{\tau_1}^{t} \exp\{-\beta(|\theta'-\theta''|)\, d\theta'\, d\theta'' = \frac{1}{\beta^2}\Big[-\exp(-\beta\tau) + 2\beta(t-\tau_1) + \exp\{-\beta(t+\tau-\tau_1)\} + \exp\{-\beta(t-\tau_2)\} - \exp\{-\beta(\tau_1-\tau_2)\}\Big]$$

<u>case C</u>

$$t + \tau > \tau_2 \geq t > \tau_1$$

$$\int_{\tau_2}^{t+\tau}\int_{\tau_1}^{t} \exp\{-\beta(|\theta''-\theta'|)\}d\theta'\, d\theta'' = \frac{1}{\beta^2}\Big[-\exp(-\beta\tau) + \exp\{-\beta(t+\tau-\tau_1)\} + \exp\{-\beta(\tau_2-t)\} - \exp\{-\beta(\tau_2-\tau_1)\}\Big]$$

APPENDIX 5

MIXING EQUATIONS FOR CONTINUOUS STATE FLOW MODEL WITH MOLECULAR DIFFUSION.

Dispersion is described by the following stochastic partial differential equation :

$$\frac{\partial C}{\partial t} = - U_x(t)\frac{\partial C}{\partial x} + D\,\frac{\partial^2 C}{\partial x^2} - U_y(t)\frac{\partial C}{\partial t} + D\,\frac{\partial^2 C}{\partial y^2} + q(t)\delta(x)\delta(y) \qquad 5.A$$

Defining a two-sided Laplace Transform by :

$$L\{C(x,y,t)\} = \bar{C}(s,p,t) = \int_{-\infty}^{\infty}\int_{-\infty}^{\infty} C(x,y,t)\,\exp(-sx)\exp(-py)\,dx\,dy$$

we obtain expressions for $L\{\frac{\partial C}{\partial x}\}$ and $L\{\frac{\partial^2 C}{\partial x^2}\}$ as follows :

$$L\{\frac{\partial C}{\partial x}\} = \int_{-\infty}^{\infty}\int_{-\infty}^{\infty} \frac{\partial C}{\partial x}\,\exp(-sx)\,\exp(-py)\,dx\,dy \qquad 5.B$$

Integrating Equation 5.B by parts and noting that $C(x,y,t) = 0$, when $x,y = -\infty$, yields :

$$L\{\frac{\partial C}{\partial x}\} = s\bar{C}(s,p,t) \quad ; \quad L\{\frac{\partial C}{\partial y}\} = p\bar{C}(s,p,t) \qquad 5.C$$

$$L\{\frac{\partial^2 C}{\partial x^2}\} = \int_{-\infty}^{\infty}\int_{-\infty}^{\infty} \frac{\partial^2 C}{\partial x^2}\,\exp(-sx)\,\exp(-py)\,dx\,dy$$

$$= \int_{-\infty}^{\infty} \left|\frac{\partial C}{\partial x}\,\exp(-sx)\right|_{-\infty}^{\infty} \exp(-py)\,dy \; -$$

$$\int_{-\infty}^{\infty}\int_{-\infty}^{\infty} (-s)\,\frac{\partial C}{\partial x}\,\exp(-sx)\,\exp(-py)\,dx\,dy$$

Assuming that $\frac{\partial C}{\partial x}$ converges sufficiently strongly as $x \to -\infty$, the first term equals zero. Substitution of Equation 5.C yields :

$$L\{\frac{\partial^2 C}{\partial x^2}\} = s^2\bar{C}(s,p,t) \quad ; \quad L\{\frac{\partial^2 C}{\partial y^2}\} = p^2\bar{C}(s,p,t) \qquad 5.D$$

Taking the Laplace Transform of Equation 5.A :

$$\frac{d\bar{C}}{dt} = -U_x(t)s\bar{C} + Ds^2\,\bar{C} - U_y(t)p\bar{C} + Dp^2\,\bar{C} + q(t) \qquad 5.E$$

and solving Equation 5.E with initial condition

$C(x,y,0) = 0 \quad ; \quad \bar{C}(s,p,0) = 0$, yields :

$$\bar{C}(s,p,t) = \int_0^t q(\tau)\ \exp\{s^2D(t-\tau) - sW_x(t,\tau) + p^2D(t-\tau) - pW_y(t,\tau)\}d\tau \qquad 5.F$$

where $W_x(t,\tau)$ and $W_y(t,\tau)$ are defined by Equations 3.11.

Noting that

$$\int_{-\infty}^{\infty} \exp\{\frac{-(x-ut)^2}{4Dt}\}\exp(-sx)\ dx = 2(\pi Dt)^{\frac{1}{2}}\ \exp(s^2Dt-sut)$$

Equation 5.F may be inverted as follows :

$$C(x,y,t) = \int_0^t \frac{q(\tau)}{4\pi D(t-\tau)}\ \exp\left(\frac{-\{x-W_x(t,\tau)\}^2 - \{y-W_y(t,\tau)\}^2}{4D(t-\tau)}\right)\ d\tau \qquad 5.G$$

<u>Mean concentration $\mu(x,y,t)$</u>

The mean concentration is defined as :

$$\mu(x,y,t) = \int_{-\infty}^{\infty}\int_{-\infty}^{\infty} c(x,y,t)\ f(w_x,t,\tau)\ f(w_y,t,\tau)\ dw_x\ dw_y \qquad 5.H$$

where,

$f(w_x,t,\tau)$ and $f(w_y,t,\tau)$ are Normal probability density functions for the Random Processes $W_x(t,\tau)$ and $W_y(t,\tau)$.

Substituting in Equation 5.H and integrating with respect to w_x and w_y by the method of completing the square finally yields Equation 3.40.

Crosscorrelation $\Phi(x_1,y_1,x_2,y_2:\tau)$

When the tracer source is a time-stationary function Q(t) the concentration at a point (x,y) is given by :

$$C(x,y,t) = \int_{-\infty}^{t} \frac{Q(\tau)}{4\pi D(t-\tau)} \exp\left(\frac{-\{x-W_x(t,\tau)\}^2 - \{y-W_y(t,\tau)\}^2}{4D(t-\tau)}\right) d\tau \quad 5.I$$

The concentration crosscorrelation between points (x_1,y_1) and (x_2,y_2) is defined as :

$$\Phi(x_1,y_1,x_2,y_2:\tau) = E\{C(x_1,y_1,t)C(x_2,y_2,t+\tau)\} \quad 5.J$$

Substituting Equation 5.I and rearranging exponential terms yields :

$$\Phi(x_1,y_1,x_2,y_2:\tau) = E\{ \int_{-\infty}^{t+\tau}\int_{-\infty}^{t} \frac{Q(\tau_1)Q(\tau_2)}{(4\pi D)^2(t-\tau_1)(t+\tau-\tau_2)}$$

$$\exp\left(\frac{-(x_1-W_{x1})^2}{4D(t-\tau_1)} - \frac{(x_2-W_{x2})^2}{4D(t+\tau-\tau_2)}\right)$$

$$\exp\left(\frac{-(y_1-W_{y1})^2}{4D(t-\tau_1)} - \frac{(y_2-W_{y2})^2}{4D(t+\tau-\tau_2)}\right) d\tau_1\, d\tau_2\} \quad 5.K$$

Since the tracer source function Q(t) and the Random Processes $W_x(t,\tau)$, $W_y(t,\tau)$ are mutually independent Equation 5.K may be written as :

$$\Phi(x_1,y_1,x_2,y_2:\tau) = \int_{-\infty}^{t+\tau}\int_{-\infty}^{t} \frac{E\{Q(\tau_1)Q(\tau_2)\}}{(4\pi D)^2(t-\tau_1)(t+\tau-\tau_2)}$$

$$\int_{-\infty}^{\infty}\int_{-\infty}^{\infty} \exp\left(\frac{-(x_1-w_{x1})^2}{4D(t-\tau_1)} - \frac{(x_2-w_{x2})^2}{4D(t+\tau-\tau_2)}\right) f(w_{x1},w_{x2})\, dw_{x1}\, dw_{x2}$$

$$\int_{-\infty}^{\infty}\int_{-\infty}^{\infty} \exp\left(\frac{-(y_1-w_{y1})^2}{4D(t-\tau_1)} - \frac{(y_2-w_{y2})^2}{4D(t+\tau-\tau_2)}\right) f(w_{y1},w_{y2})\, dw_{y1}\, dw_{y2}\, d\tau_1\, d\tau_2 \quad 5.L$$

where,

$f(w_{x1},w_{x2})$ = joint Normal probability density function for W_{x1} and W_{x2}.

$f(w_{y1},w_{y2})$ = joint Normal probability density function for W_{y1} and W_{y2}.

The above density functions have the following form (see Equations 3.29) :

$$f(w_{x1},w_{x2}) = \frac{1}{2\pi(1-r^2)^{\frac{1}{2}}} \exp\left[\frac{-1}{(1-r^2)}\left\{\frac{(w_{x1}-m_{1x,1})^2}{\sigma_{1,1}^2} - \frac{2r(w_{x1}-m_{1x,1})(w_{x2}-m_{1x,2})}{\sigma_{1,1}\,\sigma_{1,2}} - \frac{(w_{x2}-m_{1x,2})^2}{\sigma_{1,2}^2}\right\}\right]$$

$$f(w_{y1},w_{y2}) = \frac{1}{2\pi(1-r^2)^{\frac{1}{2}}} \exp\left[\frac{-1}{(1-r^2)}\left\{\frac{(w_{y1}-m_{1y,1})^2}{\sigma_{1,1}^2} - \frac{2r(w_{y1}-m_{1y,1})(w_{y2}-m_{1y,2})}{\sigma_{1,1}\,\sigma_{1,2}} - \frac{(w_{y2}-m_{1y,2})^2}{\sigma_{1,2}^2}\right\}\right] \quad 5.M$$

Substituting Equations 5.M in Equation 5.L and carrying out the integrations with respect to w_{x1},w_{x2},w_{y1} and w_{y2} by the method of completing the square yields :

$$\Phi(x_1,y_1,x_2,y_2:\tau) = \int_{-\infty}^{t+\tau}\int_{-\infty}^{t} \frac{E\{Q(\tau_1)Q(\tau_2)\}}{(4\pi D)^2(t-\tau_1)(t+\tau-\tau_2)\{2\pi\sigma_{1,1}\sigma_{1,2}(1-r^2)^{\frac{1}{2}}\}^2}$$

$$\pi^2\left\{\frac{1}{\alpha_1}+\frac{1}{\beta_1}\right\}^{-1}\left[\frac{1}{\alpha_2}+\frac{1}{\beta_2}-\left\{\frac{1}{\alpha_1}+\frac{1}{\beta_1}\right\}^{-1}\frac{r^2}{(1-r^2)^2\gamma^2}\right]^{-1}$$

$$\exp-\left[\frac{x_1^2}{\alpha_1}+\frac{x_2^2}{\alpha_2}+\frac{m_{1x,1}^2}{\beta_1}+\frac{m_{1x,2}^2}{\beta_2}-\frac{2rm_{1x,1}m_{1x,2}}{(1-r^2)\,\gamma}-\left\{\frac{1}{\alpha_1}+\frac{1}{\beta_1}\right\}^{-1}\right.$$

$$\left.\left\{\left(\frac{x_1}{\alpha_1}+\frac{m_{1x,1}}{\beta_1}\right)^2+\frac{r^2m_{1x,2}^2}{(1-r^2)^2\gamma^2}-\frac{2rm_{1x,2}}{(1-r^2)\gamma}\left(\frac{x_1}{\alpha_1}+\frac{m_{1x,1}}{\beta_1}\right)\right\}\right]$$

$$\exp\left[\left(\frac{1}{\alpha_2}+\frac{1}{\beta_2}-\{\frac{1}{\alpha_1}+\frac{1}{\beta_1}\}^{-1}\frac{r^2}{(1-r^2)^2\gamma^2}\right)^{-1}\left(\frac{x_2}{\alpha_2}-\frac{rm_{1x,1}}{(1-r^2)\gamma}+\frac{m_{1x,2}}{\beta_2}+\right.\right.$$

$$\left.\left.\{\frac{1}{\alpha_1}+\frac{1}{\beta_1}\}^{-1}[\frac{r}{(1-r^2)\gamma}\{\frac{x_1}{\alpha_1}+\frac{m_{1x,1}}{\beta_1}\}-\frac{r^2m_{1x,2}}{(1-r^2)^2\gamma^2}]\right)^2\right]$$

$$\exp-\left[\frac{y_1^2}{\alpha_1}+\frac{y_2^2}{\alpha_2}+\frac{m_{1y,1}^2}{\beta_1}+\frac{m_{1y,2}^2}{\beta_2}-\frac{2rm_{1y,1}m_{1y,2}}{(1-r^2)\gamma}-\{\frac{1}{\alpha_1}+\frac{1}{\beta_1}\}^{-1}\right.$$

$$\left.\{\left(\frac{y_1}{\alpha_1}+\frac{m_{1y,1}}{\beta_1}\right)^2+\frac{r^2m_{1y,2}^2}{(1-r^2)^2\gamma^2}-\frac{2rm_{1y,2}}{(1-r^2)\gamma}\left(\frac{y_1}{\alpha_1}+\frac{m_{1y,1}}{\beta_1}\right)\}\right]$$

$$\exp\left[\left(\frac{1}{\alpha_2}+\frac{1}{\beta_2}-\{\frac{1}{\alpha_1}+\frac{1}{\beta_1}\}^{-1}\frac{r^2}{(1-r^2)^2\gamma^2}\right)^{-1}\left(\frac{y_2}{\alpha_2}-\frac{rm_{1y,1}}{(1-r^2)\gamma}+\frac{m_{1y,2}}{\beta_2}+\right.\right.$$

$$\left.\left.\{\frac{1}{\alpha_1}+\frac{1}{\beta_1}\}^{-1}[\frac{r}{(1-r^2)\gamma}\{\frac{y_1}{\alpha_1}+\frac{m_{1y,1}}{\beta_1}\}-\frac{r^2m_{1y,2}}{(1-r^2)^2\gamma^2}]\right)^2\right]d\tau_1\,d\tau_2$$

where,

$$\alpha_1 = 4D(t-\tau_1) \quad ; \quad \alpha_2 = 4D(t+\tau-\tau_2)$$

$$\beta_1 = (1-r^2)\sigma_{1,1}^2 \quad ; \quad \beta_2 = (1-r^2)\sigma_{1,2}^2$$

$$\gamma = \sigma_{1,1}\sigma_{1,2}$$

A transformation of variables according to Equations 3.31 finally yields Equation 3.44.

APPENDIX 6

INTRODUCTION OF FLOW PARAMETER α

It is assumed that the random process of velocity fluctuations is described by the following stochastic differential equation :

$$\frac{dU'(t)}{dt} + \beta U'(t) = \beta N_{\alpha}(t) \qquad 6.A$$

where,

$N_{\alpha}(t)$ has the following White Noise properties :

$$R_{N_{\alpha}}(\tau) = E\{N_{\alpha}(t)N_{\alpha}(t+\tau)\} = \alpha\delta(\tau)$$

$$PSD_{N_{\alpha}}(w) = \alpha \qquad 6.B$$

Equation 6.A may be integrated as follows :

$$U'(t) = \int_{0}^{t} \beta N_{\alpha}(\tau) \exp\{-\beta(t-\tau)\} \, d\tau \qquad 6.C$$

The autocorrelation of $U'(t)$ is defined by :

$$R_{o}(t_1,t_2) = E\{U'(t_1)U'(t_2)\}$$

Substituting Equation 6.C and taking the Expected Value operation inside the integral yields :

$$R_{o}(t_1,t_2) = \beta^2 \int_{0}^{t_2}\int_{0}^{t_1} E\{N_{\alpha}(\tau_1)N_{\alpha}(\tau_2)\} \exp\{-\beta(t_1+t_2-\tau_1-\tau_2)\} \, d\tau_1 \, d\tau_2 \qquad 6.D$$

From Equations 6.B and 6.D it follows that :

$$R_o(t_1,t_2) = \beta^2 \int_0^{t_2}\int_0^{t_1} \alpha\delta(\tau_1-\tau_2)\ \exp\{-\beta(t_1+t_2-\tau_1-\tau_2)\}d\tau_1\ d\tau_2 \qquad 6.E$$

Integrating Equation 6.E with respect to τ_1 and τ_2 for $t_1 > t_2$ yields :

$$R_o(t_1,t_2) = \frac{\alpha\beta}{2} \left(\exp\{-\beta(t_1-t_2)\} - \exp\{-\beta(t_1+t_2)\}\right) \qquad 6.F$$

For large values of t_1,t_2 the second exponential term of Equation 6.F is small and may be neglected. Hence :

$$R_o(t_1-t_2) = \frac{\alpha\beta}{2} \exp\{-\beta(t_1-t_2)\} \qquad 6.G$$

From Equations 6.G, 3.3, 5.21 it follows that :

$$\sigma_o^2 = \frac{\alpha\beta}{2}$$

APPENDIX 7

NOTE ON UNITS OF q(t) and C(t)

From equation 1.1 it follows that the units of $q(t) \cdot \delta(x) \cdot \delta(y)$ are $\frac{\text{concentration}}{\text{time}}$. Since concentration readings are integrated across the width of the tank (d), the units of concentration are $\frac{\text{mass}}{\text{area}}$ and the units of q(t) become $\frac{\text{mass}}{\text{time}}$. (see section 4.4)

The values of concentration actually used are in terms of mls. of concentrated tracer solution per V_c cu. ft. of water, where V_c = volume of water used in calibration of probes.

The values of q(t) actually measured are in terms of mls. of diluted (1:10) tracer solution per minute. Hence in order to compare the values of q obtained from regressions with $q'_{measured}$ the following conversion factor must be used :

$$q_{measured} = \frac{V}{10 \times 60 \times d} \quad q'_{measured}$$

	V_c/d	$q'_{measured}$	$q_{measured}$
Runs 1, 2	11.84	12.5	0.247
Runs 3, 4, 5, 6, 7, 8, 9.	11.94	15	0.3

The tracer flow rate was measured by noting the steady rotameter reading with the solenoid valve fully opened. (see Figure 4.1)

APPENDIX 8

DETAILS OF EQUIPMENT

(i) Photocells

Lange Gmbh. Berlin ; Type Si - 14.

(ii) Amplifiers

Beckman	Data Amp.	Type	491.
	Power Supply	Type	392.
	Input Coupler	Type	9801.

(iii) Frequency Modulators

Wavetek Voltage Controlled Generator ; Model 111.

(iv) Taperecorders

Philips International ; Type EL 3549 A / 00.

(v) Data processing Unit (see photograph on page 139)

Philips EL 3549 A/00 Taperecorder

Philips PW 4230 Scalers

Philips PW 4260 Timer

Philips PW 4201 Controller

Philips PW 4210 Power Supply

Philips PW 4211 Power Supply

Philips PW 4209 Printer Control

Addo-X Model 13-0341 - Printer

I.B.M. Card Punching machine ; Type 024.

(vi) P.R.B.S. Signal Generator

Control Logic, S.A.

(vii) Hot Film Anemometer

Flow Corporation U.S.A.

Constant Temp. Anemometer Series 900 - 1

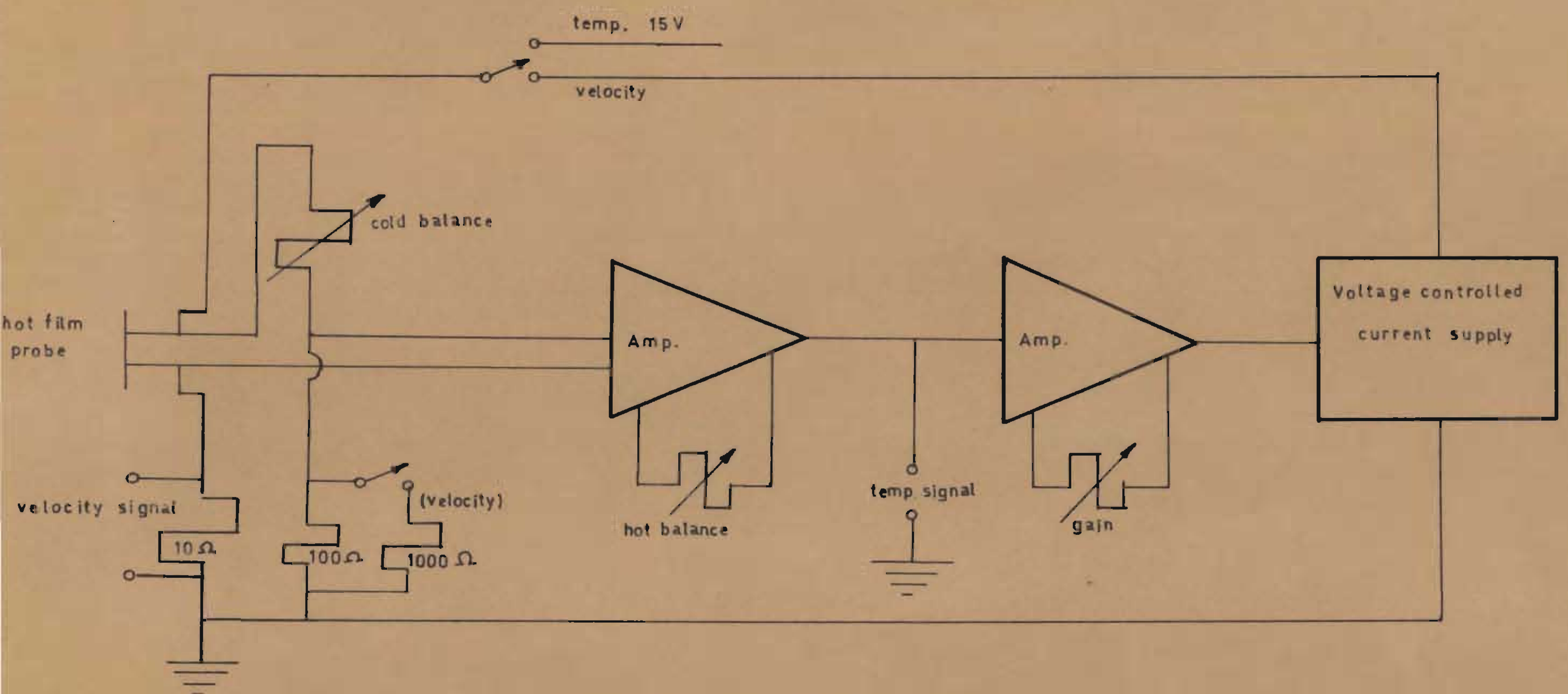

HOT FILM ANEMOMETER BRIDGE CIRCUIT

FIG. 8-A

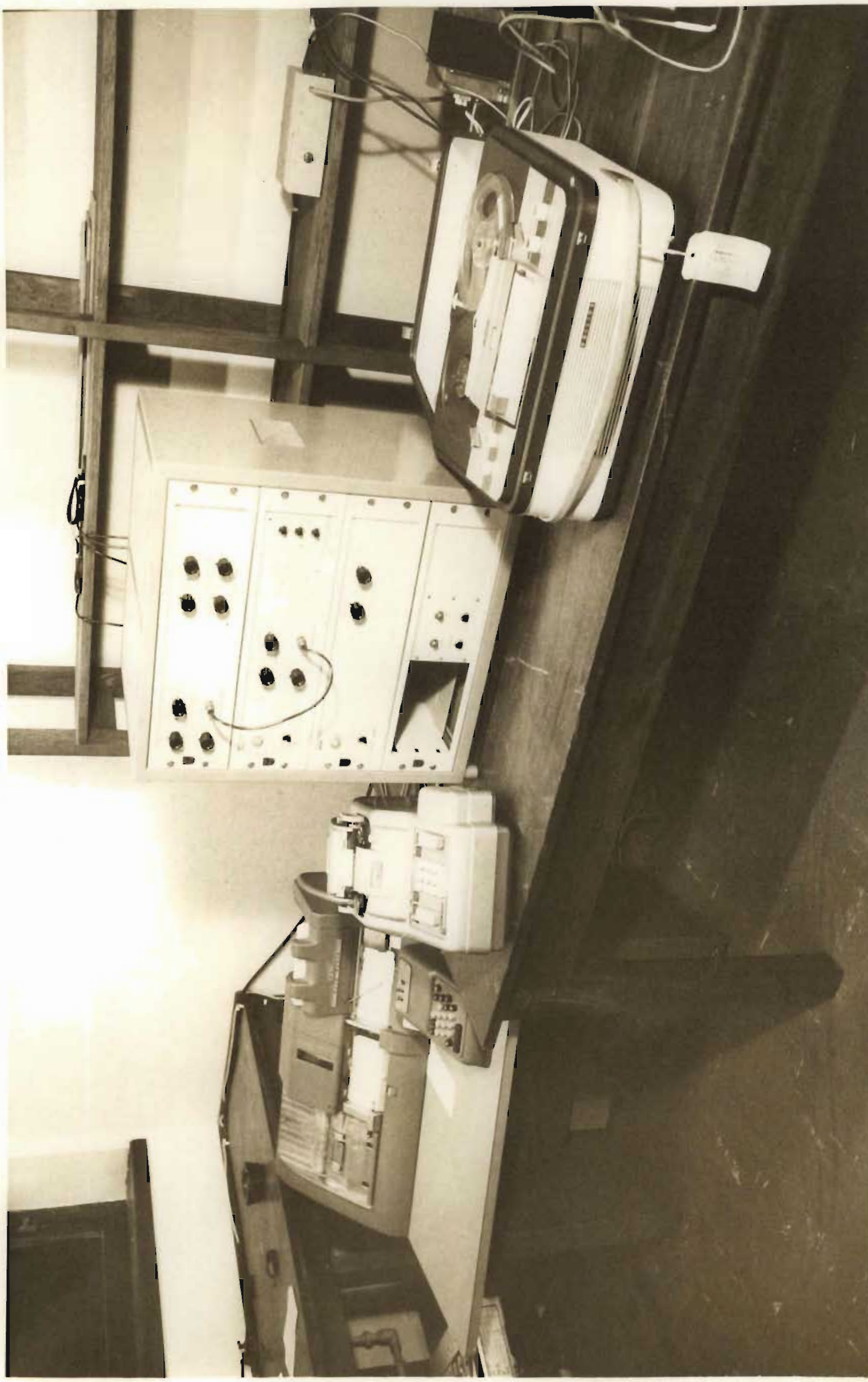

Velocity and Temp. Monitor Series 900-2

(see Figure 8.A)

Sensor Type B-1-N

****